

2

NSWC TR 81-113

A135292

# QUASI-STATIC COMPACTION STUDIES FOR DDT INVESTIGATIONS: INERT MATERIALS

BY WAYNE L. ELBAN    STEPHEN B. GROSS    KIBONG KIM    RICHARD R. BERNECKER  
RESEARCH AND TECHNOLOGY DEPARTMENT

1 DECEMBER 1982

Approved for public release, distribution unlimited.

DTIC  
ELECTE  
DEC 2 1983  
S B



## NAVAL SURFACE WEAPONS CENTER

Dahlgren, Virginia 22448 • Silver Spring, Maryland 20910

DTIC FILE COPY

83 12 01 017

UNCLASSIFIED

SECURITY CLASSIFICATION OF THIS PAGE (When Data Entered)

| REPORT DOCUMENTATION PAGE  |  | READ INSTRUCTIONS<br>BEFORE COMPLETING FORM |            |          |             |                |                            |                  |            |                |        |  |
|--|--|---|------------|----------|-------------|----------------|----------------------------|------------------|------------|----------------|--------|--|
| 1. REPORT NUMBER<br>NSWC TR 81-113   | 2. GOVT ACCESSION NO.<br><b>A135292</b>  | 3. RECIPIENT'S CATALOG NUMBER               |            |          |             |                |                            |                  |            |                |        |  |
| 4. TITLE (and Subtitle)<br>QUASI-STATIC COMPACTION STUDIES FOR DDT INVESTIGATIONS: INERT MATERIALS   | 5. TYPE OF REPORT & PERIOD COVERED   |   |            |          |             |                |                            |                  |            |                |        |  |
|  | 6. PERFORMING ORG. REPORT NUMBER   |   |            |          |             |                |                            |                  |            |                |        |  |
| 7. AUTHOR(s)<br>Wayne L. Elban, Stephen B. Gross, Kibong Kim, and Richard R. Bernecker   | 8. CONTRACT OR GRANT NUMBER(s)   |   |            |          |             |                |                            |                  |            |                |        |  |
| 9. PERFORMING ORGANIZATION NAME AND ADDRESS<br>Naval Surface Weapons Center (Code R13)<br>White Oak<br>Silver Spring, MD 20910   | 10. PROGRAM ELEMENT, PROJECT, TASK AREA & WORK UNIT NUMBERS<br>N0003080WR02453; SSP013;<br>N0003081WR22412; SSP013;<br>N0003082WR22412; SSP013 |   |            |          |             |                |                            |                  |            |                |        |  |
| 11. CONTROLLING OFFICE NAME AND ADDRESS  | 12. REPORT DATE<br>1 December 1982   |   |            |          |             |                |                            |                  |            |                |        |  |
|  | 13. NUMBER OF PAGES<br>97  |   |            |          |             |                |                            |                  |            |                |        |  |
| 14. MONITORING AGENCY NAME & ADDRESS (if different from Controlling Office)  | 15. SECURITY CLASS. (of this report)<br>UNCLASSIFIED   |   |            |          |             |                |                            |                  |            |                |        |  |
|  | 15a. DECLASSIFICATION/DOWNGRADING SCHEDULE   |   |            |          |             |                |                            |                  |            |                |        |  |
| 16. DISTRIBUTION STATEMENT (of this Report)<br>Approved for public release; distribution unlimited.  |  |   |            |          |             |                |                            |                  |            |                |        |  |
| 17. DISTRIBUTION STATEMENT (of the abstract entered in Block 20, if different from Report)   |  |   |            |          |             |                |                            |                  |            |                |        |  |
| 18. SUPPLEMENTARY NOTES  |  |   |            |          |             |                |                            |                  |            |                |        |  |
| 19. KEY WORDS (Continue on reverse side if necessary and identify by block number)<br><table border="0"> <tr> <td>Compaction</td> <td>Melamine</td> </tr> <tr> <td>Porous Beds</td> <td>Sound Velocity</td> </tr> <tr> <td>Deflagration to Detonation</td> <td>Vickers Hardness</td> </tr> <tr> <td>Transition</td> <td>Shore Hardness</td> </tr> <tr> <td>Teflon</td> <td></td> </tr> </table>  |  |   | Compaction | Melamine | Porous Beds | Sound Velocity | Deflagration to Detonation | Vickers Hardness | Transition | Shore Hardness | Teflon |  |
| Compaction   | Melamine   |   |            |          |             |                |                            |                  |            |                |        |  |
| Porous Beds  | Sound Velocity   |   |            |          |             |                |                            |                  |            |                |        |  |
| Deflagration to Detonation   | Vickers Hardness   |   |            |          |             |                |                            |                  |            |                |        |  |
| Transition   | Shore Hardness   |   |            |          |             |                |                            |                  |            |                |        |  |
| Teflon   |  |   |            |          |             |                |                            |                  |            |                |        |  |
| 20. ABSTRACT (Continue on reverse side if necessary and identify by block number)<br><p>Extensive quasi-static compaction experiments were performed on porous beds of two powdered inert materials: Teflon 7C, a highly crystalline polymer, and melamine, a molecular crystal. These two materials were selected to be somewhat representative of the range of deformation behavior that can occur for high energy propellants and their crystalline energetic ingredients, respectively. This quasi-static compaction work is a companion study to an investigation of the dynamic compaction behavior performed by other</p> |  |   |            |          |             |                |                            |                  |            |                |        |  |

UNCLASSIFIED

SECURITY CLASSIFICATION OF THIS PAGE (When Data Entered)

→ investigators on these two materials. It provides insight into the dynamic experiments and helps in their modeling as well as in modeling the complete DDT (deflagration to detonation transition) process when significant compaction occurs.

Applied force, transmitted force, and porous bed displacement were measured simultaneously during the quasi-static compaction experiments. An average axial compressive force within the granular material comprising a unit cross-sectional area of the porous bed, called the "intragranular stress," was then calculated as a function of percent theoretical maximum density for a portion of the compaction data. Initial measurements of sound velocity and hardness (Vickers and Shore) on various compacted samples are given. ↗

UNCLASSIFIED

SECURITY CLASSIFICATION OF THIS PAGE (When Data Entered)

## FOREWORD

This work was supported primarily by the High Energy Propellant Safety (HEPS) Program sponsored by the Strategic Systems Project Office under work request numbers N0003080WR02453 SSPO13, N0003081WR12412 SSPO13, and N0003082-WR22412 SSPO13. The compaction measurements on melamine were funded by the NAVSEA 6.2 Explosives Block. The results and conclusions given in this report regarding the quasi-static compaction behavior of two inert materials, Teflon 7C and melamine, chosen to simulate roughly the deformation behavior of energetic materials should be of help to those interested in investigating the quasi-static compaction of elastomeric plastic bonded explosives and high energy propellants as well as crystalline secondary explosives. This work also relates to dynamic compaction experiments performed on the same inert materials and aids physical and numerical modeling efforts describing DDT in porous beds of energetic materials. Further, this work has application to other areas where the compaction of energetic materials occurs including the pressing of primary and secondary explosives and pyrotechnic compositions to be used in laboratory research and development investigations and in production ordnance items. Initial results from measurements of sound velocity and hardness on compacted samples are included in Appendices. The identification of any manufacturer and/or product in this report does not imply endorsement or criticism by the Naval Surface Weapons Center.

Approved by:



J. F. PROCTOR, Head  
Energetic Materials Division



|                     |                      |                                     |
|---------------------|----------------------|-------------------------------------|
| Accession No.       |                      | <input checked="" type="checkbox"/> |
| NTIS                |                      | <input checked="" type="checkbox"/> |
| DTIC                |                      | <input type="checkbox"/>            |
| Unannounced         |                      | <input type="checkbox"/>            |
| Justification       |                      | <input type="checkbox"/>            |
| By _____            |                      |                                     |
| Distribution/ _____ |                      |                                     |
| Availability Codes  |                      |                                     |
| Dist                | Avail and/or Special |                                     |
| A-1                 |                      |                                     |

PREFACE

The authors thank N. C. Vogel for his help with the recording equipment used in the compaction experiments and G. B. Green for his help with the preliminary single force compaction measurements. E. T. Toton and H. D. Jones helped in the NSWC I analytic scheme, and T. A. Orlow developed a numerical technique and computer program for obtaining the unknown parameters in the equation of state used in the Burchett, Birnbaum, and Oien analytic scheme. Numerous helpful discussions with H. W. Sandusky on the dynamic compaction behavior of Teflon 7C and melamine are gratefully recognized. The authors gratefully acknowledge the helpful discussions on ultrasonic sound velocity measurements with G. V. Blessing. R. W. Armstrong provided considerable insight into the hardness measurements that were performed on the compacted Teflon 7C samples. One or more helpful discussions were held with R. W. Warfield on the compressibility of Teflon and its phase transitions.

## CONTENTS

| <u>Section</u> |  | <u>Page</u> |
|----------------|--|-------------|
| I              | INTRODUCTION.....  | 1           |
| II             | EXPERIMENTAL.....  | 5           |
| III            | COMPACTION DATA REDUCTION.....   | 13          |
| IV             | ANALYSES TO GIVE INTRAGRANULAR STRESS AND PARTICLE-WALL<br>FRICTION PARAMETER.....   | 15          |
| V              | RESULTS AND DISCUSSION.....  | 25          |
| VI             | SUMMARY AND CONCLUSIONS.....   | 45          |
| VII            | BIBLIOGRAPHY.....  | 47          |
| VIII           | NOMENCLATURE.....  | 51          |
|                | APPENDIX A -- SIEVE ANALYSES OF MELAMINE.....  | A-1         |
|                | APPENDIX B -- STEP-BY-STEP PROCEDURE OF A COMPLETE COMPACTION<br>EXPERIMENT (TWO FORCE MEASUREMENTS).....                          | B-1         |
|                | APPENDIX C -- CORRECTION IN COMPACTION APPARATUS ASSEMBLY LENGTH.....  | C-1         |
|                | APPENDIX D -- SOUND VELOCITY MEASUREMENTS ON COMPACTED MELAMINE AND<br>TEFLON 7C SAMPLES.....                                      | D-1         |
|                | APPENDIX E -- COMPILATION OF TEFLON 7C AND MELAMINE COMPACTION DATA AND<br>INTRAGRANULAR STRESS RESULTS FROM VARIOUS ANALYSES..... | E-1         |
|                | APPENDIX F -- HARDNESS STUDIES OF COMPACTED TEFLON 7C SAMPLES.....   | F-1         |

## ILLUSTRATIONS

| <u>Figure</u> |  | <u>Page</u> |
|---------------|--|-------------|
| 1             | PHOTOGRAPHS OF AS-RECEIVED TEFLON 7C AND MELAMINE.....   | 6           |
| 2             | SCHEMATIC OF APPARATUS FOR MAKING APPLIED FORCE MEASUREMENTS<br>DURING COMPACTION OF POROUS BEDS.....  | 9           |
| 3             | SCHEMATIC OF APPARATUS FOR MAKING APPLIED AND TRANSMITTED FORCE<br>MEASUREMENTS DURING COMPACTION OF POROUS BEDS.....  | 10          |
| 4             | FREE-BODY DIAGRAMS WITH FORCE BALANCES FOR THE COMPACTION OF<br>POROUS BEDS.....   | 16          |
| 5             | SEMILOGARITHMIC VARIATION OF TRANSMITTED FORCE VERSUS BED<br>LENGTH AT CONSTANT APPLIED FORCE FOR COMPACTED TEFLON 7C.....   | 18          |
| 6             | SEMILOGARITHMIC VARIATION OF TRANSMITTED FORCE VERSUS BED<br>LENGTH AT CONSTANT APPLIED FORCE FOR COMPACTED MELAMINE.....  | 19          |
| 7             | SCHEMATIC OF INCREMENTALLY DIVIDED POROUS BED (NSWC II ANALYSIS)..   | 21          |
| 8             | APPLIED STRESS VERSUS $\Sigma$ TMD FOR COMPACTED TEFLON 7C.....  | 26          |
| 9             | SEMILOGARITHMIC VARIATION OF APPLIED STRESS VERSUS $\Sigma$ TMD FOR<br>COMPACTED TEFLON 7C.....  | 28          |
| 10            | TRANSMITTED FORCE VERSUS APPLIED FORCE FOR COMPACTED TEFLON 7C<br>AND MELAMINE.....  | 29          |
| 11            | APPLIED STRESS VERSUS $\Sigma$ TMD FOR COMPACTED TEFLON 7C AND MELAMINE...   | 30          |
| 12            | SEMILOGARITHMIC VARIATION OF INTRAGRANULAR STRESS AND PARTICLE-<br>WALL FRICTION PARAMETER VERSUS $\Sigma$ TMD FOR COMPACTED TEFLON 7C<br>USING KUO, MOORE, AND YANG ANALYSIS..... | 33          |
| 13            | SEMILOGARITHMIC VARIATION OF INTRAGRANULAR STRESS AND PARTICLE-<br>WALL FRICTION PARAMETER VERSUS $\Sigma$ TMD FOR COMPACTED TEFLON 7C<br>USING NSWC I ANALYSIS.....               | 34          |
| 14            | SEMILOGARITHMIC VARIATION OF INTRAGRANULAR STRESS AND PARTICLE-<br>WALL FRICTION PARAMETER VERSUS $\Sigma$ TMD FOR COMPACTED MELAMINE<br>USING KUO, MOORE, AND YANG ANALYSIS.....  | 39          |
| 15            | SEMILOGARITHMIC VARIATION OF INTRAGRANULAR STRESS AND PARTICLE-<br>WALL FRICTION PARAMETER VERSUS $\Sigma$ TMD FOR COMPACTED MELAMINE<br>USING NSWC I ANALYSIS.....                | 42          |
| A-1           | PARTICLE SIZE ANALYSES OF MELAMINE.....  | A-3         |
| C-1           | APPLIED FORCE VERSUS STEEL COLUMN DEFLECTION.....  | C-2         |
| D-1           | SCHEMATIC OF LEXAN DDT TUBE CONTAINING POROUS BED FOR MAKING<br>SOUND SPEED MEASUREMENTS.....  | D-2         |
| D-2           | BLOCK DIAGRAM OF BROADBAND ULTRASONIC APPARATUS OPERATING IN<br>DIRECT CONTACT PULSE-ECHO.....   | D-3         |
| D-3           | BLOCK DIAGRAM OF BROADBAND ULTRASONIC APPARATUS OPERATING IN<br>THROUGH-TRANSMISSION WITH DELAY ROD.....   | D-6         |
| D-4           | AXIAL LONGITUDINAL VELOCITY VERSUS $\Sigma$ TMD FOR COMPACTED TEFLON<br>7C SAMPLES AND TEFLON BAR STOCK.....   | D-11        |
| D-5           | SEMILOGARITHMIC VARIATION OF LONGITUDINAL VELOCITY VERSUS $\Sigma$ TMD<br>FOR BARE CHARGES OF COMPACTED TEFLON 7C SAMPLES.....   | D-13        |

ILLUSTRATIONS (Cont.)

| <u>Figure</u> |  | <u>Page</u> |
|---------------|--|-------------|
| D-6           | LONGITUDINAL MODULUS VERSUS %TMD OBTAINED FROM LONGITUDINAL VELOCITY MEASUREMENTS ON BARE CHARGES OF COMPACTED TEFLON 7C SAMPLES.....                              | D-14        |
| D-7           | SEMILOGARITHMIC VARIATION OF LONGITUDINAL MODULUS VERSUS %TMD OBTAINED FROM LONGITUDINAL VELOCITY MEASUREMENTS ON BARE CHARGES OF COMPACTED TEFLON 7C SAMPLES..... | D-15        |
| F-1           | DIAMOND PYRAMID (VICKERS) HARDNESS VERSUS RADIAL DISTANCE ALONG TOP SURFACE OF COMPACTED TEFLON 7C SAMPLES.....  | F-2         |
| F-2           | SHORE A-2 HARDNESS VERSUS %TMD FOR COMPACTED TEFLON 7C SAMPLES....   | F-3         |
| F-3           | SHORE D HARDNESS VERSUS %TMD FOR COMPACTED TEFLON 7C SAMPLES.....  | F-4         |

## TABLES

| <u>Table</u> |   | <u>Page</u> |
|--------------|---|-------------|
| 1            | LEAST SQUARES ANALYSES OF THE LINEAR $F_c - F_a$ DEPENDENCY FOR COMPACTED TEFLON 7C.....  | 31          |
| 2            | OBSERVATIONS FROM KUO, MOORE, AND YANG ANALYSIS OF TEFLON 7C COMPACTION DATA.....   | 35          |
| 3            | OBSERVATIONS FROM NSWC I ANALYSIS OF TEFLON 7C COMPACTION DATA.....   | 35          |
| 4            | DIFFERENCES IN INTRAGRANULAR STRESS VALUES COMPUTED FROM KUO, MOORE, AND YANG ANALYSIS AND FROM NSWC I ANALYSIS OF TEFLON 7C COMPACTION DATA..... | 36          |
| 5            | LEAST SQUARES ANALYSES OF THE LINEAR $F_c - F_a$ DEPENDENCY FOR COMPACTED MELAMINE.....   | 38          |
| 6            | OBSERVATIONS FROM KUO, MOORE, AND YANG ANALYSIS OF MELAMINE COMPACTION DATA.....  | 42          |
| 7            | OBSERVATIONS FROM NSWC I ANALYSIS OF MELAMINE COMPACTION DATA.....  | 42          |
| 8            | DIFFERENCES IN INTRAGRANULAR STRESS VALUES COMPUTED FROM KUO, MOORE, AND YANG ANALYSIS AND FROM NSWC I ANALYSIS OF MELAMINE COMPACTION DATA.....  | 43          |
| A-1          | SIEVE ANALYSES OF MELAMINE.....   | A-2         |
| D-1          | SOUND VELOCITY MEASUREMENTS ON VARIOUS LIQUIDS WHILE CONTAINED IN A LEXAN DDT TUBE.....   | D-4         |
| D-2          | LONGITUDINAL VELOCITY MEASUREMENTS ON COMPACTED MELAMINE POWDER WHILE CONTAINED IN A LEXAN DDT TUBE.....  | D-4         |
| D-3          | LONGITUDINAL VELOCITY MEASUREMENTS ON COMPACTED TEFLON 7C POWDER WHILE CONTAINED IN A LEXAN DDT TUBE.....   | D-7         |
| D-4          | LONGITUDINAL VELOCITY MEASUREMENTS ON BARE CHARGES OF COMPACTED TEFLON 7C POWDER.....   | D-9         |
| D-5          | LONGITUDINAL VELOCITY MEASUREMENTS ON BARE CHARGES OF TEFLON 7C POWDER COMPACTED USING THE INSTRON UNIVERSAL TESTING MACHINE.....                 | D-10        |
| D-6          | LONGITUDINAL VELOCITY MEASUREMENTS ON TEFLON BAR STOCK.....   | D-10        |
| E-1          | COMPACTION DATA FOR 5g TEFLON 7C SAMPLES.....   | E-2         |
| E-2          | COMPACTION DATA FOR 10g TEFLON 7C SAMPLES.....  | E-3         |
| E-3          | COMPACTION DATA FOR 15g TEFLON 7C SAMPLES.....  | E-5         |
| E-4          | COMPACTION DATA FOR 20g TEFLON 7C SAMPLES.....  | E-6         |
| E-5          | COMPACTION DATA FOR 25g TEFLON 7C SAMPLES.....  | E-8         |
| E-6          | COMPACTION DATA FOR 5g MELAMINE SAMPLES.....  | E-9         |
| E-7          | COMPACTION DATA FOR 10g MELAMINE SAMPLES.....   | E-10        |
| E-8          | COMPACTION DATA FOR 15g MELAMINE SAMPLES.....   | E-11        |
| E-9          | COMPACTION DATA FOR 20g MELAMINE SAMPLES.....   | E-12        |
| E-10         | COMPACTION DATA FOR 25g MELAMINE SAMPLES.....   | E-13        |
| E-11         | INTRAGRANULAR STRESS RESULTS FROM VARIOUS ANALYSES OF TEFLON 7C COMPACTION DATA.....  | E-14        |
| E-12         | INTRAGRANULAR STRESS RESULTS FROM VARIOUS ANALYSES OF MELAMINE COMPACTION DATA.....   | E-16        |

## I. INTRODUCTION

Using a flash radiography system, it has been demonstrated clearly that appreciable dynamic compaction occurs in the deflagration to detonation transition (DDT) process in porous beds of energetic materials confined in the optical DDT tube.<sup>1-3</sup> It is envisioned that compaction can result from:

- (1) firing of the ignitor,
- (2) propagation of a convective ignition front, and
- (3) reaction during propagation of compressive waves.

Consequently, it is of interest to perform compaction measurements on porous beds of energetic materials in order to obtain a compaction law (stress versus percent theoretical maximum density (% TMD)) that will provide data on the stress level necessary to achieve a given % TMD. Identification of compaction mechanisms with their possible relation to hot spot formation and the role that this has in the DDT process is also important.

To assist in modeling the combustion of a porous bed of some energetic material that is undergoing compaction, it is necessary to determine the compaction behavior of the porous bed itself without the complication of the container or mold wall effect. Kuo, Moore, and Yang<sup>4</sup> have reported a determination of this boundary contribution, called the particle-wall friction

---

<sup>1</sup>Bernecker, R. R., Sandusky, H. W., and Clairmont, Jr., A. R., "Compaction and the Burning to Detonation Transition at Low Confinement," in Proceedings of the 16th JANNAF Combustion Meeting, Vol. I, 10-14 Sep 1979, Publ. 1979, pp. 91-116.

<sup>2</sup>Sandusky, H. W., and Bernecker, R. R., "Transparent Tube Studies of Burning to Detonation Transition in Granular Explosives I, Preliminary Framing Camera Studies," NSWC TR 79-79, 27 Oct 1980.

<sup>3</sup>Hopkins, B. D., Butcher, A. G., Pilcher, D. T., and Beckstead, M. W., "A Comparison of DDT Calculations and Experiments for Granulated Rocket Propellant," in Proceedings of the 16th JANNAF Combustion Meeting, Vol. 3, 10-14 Sep 1979, Publ. 1979, pp. 33-49.

<sup>4</sup>Kuo, K. K., Moore, B. B., and Yang, V., "Measurement and Correlation of Intragranular Stress and Particle-Wall Friction in Granular Propellant Beds, in Proceedings of the 16th JANNAF Combustion Meeting, Vol. I, 10-14 Sep 1979, Publ. 1979, pp. 559-581. (See also "Intragranular Stress, Particle-Wall Friction and Speed of Sound in Granular Propellant Beds," Journal of Ballistics, Vol. 4, No. 1, 1980, pp. 697-730.)

parameter, as a function of porosity in quasi-static compaction studies on two deterred double-base propellants. This procedure allows the determination of the desired intragranular stress-porosity dependency, where the intragranular stress is the average axial compressive stress within the granular material comprising a unit cross-sectional area of the porous bed. This was accomplished by measuring the force on and the displacement of the top and bottom rams while the bed was compressed vertically at a low strain rate using a Tinius Olsen compression machine. The quantities of interest were then determined from equations obtained from considering the force balance on the porous bed during compaction. A more detailed discussion of these equations follows in the "Analyses to Give Intragranular Stress and Particle-Wall Friction Parameter" section. In addition, from microscopic examination of recovered samples that had been compacted, it was possible to identify two stages in the compaction process corresponding to (1) packing of particles into large interstitial voids and (2) plastic flow and fracture of particles into small voids.

The work described in this report was undertaken to design and fabricate a quasi-static compaction apparatus similar to the one used by Kuo, Moore, and Yang, allowing extensive compaction measurements to be performed on two inert materials, Teflon 7C and melamine powders. This would allow quasi-static compaction experiments to be performed later on various granular energetic materials which undergo dynamic compaction when tested in a DDT tube configuration. Two new schemes were devised for calculating intragranular stress and compared with two methods that appear in the literature. Besides the analysis developed by Kuo, Moore, and Yang,<sup>4</sup> a second analytic scheme has been described by Burchett, Birnbaum, and Oien.<sup>5</sup> Attention was given to all of these various methods of analysis to gain insight into the most reasonable approach for analyzing subsequent quasi-static compaction data obtained for energetic materials. Clearly, this is also an important consideration because compaction experiments conducted remotely are significantly more cumbersome and time consuming than the ones described in this work involving inert materials.

Emphasis was given to performing quasi-static measurements because a great deal of useful information can be obtained quickly using a relatively simple experimental set-up. The compaction data that is attained is necessary to establish and develop physical and numerical<sup>6</sup> models of the DDT mechanism(s) in porous beds of energetic materials. Clearly, rate effects are expected to be important at certain times because of the time scales involved in the DDT experiment. The effect of strain rate has been treated theoretically by Carroll

---

<sup>4</sup>Kuo, Moore, and Yang, pp. 559-581.

<sup>5</sup>Burchett, O. L., Birnbaum, M. R., and Oien, C. T., "Compaction Studies of Palladium/Aluminum Powders," in Proceedings of the 6th International Pyrotechnics Seminar, 17-21 Jul 1978, pp. 11-38.

<sup>6</sup>Sandusky, H. W., Elban, W. L., Kim, K., Bernecker, R. R., Gross, S. B., and Clairmont, Jr., A. R., "Compaction of Porous Beds of Inert Materials," in Proceedings Seventh Symposium (International) on Detonation, 16-19 Jun 1981, NSWC MP 82-334, pp. 843-856.

and Holt<sup>7</sup> and assessed experimentally by Walker,<sup>8</sup> who measured the compaction behavior of a number of powdered materials, including lead shot, ammonium nitrate (AN), trinitrotoluene (TNT), AN-TNT mixtures, and a variety of other inorganic salts, under static and dynamic loading (by drop-weight impact). It was found for each material that the resistance of the porous bed to compression by impact was always greater than the resistance to compression by static loading, and for many of the materials this difference was substantial. Whether or not similar differences occur for energetic materials currently of interest needs to be determined.

To facilitate the task of characterizing the quasi-static compaction measurements and their analyses prior to investigating the compaction behavior of energetic materials, a large number of experiments were performed on porous beds of two inert materials: Teflon 7C, a highly crystalline polymer, and melamine, a molecular crystal. These two materials were chosen to represent somewhat the range in deformation behavior that can occur for elastomeric plastic bonded explosives and high energy propellants as well as crystalline secondary explosives. In separate work, dynamic compaction experiments<sup>6,9</sup> were conducted on these two materials in which compaction resulted from the same ignition source used for DDT tube experiments.<sup>1,2</sup> The use of inert materials avoids complications associated with gas generation from the combustion of energetic materials, allowing the early stage of the DDT mechanism to be examined. This quasi-static compaction work is a companion study to the ignitor driven experiments<sup>6,9</sup> and serves to give insight into these experiments and helps in their modeling<sup>6</sup> as well as in modeling the complete DDT process when significant compaction occurs. This work also relates to quasi-static compaction studies on energetic materials including work by Kuo, Moore, and Yang<sup>4</sup> that was discussed earlier and recent work by Birkett<sup>10</sup> on various gun propellants of military interest.

---

<sup>7</sup>Carroll, M. M., and Holt, A. C., "Static and Dynamic Pore-Collapse Relations for Ductile Porous Materials," Journal of Applied Physics, Vol. 43, No. 4, 1972, pp. 1626-1636.

<sup>8</sup>Walker, E. E., "The Properties of Powders Part VI The Compressibility of Powders," Transactions of the Faraday Society, Vol. 19, No. 7, Part 1, 1923, pp. 73-82.

<sup>6</sup>Sandusky, Elban, Kim, Bernecker, Gross, and Clairmont, pp. 843-856.

<sup>9</sup>Sandusky, H. W., Bernecker, R. R., and Clairmont, Jr., A. R., "Dynamic Compaction of Inert Porous Beds," NSWC TR 81-97, to be published.

<sup>1</sup>Bernecker, Sandusky, and Clairmont, pp. 91-116.

<sup>2</sup>Sandusky and Bernecker.

<sup>4</sup>Kuo, Moore, and Yang, pp. 559-581.

<sup>10</sup>Birkett, J. A., "The Acquisition of M30A1 Propellant Rheology Data," IHTR 724, 30 Sep 1981.

## II. EXPERIMENTAL

A. PROPERTIES OF MATERIALS USED FOR COMPACTION EXPERIMENTS

1. Teflon 7C. Teflon 7C is a powdered tetrafluoroethylene molding resin manufactured by E. I. du Pont de Nemours and Company, Inc. Its properties as reported by the manufacturer, include an apparent bulk density of  $0.275 \text{ g/cm}^3$  and an average relative particle size of  $30 \mu\text{m}$ , as determined by air sedimentation. Teflon 7C has a maximum density\* of  $2.305 \text{ g/cm}^3$ , which corresponds to it being 100% crystalline. This is very nearly the case for the as-received molding powder. The maximum density possible at ambient pressure for a compacted or preformed sample is about  $2.28 \text{ g/cm}^3$ , which decreases to  $2.155$  to  $2.176 \text{ g/cm}^3$  when the sample is sintered. This occurs because Teflon 7C undergoes a crystalline to amorphous phase transition during sintering. The density is  $2.00 \text{ g/cm}^3$  for 100% amorphous material. Low magnification microscopic examination using a Zeiss Tessovar system revealed (Figure 1a) that Teflon 7C easily forms weak agglomerates. Individual particles are fibrous in appearance.

Besides being chosen in this work as a "simulant" for the deformation properties of elastomeric plastic bonded explosives and high energy (modified double-base and composite) propellants, whose DDT behavior has been studied,<sup>1,11,12</sup> Teflon 7C has served as a binder ingredient in several pressed

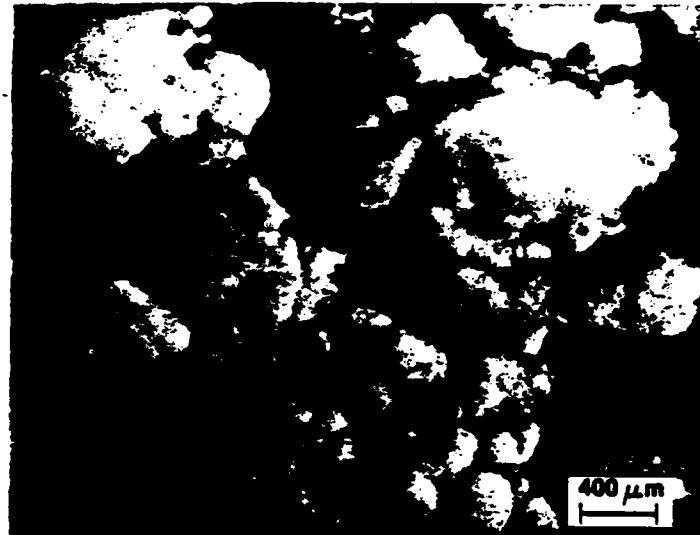
---

\*Density information on Teflon 7C was provided by L. A. Ferris, Customer Services Specialist, Fluoropolymers Division, Plastic Products and Resins Department, DuPont Company, during a telephone conversation on 4 Sep 1979.

<sup>1</sup>Bernecker, Sandusky, and Clairmont, pp. 91-116.

<sup>11</sup>Bernecker, R. R., Price, D., and Sandusky, H., "Burning to Detonation Transition in Porous Beds of a High Energy Propellant," NSWC TR 79-351, Nov 1979.

<sup>12</sup>Price, D. and Bernecker, R. R., "DDT Behavior of Porous Propellant Models and Porous Samples of Commercial Propellants" NSWC TR 80-65, 13 Mar 1980.



(A) TEFLON 7C



(B) MELAMINE

FIGURE 1. PHOTOGRAPHS OF AS-RECEIVED TEFLON 7C AND MELAMINE

explosive compositions. These include PBXW-7, the seismic charges<sup>13</sup> placed on the moon during the Apollo 17 space mission,<sup>14</sup> and an inert simulant<sup>15</sup> for the seismic explosive charges.

2. Melamine. Melamine is a molecular crystalline solid in the form of a granular powder and is supplied by the Eastman Kodak Company (stock number 1540). It has a crystal density of  $1.573/\text{cm}^3$  at  $16^\circ\text{C}$  as reported in the Handbook of Chemistry and Physics,<sup>16</sup> while a slightly lower value of  $1.561/\text{cm}^3$  is calculated from the room temperature X-ray diffraction data obtained by Varghese, O'Connell, and Maslen.<sup>17</sup> The higher value was used in performing the % TMD calculations reported in this work. Prior to using, the material was dried at  $100^\circ\text{C}$  for about 116 h. Based on sieve analyses described in Appendix A, the average particle size was found to range from 46 to 56  $\mu\text{m}$ . Low magnification microscopic examination revealed (Figure 1b) that melamine particles were irregularly shaped, with some being bonded together, and confirmed the rather wide particle size distribution determined by the sieve analyses.

Melamine was selected in this work as a "simulant" for the deformation behavior of various molecular explosive crystals, such as RDX, HMX, tetryl, and picric acid, whose DDT behavior has been studied<sup>18,19</sup> either as pure material or with wax as an additive. As was the case with the Teflon 7C, some previous experience had been obtained in compacting melamine since it is another major ingredient in the inert simulant<sup>15</sup> for the seismic explosive charges mentioned previously.

---

<sup>13</sup>Kilmer, E. E., "Plastic Bonded, Thermally Stable Explosive for an Apollo Experiment," Journal of Spacecraft and Rockets, Vol. 10, No. 7, 1973, pp. 463-466.

<sup>14</sup>Hinners, N. W., and Mason, P. V., "The Apollo-17 Surface Experiments," Astronautics and Aeronautics, Vol. 10, No. 12, 1972, pp. 40-54.

<sup>15</sup>Elban, W. L., "The Development of an Inert Simulant for HNS/Teflon Explosive," NOLTR 72-255, 14 Nov 1972.

<sup>16</sup>Weast, R. C., ed., CRC Handbook of Chemistry and Physics (Boca Raton, FL: CRC Press, Inc., 1980), p. C-406.

<sup>17</sup>Varghese, J. N., O'Connell, A. M., and Maslen, E. N., "The X-ray and Neutron Crystal Structure of 2,4,6 - Triamino - 1,3,5 - triazine (Melamine)," Acta Crystallographica, Vol. B33, Part 7, 1977, pp. 2102-2108.

<sup>18</sup>Price, D. and Bernecker, R. R., "DDT Behavior of Waxed Mixtures of RDX, HMX, and Tetryl," NSWC TR 77-96, 18 Oct 1977.

<sup>19</sup>Price, D. and Bernecker, R. R., "DDT Behavior of Ground Tetryl and Picric Acid," NSWC TR 77-175, 25 Jan 1978.

## B. PRELIMINARY SINGLE FORCE MEASUREMENTS

Some preliminary experiments involving single force measurements were performed in beginning the study of the compaction behavior of Teflon 7C powder. Axial applied force and ram displacement measurements were made using the set-up appearing in Figure 2. Either 8 or 16 g of Teflon 7C was compacted in a 25.4 mm I.D. steel (~54 mm O.D) or Lexan (~75 mm O.D.) cylindrical mold, chosen to simulate tubes used in DDT tube studies. The steel mold has a Rockwell C hardness of 58 and a highly polished (0.1 to 0.2  $\mu\text{m}$  surface finish) inner bore. By comparison, the inner bore of the Lexan tube had a surface finish ranging from 0.25 to 0.38  $\mu\text{m}$ . With the steel "boot" in position, the sample to be compacted was poured into the mold. After the hardened steel ram had been gently lowered and allowed to come to rest, the initial bed length was determined using vernier calipers to measure the overall length of the ram-mold assembly with and without sample. The loaded ram-mold assembly was placed in a universal testing machine (Instron model TT-C) and compressed at a constant crosshead speed of 5 mm/min. The onset of bed deformation was detected using a dial indicator positioned at the underside of the knurled head of the ram (Figure 2).

## C. TWO FORCE MEASUREMENTS

Although single force measurements performed using a single-acting ram provide some useful information concerning the compaction of porous beds, no determination of the dependency of the intragranular stress on % TMD can be made. An effort was undertaken to develop and characterize an apparatus suitable for evaluating this dependency. Ultimately, this apparatus is to be used remotely to conduct compaction experiments on energetic materials.

Single increment samples ranging from 5 to 25 g in 5 g increments were compressed in the apparatus represented in Figure 3 using a universal testing machine (Tinius Olsen Electomatic having a 53 kN (12000 lbf) capacity) operating at a constant crosshead speed of 1.27 mm/min. This apparatus is based upon designs reported by Kuo, Moore, and Yang,<sup>4</sup> Hausner and Sheinhartz,<sup>20</sup> and Sheinhartz, McCullough, and Zambrow.<sup>21</sup> Two strain gage load cells (Sensotec model 41) having a 89 kN capacity measured the axial applied and transmitted compressive forces; the output from each load cell was fed to a dual channel strip chart recorder (Linear model 585). A linear variable differential

---

<sup>4</sup>Kuo, Moore, and Yang, pp. 559-581.

<sup>20</sup>Hausner, H. H., and Sheinhartz, I., "Friction and Lubrication in Powder Metallurgy," in Proceedings of the 10th Annual Meeting of the Metal Powder Association, Vol. I, 1954, pp. 6-27.

<sup>21</sup>Sheinhartz, I., McCullough, H. M., and Zambrow, J. L., "Method Described for Evaluation of Lubricants in Powder Metallurgy," Journal of Metals, Vol. 6, No. 5, 1954, pp. 515-518.

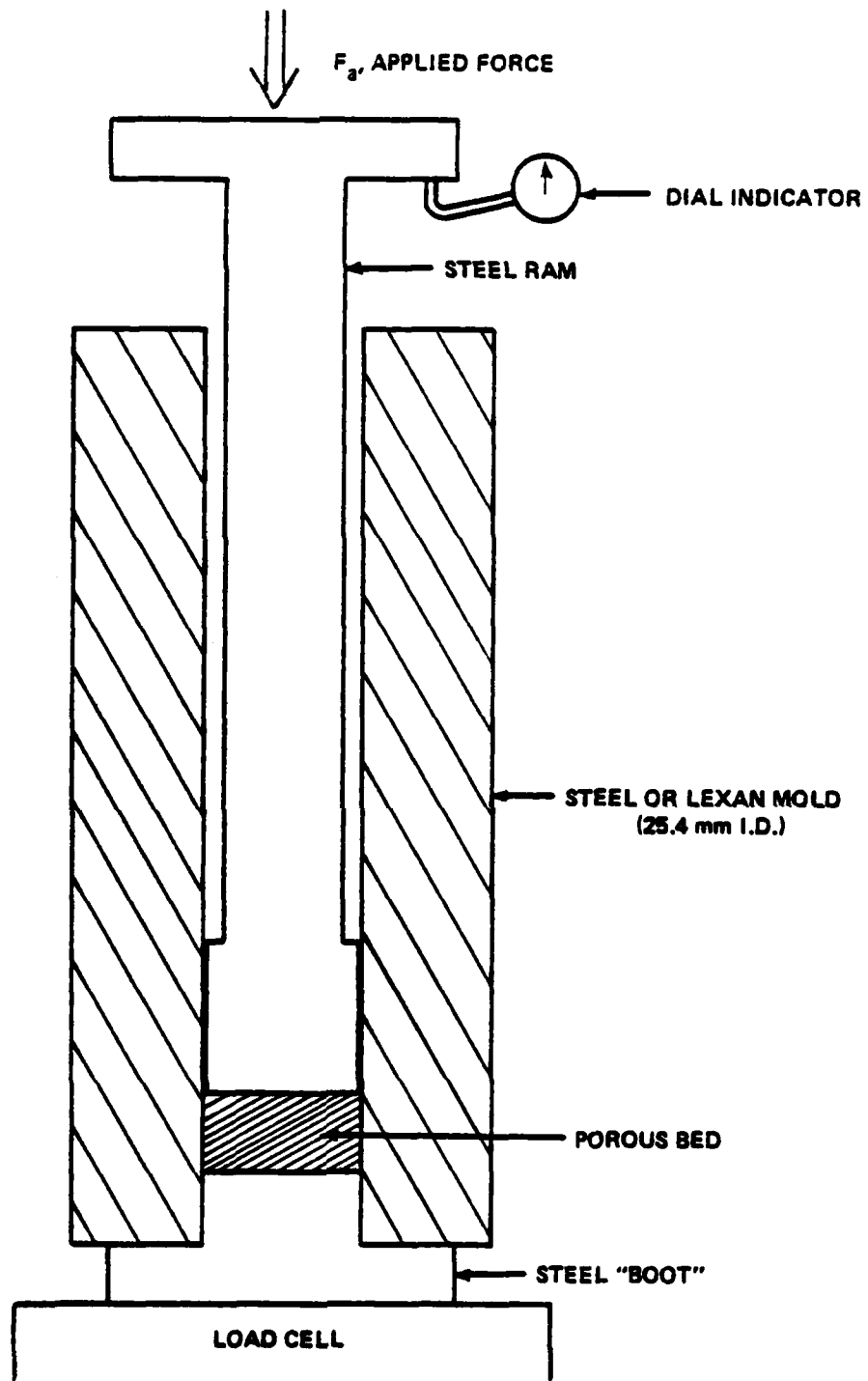
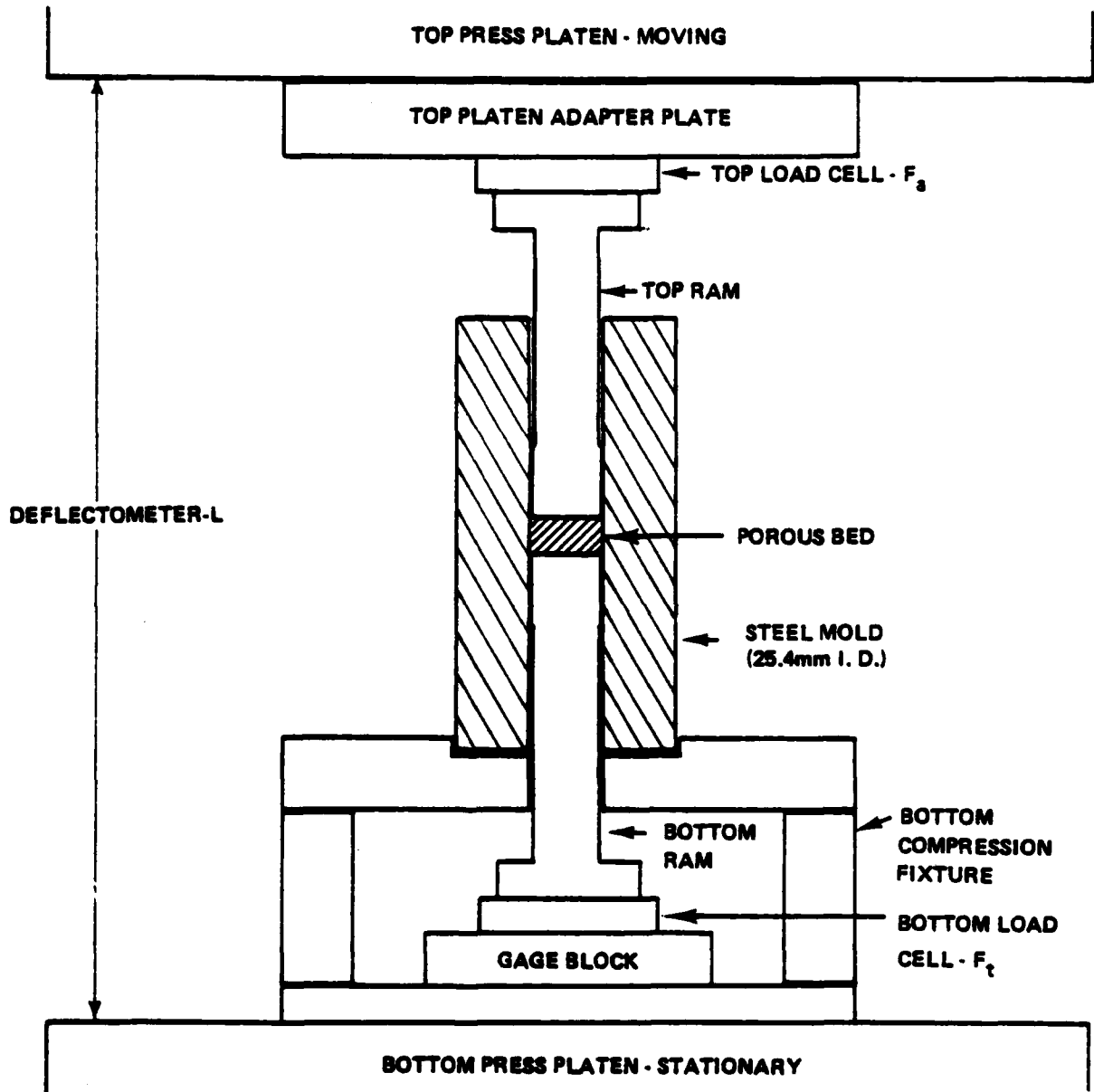


FIGURE 2. SCHEMATIC OF APPARATUS FOR MAKING APPLIED FORCE MEASUREMENTS DURING COMPACTION OF POROUS BEDS



(DESIGNED AFTER KUO, MOORE, AND YANG,<sup>4</sup> HAUSNER AND SHEINHARTZ,<sup>20</sup> AND SHEINHARTZ, McCULLOUGH, AND ZAMBROW<sup>21</sup>)

FIGURE 3. SCHEMATIC OF APPARATUS FOR MAKING APPLIED AND TRANSMITTED FORCE MEASUREMENTS DURING COMPACTION OF POROUS BEDS

transformer signal conditioner (Schaevitz Engineering model CAS-025-010) was used to interface between a deflectometer (Tinius Olsen model D-4) and a second strip chart recorder (Houston Instruments Omniscribe) to obtain top ram displacement output. Displacement measurements were calibrated and verified with a cathetometer (Ealing model S31950). The cathetometer was also used to determine the initial porous bed length and offered considerable improvement over the vernier calipers used initially in these two force measurement compaction studies as well as in the preliminary single force measurement work. The same 25.4 mm I.D. steel mold used in the preliminary single force measurements was employed in all of the two force measurement studies. A step-by-step procedure of a single compaction experiment appears in Appendix B. In all of the compaction experiments, two or more sets of data were obtained for each mass to verify reproducibility and uniformity of results.

### III. COMPACTION DATA REDUCTION

The preliminary single force data were simply treated by calculating the axial applied stress, assuming a rigid mold wall, as a function of % TMD without accounting for the elastic compression of the top ram, the steel "boot," and the load cell. Neglecting the elastic deformation of the compaction apparatus can result in a large overestimation of % TMD for a given applied stress. This occurs for two reasons. First and most importantly, there is considerable low modulus deflection, as can be seen from the plot of applied force versus steel column deflection given in Appendix C. This is much greater than what can be estimated by considering just the elastic compression of a steel column, corresponding to the compaction apparatus without a sample. Second, % TMD is a sensitive function of small changes in porous bed length because the total bed length is small for many of the samples that were compacted. It is this second consideration that necessitated replacing the vernier calipers with a cathetometer in order to measure more precisely the initial bed length before beginning the two force compaction experiments.

The remaining discussion on data reduction in this section is devoted to treating the data obtained from the two force measurement compaction studies. From the compaction procedure appearing in Appendix B, it should be noted that the compaction process was stopped at various applied force intervals. These interruptions can be seen easily on the strip chart output as a series of peaks. The tops of the peaks (axial applied force, axial transmitted force, and top ram deflection) are the points of interest for our analysis.

#### A. AXIAL APPLIED AND TRANSMITTED FORCES

The axial applied and transmitted force measurements were obtained directly from the strip chart recorder outputs that were generated by the top and bottom load cells, respectively. Either force is calculated from:

$$\text{Force} = \frac{\text{Pen Deflection Length}}{\text{Full Scale Chart Width}} \cdot \text{Force at Full Scale.} \quad (1)$$

The reading for this determination is  $\pm 0.1\%$ , while the maximum overall error of the load cell is specified by the manufacturer to be  $0.21\%$  of full scale.

B. % THEORETICAL MAXIMUM DENSITY

The % TMD of a sample compacted at some applied stress is given by

$$\% \text{ TMD} = \left( \frac{\rho_s}{\rho_c} \right) 100, \quad (2)$$

where  $\rho_s$  is the density of the compacted sample and  $\rho_c$  is the crystal density. Assuming a rigid mold wall, the sample density is calculated from

$$\rho_s = \frac{M_p}{\frac{\pi}{4} D L}, \quad (3)$$

where  $M_p$  is the total mass of the porous bed,  $D$  is the mold inner diameter, and  $L$  is the height of the compacted sample. The value of  $L$  was measured by the difference between the initial height,  $h_0$ , determined using the cathetometer, and the deflectometer reading obtained from the strip chart output after being corrected (Appendix C).

This is written as

$$L = h_0 - (\Delta l_{\text{defl}} - \epsilon), \quad (4)$$

where  $\Delta l_{\text{defl}}$  is the change in compaction assembly length and  $\epsilon$  is the correction factor.

#### IV. ANALYSES TO GIVE INTRAGRANULAR STRESS AND PARTICLE-WALL FRICTION PARAMETER

##### A. KUO, MOORE, AND YANG ANALYSIS

Initially, the reduced compaction data was analyzed according to the method, (developed by Kuo, Moore, and Yang<sup>4</sup>) that is given in Figure 4. Since the experiments are performed quasi-statically, the acceleration terms in the equations of motion are negligible. By considering the force balance for one-half of the porous bed length, an expression for intragranular stress,  $\tau_i$ , is obtained as

$$\tau_i = \frac{F_a - \tau_{wp} P_{wp} L / 2}{A (1 - \phi_{ave})}, \quad (5)$$

where  $\tau_{wp}$  is the particle-wall friction stress,  $F_a$  is the force applied to the top ram,  $P_{wp}$  is the contact perimeter between particles and tube wall,  $L$  is the porous bed length,  $A$  is the cross-sectional area of the porous bed, and  $\phi_{ave}$  is the average fractional porosity. The force balance for the entire porous bed length gives

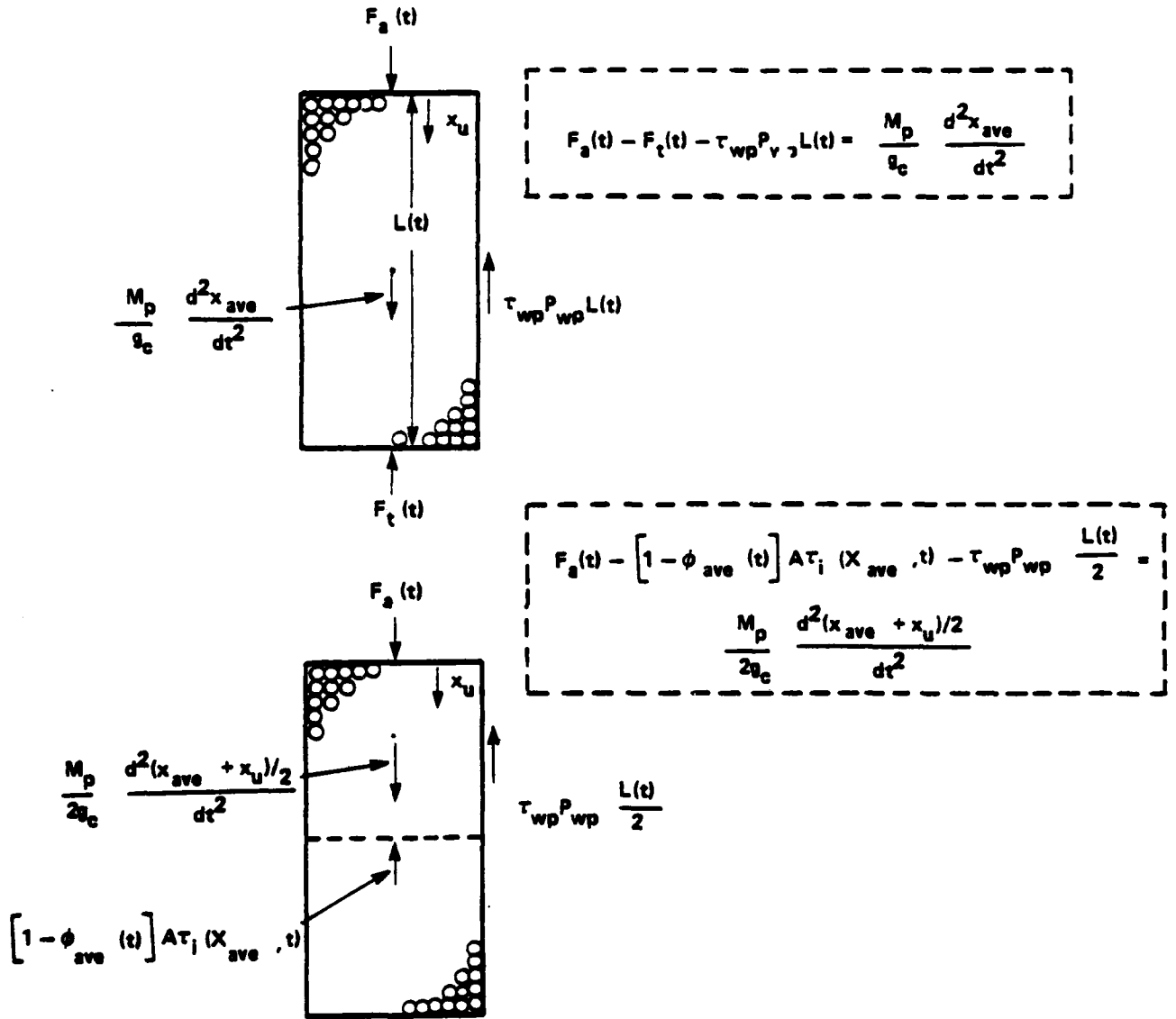
$$\tau_{wp} P_{wp} = \frac{F_a - F_t}{L}, \quad (6)$$

where  $F_t$  is the force transmitted to the bottom ram.

From this, the so-called particle-wall friction parameter ( $\tau_{wp} P_{wp} / \pi D$ ) is easily calculated, having units of stress. In calculating this quantity, the inner diameter of the mold,  $D$ , is assumed to be constant. In Figure 4,  $M_p$  is the total mass of the porous bed,  $x_u$  is the axial location of the upper porous bed-ram interface,  $x_{ave}$  is the axial location of the midplane of the porous bed,  $t$  is time, and  $g_c$  is the appropriate unit conversion factor.

---

<sup>4</sup>Kuo, Moore, and Yang, pp. 559-581.



(TAKEN FROM KUO, MOORE, AND YANG<sup>4</sup>)

FIGURE 4. FREE-BODY DIAGRAMS WITH FORCE BALANCES FOR THE COMPACTION OF POROUS BEDS

B. ANALYSIS ALLOWING  $\tau_{wp} P_{wp}$  TO VARY WITH POROUS BED LENGTH (NSWC I ANALYSIS)

The previous analysis has made several assumptions. One is that the quantity  $\tau_{wp} P_{wp}$  remains constant along the length of the porous bed, and clearly this is not physically realistic. An attempt was made to calculate intragranular stress and particle-wall friction parameter without introducing this simplification.<sup>6</sup> Neglecting the acceleration term, the top force balance appearing in Figure 4 is modified to be

$$F_a - F = \int_0^L \tau_{wp} P_{wp} dt, \quad (7)$$

where  $F$  is the axial force at  $l$  and  $\tau_{wp} P_{wp}$  is allowed to vary with  $l$  in an unspecified manner. To evaluate this integral the analysis that follows was performed. From plots of the semilogarithmic variation of transmitted force versus bed length made at essentially constant applied force (Figures 5 and 6), the following relation is observed

$$F_t = F_a e^{-K_1 L} \quad (8a)$$

Based on this, it is assumed\* that the axial force distribution for a given compacted bed is

$$F_t = F_a e^{-K_1 l} \quad (8b)$$

Substituting this expression into Equation (7) and differentiating the resultant integral equation yields

$$\tau_{wp} P_{wp} = K_1 F_a e^{-K_1 l} \quad (9)$$

The intragranular stress at the midplane (i.e.,  $l = L/2$ ) now becomes

$$\tau_i = \frac{F_a e^{-K_1 L/2}}{A(1-\phi_{ave})} \quad (10)$$

<sup>6</sup>Sandusky, Elban, Kim, Bernecker, Gross, and Clairmont, pp. 843-856.

\*This results in a constant proportionality between  $\tau_{wp} P_{wp}$  and the normal stress,  $\sigma$ , which was assumed by Burchett, Birnbaum, and Oien.<sup>5</sup> More detail regarding their analysis and its application to the compaction data for Teflon 7C and melamine will follow.

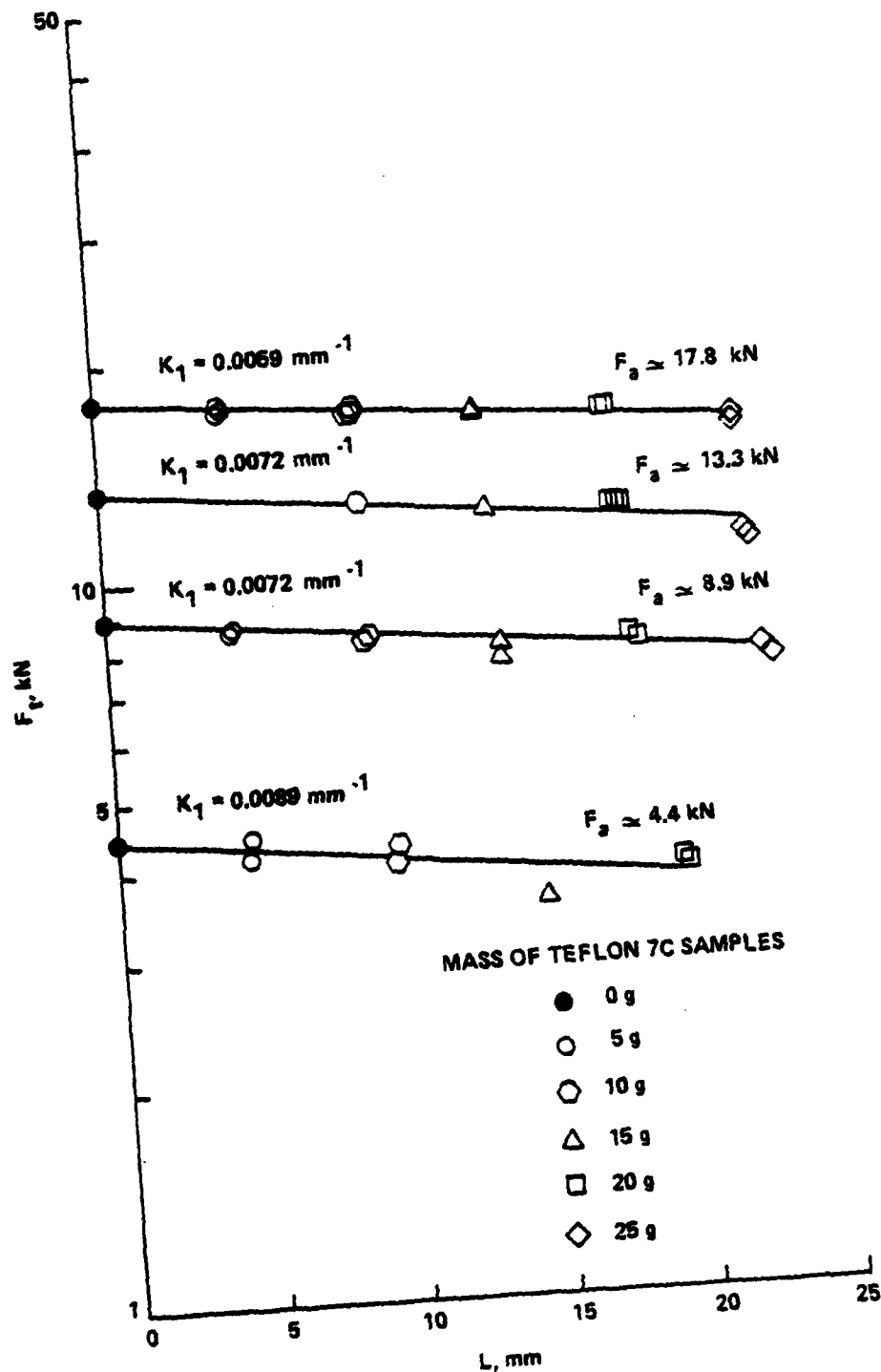


FIGURE 5. SEMILOGARITHMIC VARIATION OF TRANSMITTED FORCE VERSUS BED LENGTH AT CONSTANT APPLIED FORCE FOR COMPACTED TEFLON 7C

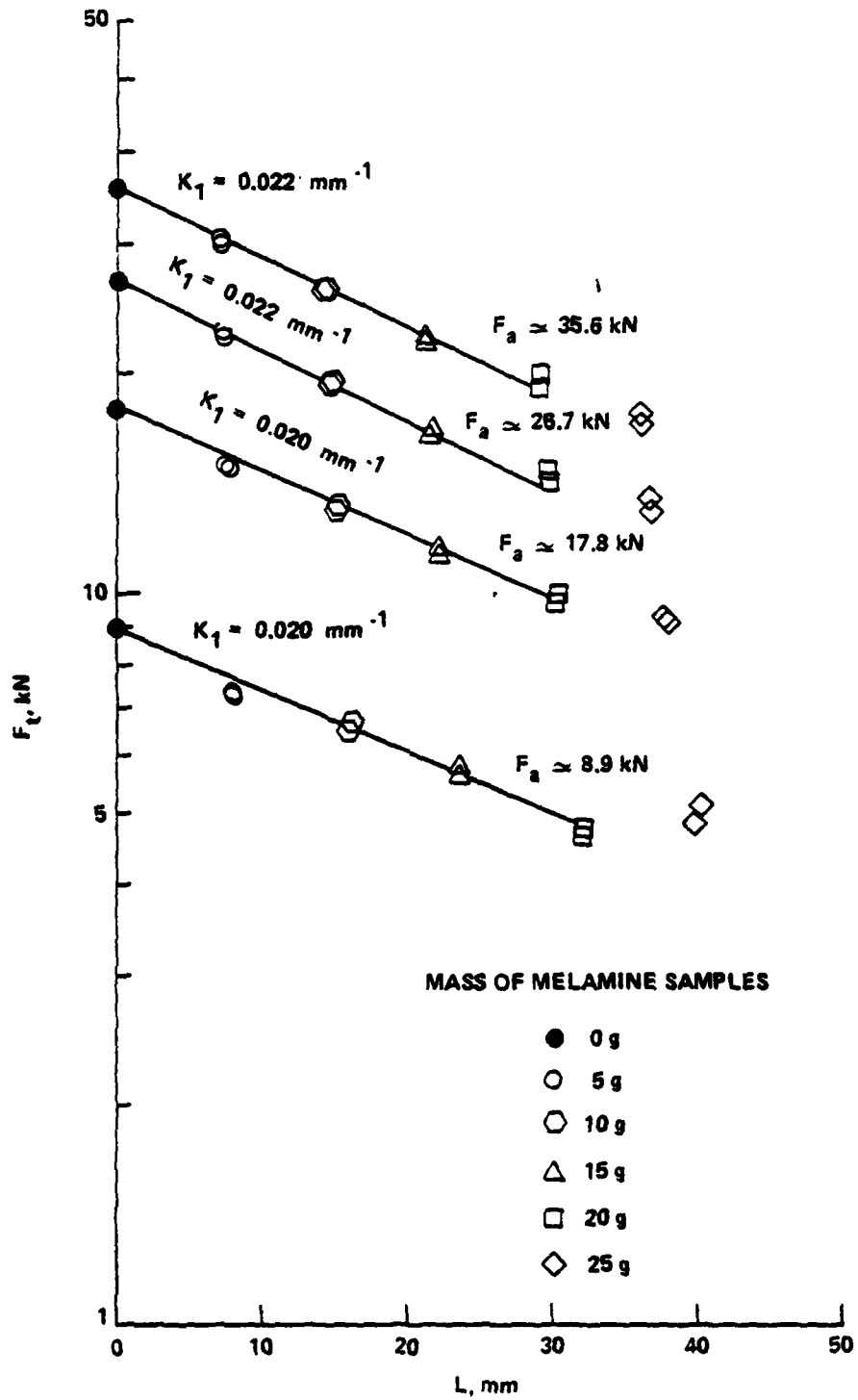


FIGURE 8. SEMILOGARITHMIC VARIATION OF TRANSMITTED FORCE VERSUS BED LENGTH AT CONSTANT APPLIED FORCE FOR COMPACTED MELAMINE

C. ANALYSIS BY DIVIDING THE POROUS BED INTO INCREMENTS (NSWC II ANALYSIS)

The first two analyses assume that the axial density (or % TMD) profile in the compacted bed is linear. This is reasonable if the L/D ratio is small or alternatively, if the frictional stress itself is small. Separately, there is the question of what complications arise from failing to account for the radial stress distribution that exists in the compacted column because of the top and bottom porous bed-ram interfaces. The effect of radial stress distribution is ignored in all of this work except to say that it would be more pronounced in the shorter columns of material. Thus, it is desirable to devise an additional analytic scheme,<sup>22</sup> without assuming a linear density profile, for treating longer columns of compacted material where the effect of the radial stress distribution would be reduced. Developing a refined analysis for longer porous beds is also important because of the obvious shortcoming in using the NSWC I analysis for the 25 g melamine data. That is, this data did not follow (Figure 6) the exponential dependency observed for the other melamine samples and hence could not be analyzed by this method.

However, refining the analysis to allow for a non-linear axial density distribution, while determining the axial stress gradient, poses a difficult problem since only three parameters ( $F_a$ ,  $F_t$ , and  $L$ ) were measured in the compaction experiments. A definite resolution of the stress and density distributions is not possible without additional approximations in the analytic scheme. Considering the porous bed to be divided into a number of small axial increments, it is assumed that each increment will have the same  $F_t/F_a$  ratio as long as the mass of each increment is constant (Figure 7). This is reasonable because of the linear relationship that was measured (next section of this report) between the axial transmitted and axial applied forces for both Teflon 7C and melamine. Thus, it is expected that all of the increments of the same mass will behave similarly in the compaction of a long column comprised of these increments. It is now possible to generate an unambiguous axial force profile given by

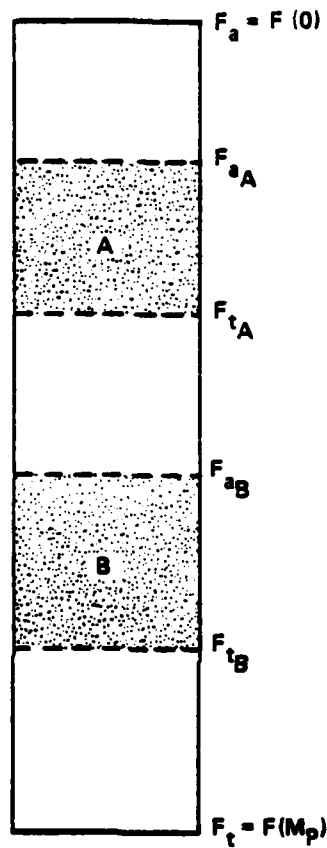
$$F(m) = F_a \left( \frac{F_t}{F_a} \right)^{\frac{m}{M_p}}, \quad (11)$$

where  $M_p$  is the mass of the total column, and  $m$  is the mass coordinate taken from the top face (Figure 7). Therefore,

$$F(0) = F_a \text{ and} \quad (12a)$$

$$F(M_p) = F_t. \quad (12b)$$

<sup>22</sup>Kim, K., "Incremental Data Reduction Method for Static Compaction Experiments," presented at 1982 JANNAF Propulsion Systems Hazards Meeting, 19-21 Apr 1982, China Lake, CA.



$$\frac{F_{tA}}{F_{aA}} = \frac{F_{tB}}{F_{aB}}$$

WHEN THE MASSES OF INCREMENTS A AND B ARE EQUAL

FIGURE 7. SCHEMATIC OF INCREMENTALLY DIVIDED POROUS BED (NSWC II ANALYSIS)

An additional approximation is needed to generate the axial density profile. To achieve this, an approach was taken to "guess" initially a set of data points for the stress-density relationship and then to correct the set based on the measured parameters by successive iteration. The procedure is outlined as follows:

1. Selection of the Initial Approximation. Begin by choosing a stress-density profile in tabular form to serve as the first approximation. The stress-density profile obtained from either of the first two methods is a good candidate.

2. First Correction of the Initial Approximation. With the stress profile obtained previously using Equation (11) and the initial approximation for the stress-density profile, the corresponding increment heights are calculated and summed. This calculated total column height is compared with the measured L. A correction factor is calculated from

$$\alpha_c = \frac{\text{measured } L}{\text{calculated } L} \quad (13)$$

It is then assumed that this correction factor can be uniformly applied to each of the porous bed increments to obtain the first corrected density profile.

3. Additional Corrections. The above procedure can be continued as appropriate to further refine the density profile.

#### D. SECOND ANALYSIS BY DIVIDING THE POROUS BED INTO INCREMENTS (BURCHETT, BIRNBAUM, AND OIEN ANALYSIS)

A separate incremental analysis of the compaction of porous beds of palladium/aluminum powders has been reported by Burchett, Birnbaum, and Oien.<sup>5</sup> This analysis is based on having a suitable equation of state, which for the palladium/aluminum powder compaction data was found to be of the form

$$\sigma = \sigma_o \left[ 1 - \left( \frac{\alpha - 1}{\alpha_o - 1} \right)^a \right]^b \quad (14)$$

where  $a$ ,  $b$ , and  $\sigma_o$  are unknown parameters, and  $\alpha_o$  and  $\alpha$  are the initial porosity and the porosity at a particular normal stress  $\sigma$ , respectively. In this case, porosity is defined as the ratio of the void free reference density,  $\rho_r$  (or crystal density,  $\rho_c$ ), to the powder density,  $\rho$ . It is assumed that the powder has compacted isostatically. Since this approach has been discussed<sup>5</sup> in detail, only limited comments and equations will be given for the purposes of this work.

---

<sup>5</sup>Burchett, Birnbaum, and Oien, pp. 11-38.

A similar integral equation force balance to that of Equation (7) was used with the integrand being of the form  $\pi D f \sigma(Z)$ , where  $D$  is the mold inner diameter,  $f$  is the coefficient of friction between the mold and the powder, and  $\sigma$  varies with axial position,  $Z$ . Since the  $\sigma(Z)$  dependency was not determined experimentally and thus is unknown, this integral can not be evaluated directly either. The analysis proceeds by dividing the compacted powder of overall length  $L$  into  $n$  equal axial increments and by assuming a linear variation of  $\sigma$  through the axial increment. This allows the transmitted stress on the bottom ram,  $\sigma_t$ , to be given in terms of the applied stress on the top ram,  $\sigma_a$ , as

$$\sigma_t = \sigma_a \left( \frac{nD - 2Lf}{nD + 2Lf} \right)^n, \quad (15)$$

which can be solved for  $f$  to yield

$$f = \frac{nD}{2L} \frac{\left[ 1 - \left( \frac{\sigma_t}{\sigma_a} \right)^{1/n} \right]}{\left[ 1 + \left( \frac{\sigma_t}{\sigma_a} \right)^{1/n} \right]}. \quad (16)$$

For the  $j^{\text{th}}$  increment, Equation (14) can be manipulated to give

$$\frac{\rho_j}{\rho_r} = \frac{1}{1 + (\alpha_0 - 1) \left[ 1 - \left( \frac{\sigma_j}{\sigma_0} \right)^{1/b} \right]^{1/a}}, \quad (17)$$

where

$$\sigma_j = \sigma_a \left( \frac{nD - 2Lf}{nD + 2Lf} \right)^j. \quad (18)$$

Thus, determining correct values of  $a$ ,  $b$ , and  $\sigma_0$  for the compaction data of interest allows, for comparison with the other three analytic approaches used in this work, the calculation of the intragranular stress at the midplane (i.e.,  $\tau_i = \sigma_j / (1 - \phi_{\text{ave}})$  where  $j = n/2$ ) as a function of density or % TMD ( $100\rho_{n/2}/\rho_r$ ) at the midplane.

## V. RESULTS AND DISCUSSION

A. TEFLON 7C COMPACTION

1. Preliminary Single Force Measurements. The variation of applied stress with % TMD for compacting 8 and 16 g of Teflon 7C powder in steel and Lexan molds appears in Figure 8. The effect of friction at the particle-wall interface appears to be manifested, particularly at the higher stress levels, by the lower density achieved in the 16 g experiment relative to the 8 g experiment. This was observed to be the case for both molds. Similar behavior was observed in comparing the results for the two different molds. Higher densities at constant applied stress were achieved in the steel mold; this is attributed to the smoother inside surface finish of the steel mold since the opposite trend should occur if only the elastic deformation of the two mold materials is considered.

In studying Figure 8, it is difficult to determine whether any change in compaction mechanism has occurred. However, Donachie and Burr<sup>23</sup> have addressed this in considerable detail in their investigation on compacting copper powder. A semilogarithmic plot of compaction pressure versus % relative void content was found to be an advantageous way of presenting the data to elucidate changes in compaction mechanisms. A similar type plot ( $\tau_i$  versus % TMD) was adopted in this work. With the help of microhardness measurements and metallographic examination, three distinct stages were identified<sup>23</sup> to occur during compaction as follows:

- I. transitional restacking (particles flowing past one another without significant plastic deformation)
- II. plastic deformation of particles
- III. cold working with or without particle fragmentation.

It is clear that since transitional restacking only involved relative shifting of particles in the absence of plastic deformation, porous beds compacted during this stage lacked appreciable mechanical strength and reverted back to powder in an unconfined state. Following transitional restacking, the particles became fixed in their positions and began to deform plastically to fill the voids in the bed. During the plastic deformation stage, interparticle bonds develop giving a coherent body that could be removed from the mold intact and be handled.

---

<sup>23</sup>Donachie, M. J., and Burr, M. F., "Effects of Pressing of Metal Powders," Journal of Metals, Vol. 15, No. 7, 1963, pp. 849-854.

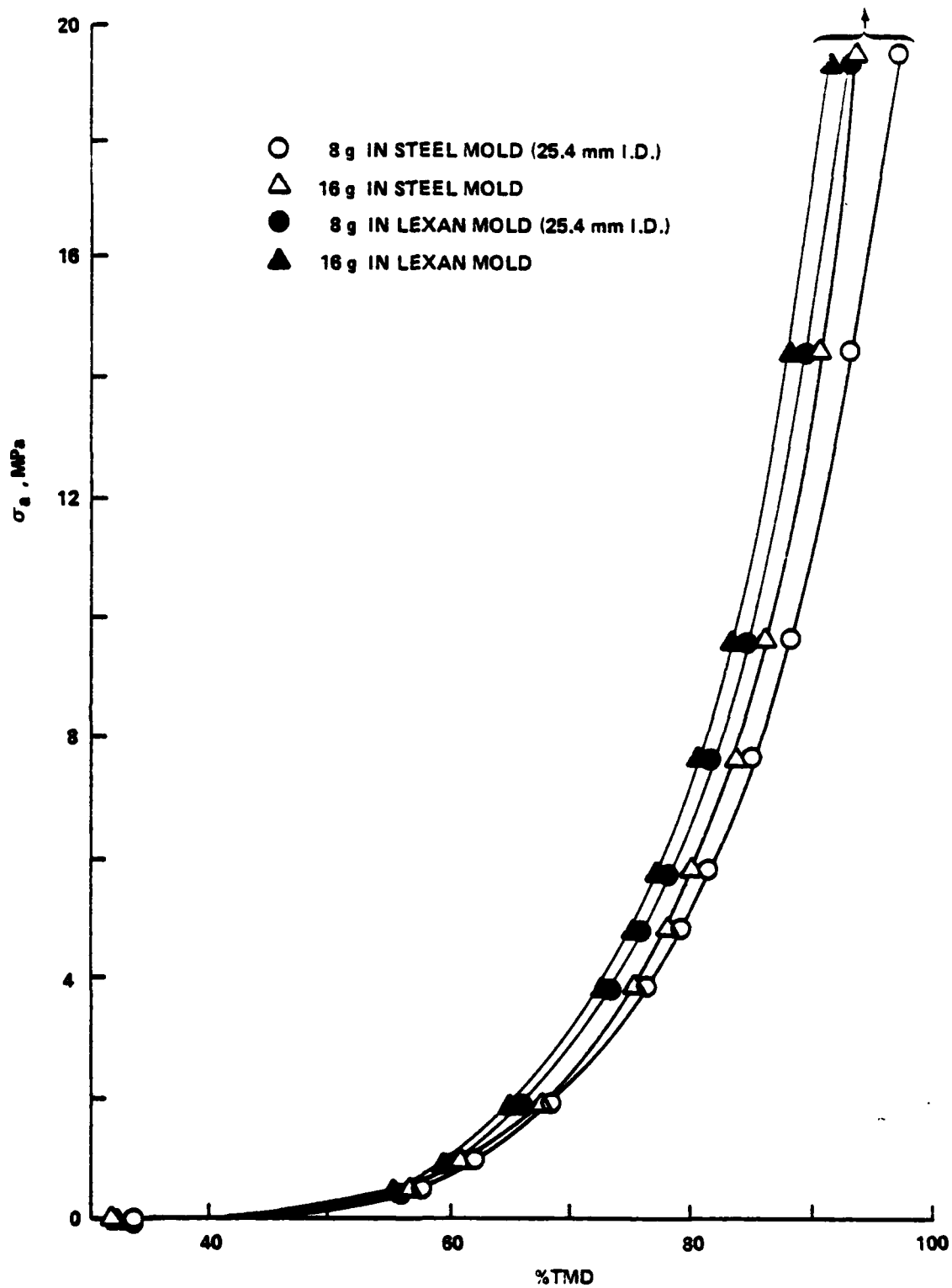


FIGURE 8. APPLIED STRESS VERSUS %TMD FOR COMPACTED TEFLON 7C

Additional discussion on these three mechanisms of compaction for several types of materials was presented by Clyens and Johnson,<sup>24</sup> who emphasized that several mechanisms can occur simultaneously. Indeed, depending on the mechanical properties of the powder some may be virtually missing. For highly ductile materials, stages I and III would not be very important, while stage II would not be significant for hard, brittle powders.

A plot of the semilogarithmic variation of applied stress versus % TMD (100-% relative void content) for 8 g of Teflon 7C powder compacted in the steel and Lexan molds appears in Figure 9. Two apparent stages of compaction (denoted I' and II') were found. However, these stages apparently do not correspond to stages I and II observed by Donachie and Burr,<sup>23</sup> since unconfined samples at 52.9 and 59.9% TMD did have sufficient strength to permit longitudinal sound velocity measurements (Appendix D), although they tended to crumble somewhat. Exactly what is happening microstructurally to the particles while the bed is being compacted during stages I' and II' was not determined, but it is certain that considerable plastic deformation is occurring.

Axial longitudinal sound velocity measurements were made on each compacted cylinder of Teflon 7C powder after removal from its mold, and these results are listed in Table D-5 in Appendix D. All of these cylinders were pressed to higher stress levels than what appears in Figure 8 before being tested ultrasonically. These values correlate well with the bare cylinder data (Appendix D) given in Table D-4 and simply extend the curve appearing in Figure D-4 to higher % TMD.

2. Two Force Measurements. Plots of transmitted force versus applied force and applied stress versus % TMD (an average quantity for the total sample) are given in Figures 10 and 11, respectively. Only one set of data each for the 5 (Run #54TF) and 25 (Run #68TF) g samples of Teflon 7C is included. For all of the Teflon 7C data (Appendix E) a highly linear relationship was found between the transmitted force and the applied force over the entire applied force range. Least squares analysis was performed on all of the data (Table 1) and for each individual experiment, the correlation coefficient, when used with the number of data points defining the straight line, gave a confidence level in excess of 99.99%. Similarly, a linear dependency has been reported in several studies on metal powders.<sup>20,21,25</sup> As observed for the preliminary single force measurements, the variation of applied stress versus % TMD is highly non-linear, being convex to the abscissa.

---

<sup>24</sup>Clyens, S., and Johnson, W., "The Dynamic Compaction of Powdered Materials," Materials Science and Engineering, Vol. 30, No. 2, 1977, pp. 121-139.

<sup>23</sup>Donachie, and Burr, pp. 849-854.

<sup>20</sup>Hausner, and Sheinhartz, pp. 6-27.

<sup>21</sup>Sheinhartz, McCullough, and Zambrow, pp. 515-518.

<sup>25</sup>Leopold, P. M., and Nelson, R. C., "The Effect of Die-Wall Lubrication and Admixed Lubricant on the Compaction of Sponge-Iron Powder 1. Effect of Lubrication on Powder Compaction," International Journal of Powder Metallurgy, Vol. 1, No. 3, 1965, pp. 37-44.

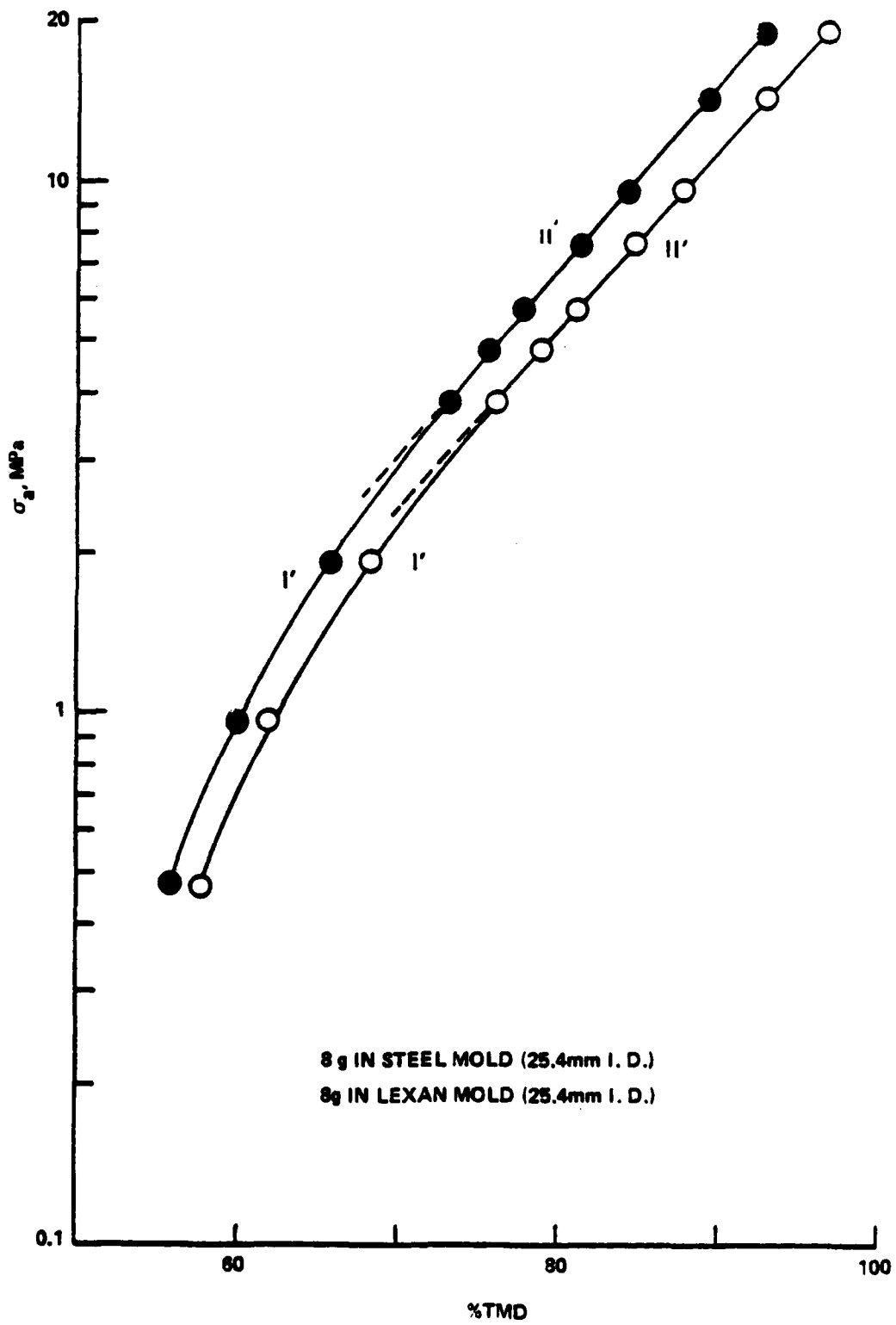


FIGURE 9. SEMILOGARITHMIC VARIATION OF APPLIED STRESS VERSUS %TMD FOR COMPACTED TEFLON 7C

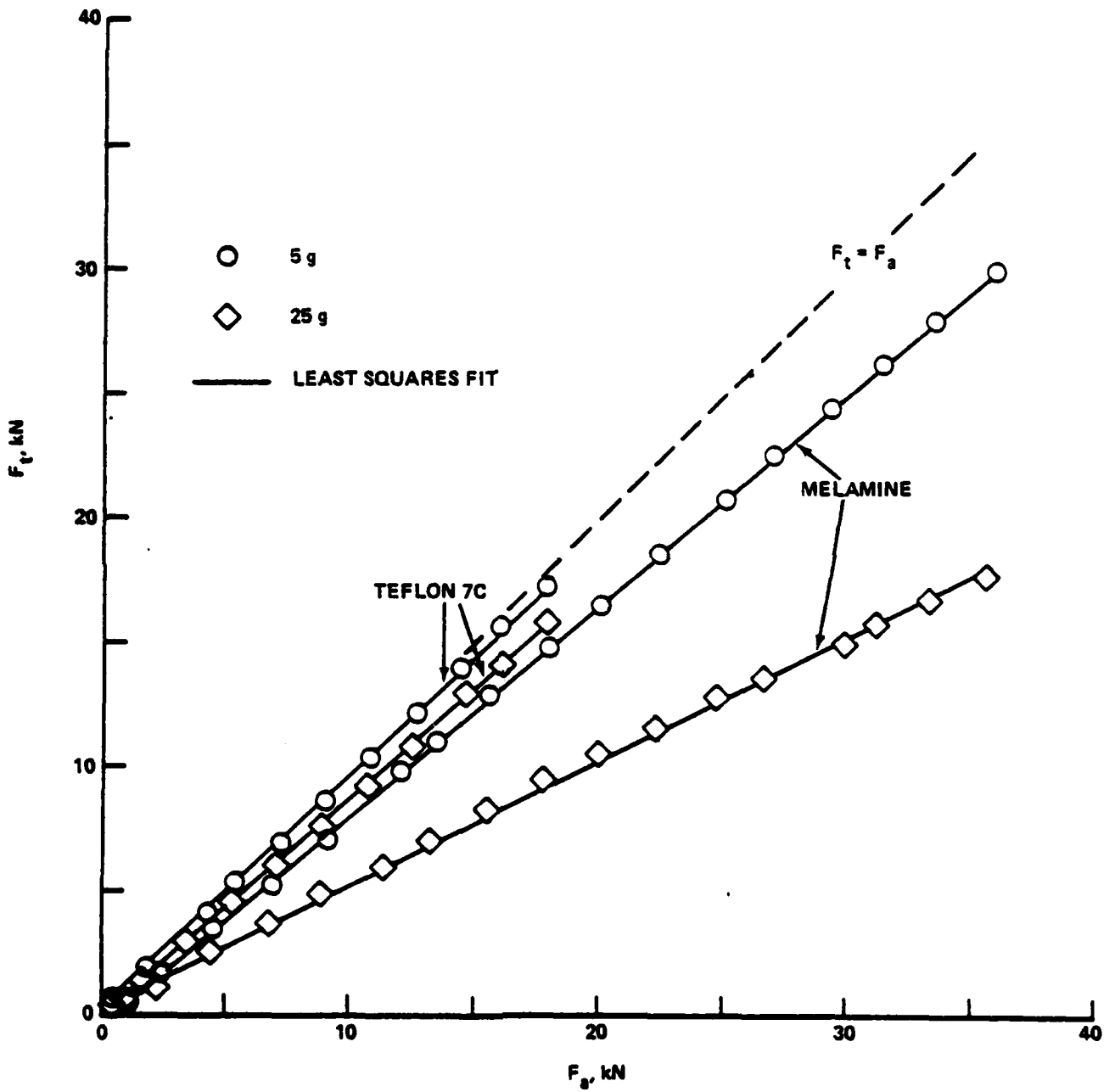


FIGURE 10. TRANSMITTED FORCE VERSUS APPLIED FORCE FOR COMPACTED TEFLON 7C AND MELAMINE

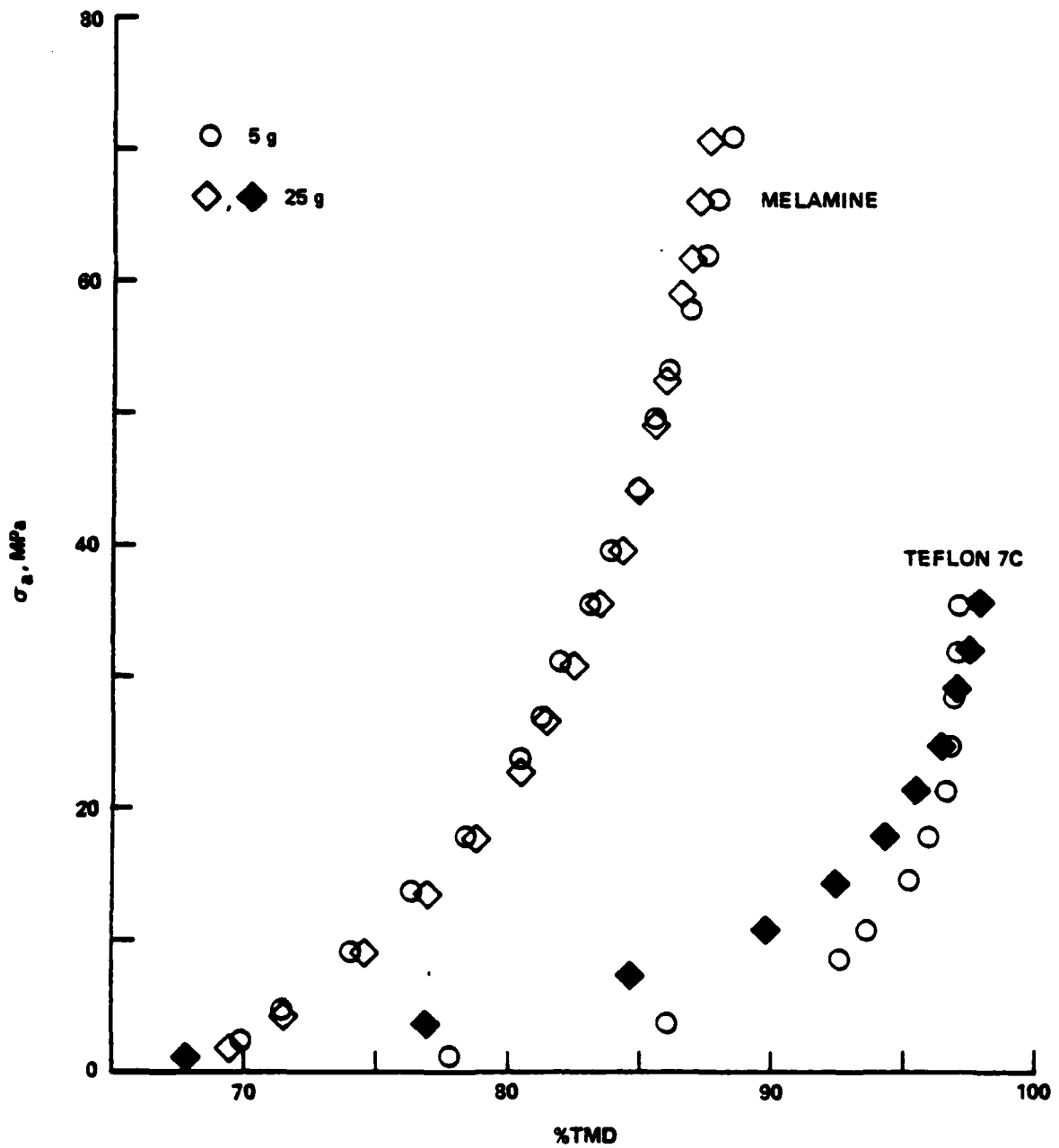


FIGURE 11. APPLIED STRESS VERSUS %TMD FOR COMPACTED TEFLON 7C AND MELAMINE

TABLE 1. LEAST SQUARES ANALYSES OF THE LINEAR  $F_t - F_a$  DEPENDENCY FOR COMPACTED TEFLON 7C

| <u>Sample Mass*, g</u> | <u>Run Number</u> | <u>Slope</u> | <u>Intercept, kN</u> | <u>Correlation Coefficient</u> |
|------------------------|-------------------|--------------|----------------------|--------------------------------|
| 5                      | 54TF              | 0.963        | -0.083               | 0.999                          |
|                        | 57TF              | 0.966        | -0.083               | 0.999                          |
|                        | 59TF              | 0.966        | -0.050               | 0.999                          |
| 10                     | 60TF              | 0.936        | -0.207               | 0.999                          |
|                        | 61TF              | 0.919        | -0.191               | 0.999                          |
|                        | 83TF              | 0.950        | -0.165               | 0.999                          |
|                        | 84TF              | 0.942        | -0.054               | 0.999                          |
| 15                     | 62TF              | 0.913        | -0.238               | 0.999                          |
|                        | 70TF              | 0.921        | -0.328               | 0.999                          |
| 20                     | 65TF              | 0.919        | -0.113               | 0.999                          |
|                        | 66TF              | 0.918        | -0.148               | 0.999                          |
|                        | 85TF              | 0.898        | -0.116               | 0.999                          |
|                        | 86TF              | 0.901        | -0.159               | 0.999                          |
| 25                     | 68TF              | 0.875        | -0.372               | 0.999                          |
|                        | 69TF              | 0.887        | -0.250               | 0.999                          |

\*The initial L/D ratio ranged from 0.22 for the 5 g samples to 1.3 for the 25 g samples. These values for Teflon 7C compare to an initial L/D ratio of about 2.7 for the two ball propellants studied by Kuo, Moore, and Yang.<sup>4</sup>

A portion of the Teflon 7C compaction data (one complete experiment each for the 5, 15, and 25 g samples) was first analyzed according to the method described by Kuo, Moore, and Yang.<sup>4</sup> Semilogarithmic plots of intragranular stress and particle-wall friction parameter versus % TMD are given in Figure 12. Some observations concerning these plots appear in Table 2. Perhaps most important is the small value, not exceeding 0.079, of the  $(\tau_{wp} P_{wp}/\pi D)/\tau_i$  ratio. This is consistent with the well-known lubrication qualities of Teflon.

As mentioned previously, it is assumed in the Kuo, Moore, and Yang analysis that the radial and axial density variations in the compacted sample are minimal and that these densities can be represented properly by average values (Equation (5)). To assess the radial gradient present, microhardness<sup>26</sup> experiments were performed on two highly compacted samples (% TMD > 95) of Teflon 7C. The results from this work are described in Appendix F. The hardness was found to increase in the annular region near the circumference of the sample. It would be interesting to perform similar experiments on lower % TMD samples. In addition, Shore hardness measurements were made on a number of compacted Teflon 7C samples having densities ranging from 52 to 97% TMD. These results are also given in Appendix F.

The same Teflon 7C compaction data was also analyzed<sup>6</sup> using the NSWC I method in which  $\tau_{wp} P_{wp}$  is allowed to vary along the length of the porous bed. Appearing in Figure 13 are semilogarithmic plots of intragranular stress and particle-wall friction parameter versus % TMD that were obtained from averaging the  $K_1$  values in Figure 5. Some observations concerning these plots are found in Table 3. With the NSWC I analysis, the value of the  $(\tau_{wp} P_{wp}/\pi D)/\tau_i$  ratio was more regular and did not exceed 0.045.

Although the observations given in Tables 2 and 3 are comparable qualitatively, some quantitative variation does exist in the intragranular stress values computed by the two approaches for compaction of Teflon 7C. Various % differences are listed in Table 4. The maximum difference occurs at the lowest applied force levels, and the difference tends to a minimum as the applied force is increased, indicating that any density gradients that occur during the early stages of compaction are being diminished as the % TMD is increased. Rather small "representative" % differences are obtained from the two methods of analysis. This suggests that the invariant  $\tau_{wp} P_{wp}$  assumption<sup>4</sup> is quite adequate for analyzing the Teflon 7C compaction data, especially since the magnitude of  $\tau_{wp} P_{wp}$  is so small.

---

<sup>4</sup>Kuo, Moore, and Yang, pp. 559-581.

<sup>26</sup>Westbrook, J. H., and Conrad, H., eds. The Science of Hardness Testing and Its Research Applications (Metals Park, Ohio: American Society for Metals, 1973).

<sup>6</sup>Sandusky, Elban, Kim, Bernecker, Gross, and Clairmont, pp. 843-856.

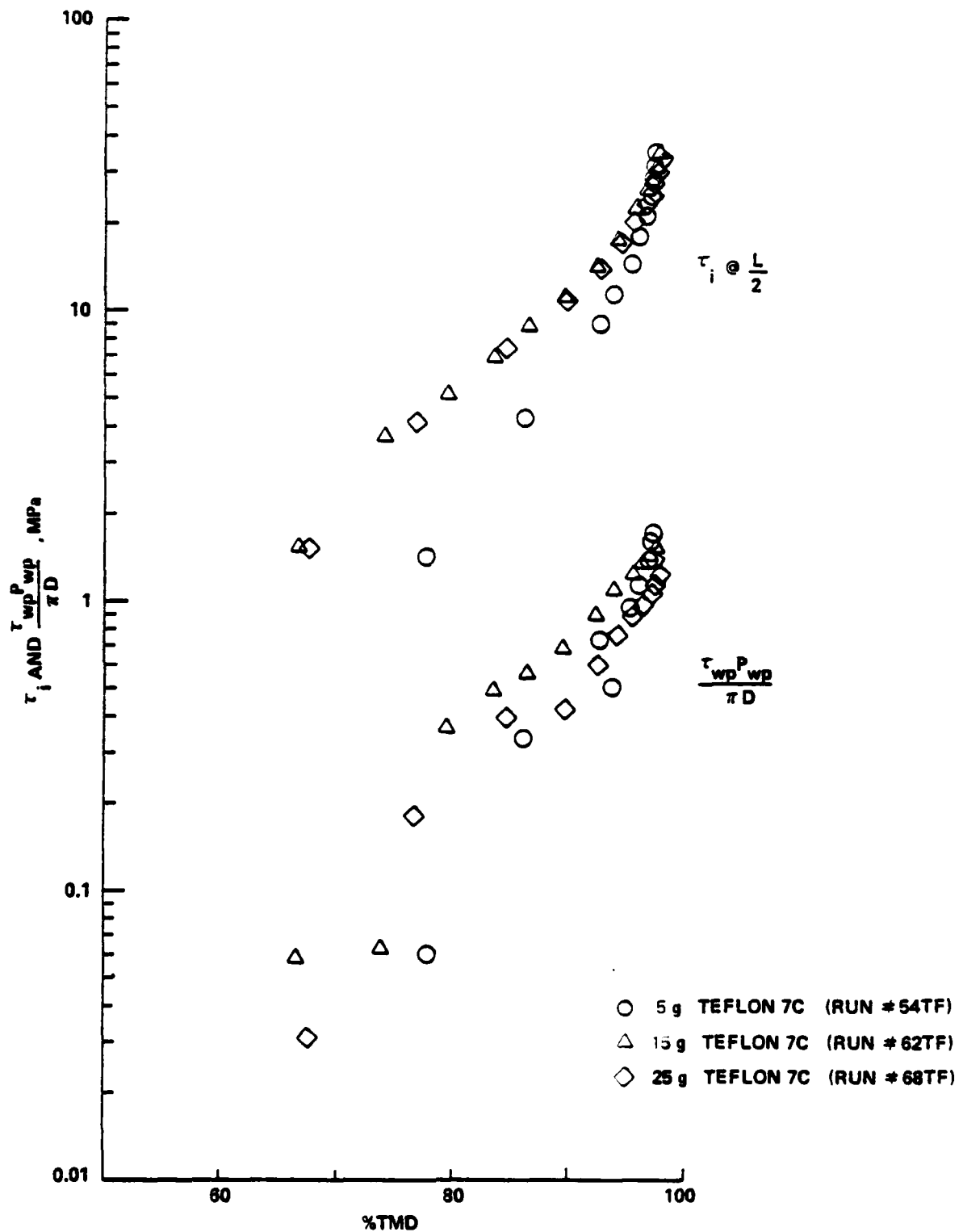


FIGURE 12. SEMILOGARITHMIC VARIATION OF INTRAGRANULAR STRESS AND PARTICLE-WALL FRICTION PARAMETER VERSUS %TMD FOR COMPACTED TEFLON 7C USING KUO, MOORE, AND YANG ANALYSIS

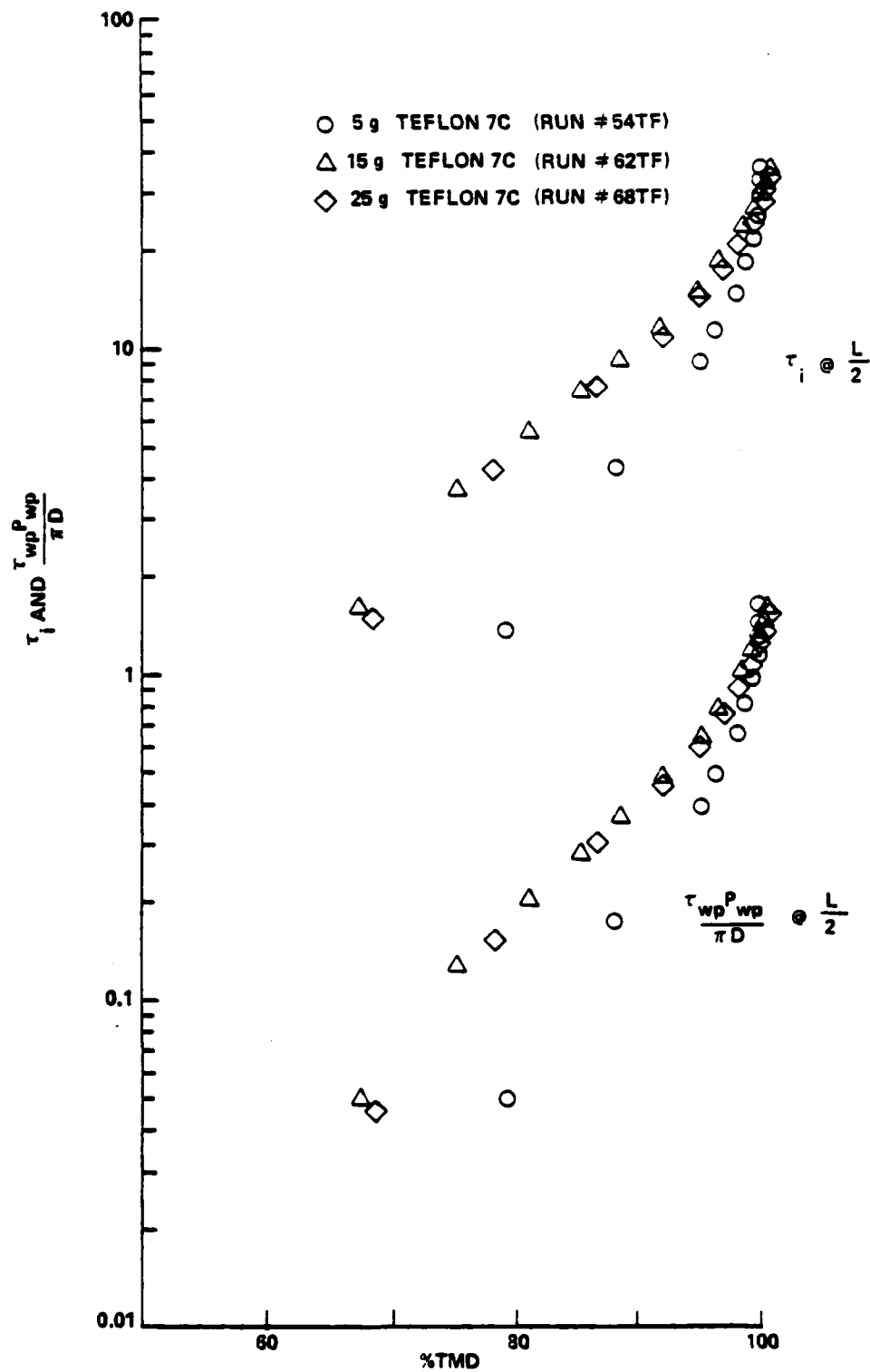


FIGURE 13. SEMILOGARITHMIC VARIATION OF INTRAGRANULAR STRESS AND PARTICLE-WALL FRICTION PARAMETER VERSUS %TMD FOR COMPACTED TEFLON 7C USING NSWC I ANALYSIS

TABLE 2. OBSERVATIONS FROM KUO, MOORE, AND YANG ANALYSIS  
OF TEFLON 7C COMPACTION DATA

|                                  |  |
|----------------------------------|--|
| Ordering of $\tau_i$             | 5 g < 25 g < 15 g @ Constant<br>% TMD <~97       |
|                                  | 25 g < 5 g < 15 g @ Constant<br>% TMD >~97       |
| Appearance of<br>$\tau_i$ Curves | Spread Out and Merging Together<br>at % TMD > 96 |
| $(\tau_{wp}P_{wp}/\pi D)/\tau_i$ |  |
| 5 g                              | 0.045 + 0.079                                    |
| 15 g                             | 0.017 + 0.071                                    |
| 25 g                             | 0.021 + 0.053                                    |

TABLE 3. OBSERVATIONS FROM NSWC I ANALYSIS  
OF TEFLON 7C COMPACTION DATA

|                                  |  |
|----------------------------------|--|
| Ordering of $\tau_i$             | Same as for Kuo, Moore, and<br>Yang Analysis |
| Appearance of<br>$\tau_i$ curves | Same as for Kuo, Moore, and<br>Yang Analysis |
| $(\tau_{wp}P_{wp}/\pi D)/\tau_i$ |  |
| 5 g                              | 0.036 + 0.045                                |
| 15 g                             | 0.031 + 0.045                                |
| 25 g                             | 0.032 + 0.045                                |

TABLE 4. DIFFERENCES IN INTRAGRANULAR STRESS VALUES COMPUTED FROM KUO, MOORE, AND YANG ANALYSIS AND FROM NSWC I ANALYSIS OF TEFLON 7C COMPACTION DATA

| <u>Sample Mass, g</u> | <u>Maximum</u> | <u>% Difference</u><br><u>Minimum</u> | <u>"Representative"</u> |
|-----------------------|----------------|---------------------------------------|-------------------------|
| 5                     | 4.3            | 0.04                                  | 0.1 → 1                 |
| 15                    | 4.9            | 0.2                                   | 0.2 → 3                 |
| 25                    | 4.2            | 0.2                                   | 0.4 → 2                 |

No attempt was made to calculate the intragranular stress from the Teflon 7C compaction data using the first incremental (NSWC II) analytic method because of the very small wall friction contribution. However, the 25 g Teflon 7C compaction data treated previously was analyzed by the incremental method of Burchett, Birnbaum, and Oien.<sup>5</sup> Intragranular stress values (at the midplane) obtained using Equations (16) and (18) appear in Table E-11 and, with a few exceptions, are the same as those values calculated by the Kuo, Moore, and Yang method. The values of the coefficient of friction between the steel mold and the compacted powder calculated using Equation (16) varied from 0.03 to 0.06 (0.04 for the 97.9% TMD sample) and are in excellent agreement with the static coefficient of friction value<sup>27</sup> of 0.04 for solid Teflon polymer (polytetrafluorethylene) on steel. An attempt was also made to fit this 25 g compaction data to the equation of state given in Equation (14) that had been found to be suitable for describing the compaction of palladium/aluminum powders. This resulted in values for the unknown parameters of  $a = -0.887$ ,  $b = 0.697$ , and  $\sigma_0 = 5.16$  MPa. Thus, it was determined that this equation of state was not appropriate for the Teflon 7C compaction data.

## B. MELAMINE COMPACTION

1. Two Force Measurements. Plots of transmitted force versus applied force and applied stress versus % TMD for a representative set of 5 (Run #72TF) and 25 (Run #82TF) g melamine compaction data are included in Figures 10 and 11, respectively. As was the case for compacted Teflon 7C, a highly linear relationship was found between the transmitted force and the applied force over the entire applied force range for all of the melamine compaction data (Appendix E). The results from a least squares analysis of the various experimental runs appear in Table 5 and give a confidence level (except for the first 25 g data set) in excess of 99.99% for a linear transmitted force-applied force dependency. As with compacting Teflon 7C, the variation of applied stress versus % TMD for compacting melamine is highly non-linear, being convex to the abscissa. The separation in the Teflon 7C and melamine curves in Figure 11 demonstrates clearly the difficulty encountered in compacting melamine powder as compared to Teflon 7C powder. An applied stress of about 35 MPa compacted Teflon 7C samples in excess of 97% TMD, whereas doubling the applied stress to about 70 MPa could only compact melamine to 87 or 88% TMD.

Analogous to analyzing the Teflon 7C compaction data, one complete experiment each for the 5, 15 and 25 g samples of melamine was first treated using the method detailed by Kuo, Moore, and Yang.<sup>4</sup> Semilogarithmic plots of intragranular stress and particle-wall friction parameter versus % TMD are given in Figure 14. Some observations regarding these plots are given in Table 6. Compared to Teflon 7C, the  $(\tau_{wp}P_{wp}/\pi D)/\tau_i$  ratio for melamine was larger.

<sup>5</sup>Burchett, Birnbaum, and Oien, pp. 11-38.

<sup>27</sup>Hodgman, C. D., Weast, R. C., Shankland, R. S., and Selby, S. M., eds., Handbook of Chemistry and Physics (Cleveland: Chemical Rubber Publishing Co., 1963), p. 2221.

<sup>4</sup>Kuo, Moore, and Yang, pp. 559-581.

TABLE 5. LEAST SQUARES ANALYSES OF THE LINEAR  $F_t - F_a$  DEPENDENCY FOR COMPACTED MELAMINE

| <u>Sample Mass*, g</u> | <u>Run Number</u> | <u>Slope</u> | <u>Intercept, kN</u> | <u>Correlation Coefficient</u> |
|------------------------|-------------------|--------------|----------------------|--------------------------------|
| 5                      | 72TF              | 0.850        | -0.445               | 0.999                          |
|                        | 73TF              | 0.853        | -0.357               | 0.999                          |
| 10                     | 74TF              | 0.724        | 0.190                | 0.999                          |
|                        | 75TF              | 0.734        | -0.119               | 0.999                          |
| 15                     | 76TF              | 0.624        | 0.218                | 0.999                          |
|                        | 77TF              | 0.641        | -0.208               | 0.999                          |
| 20                     | 78TF              | 0.544        | -0.106               | 0.999                          |
|                        | 79TF              | 0.568        | -0.269               | 0.999                          |
| 25                     | 80TF              | 0.466        | 0.652                | 0.997                          |
|                        | 82TF              | 0.496        | 0.367                | 0.999                          |

---

\*The initial L/D ratio ranged from 0.35 for the 5 g samples to 1.8 for the 25 g samples. These values for melamine compare to an initial L/D ratio of about 2.7 for the two ball propellants studied by Kuo, Moore, and Yang.<sup>4</sup>

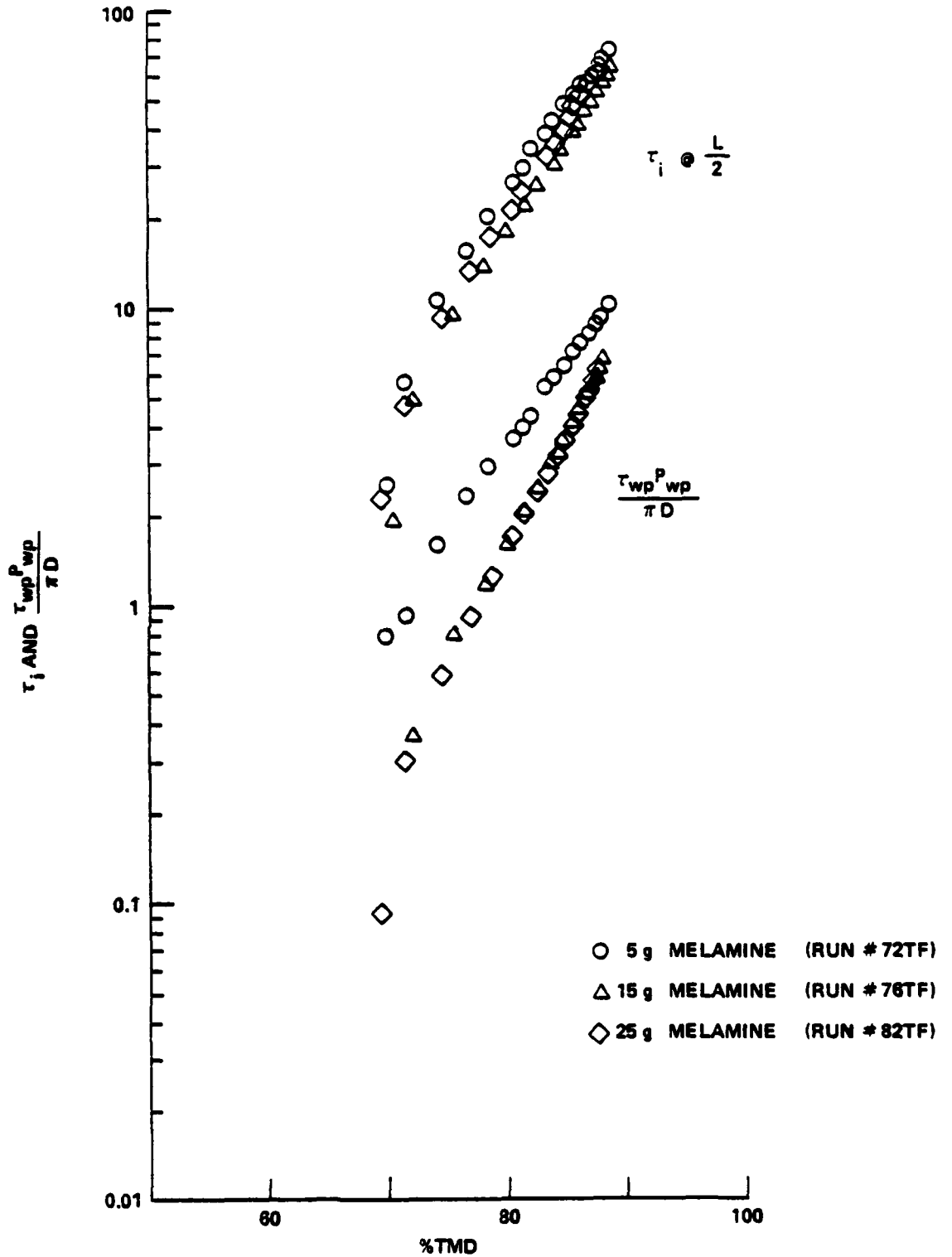


FIGURE 14. SEMILOGARITHMIC VARIATION OF INTRAGRANULAR STRESS AND PARTICLE-WALL FRICTION PARAMETER VERSUS %TMD FOR COMPACTED MELAMINE USING KUO, MOORE, AND YANG ANALYSIS

TABLE 6. OBSERVATIONS FROM KUO, MOORE, AND YANG ANALYSIS OF MELAMINE COMPACTION DATA

|                                  |                                    |
|----------------------------------|------------------------------------|
| Ordering of $\tau_i$             | 15 g < 25 g < 5 g @ Constant % TMD |
| Appearance of $\tau_i$ Curves    | Roughly Parallel                   |
| $(\tau_{wp}P_{wp}/\pi D)/\tau_i$ |                                    |
| 5 g                              | 0.13 + 0.31                        |
| 15 g                             | 0.04 + 0.12                        |
| 25 g                             | 0.04 + 0.10                        |

TABLE 7. OBSERVATIONS FROM NSWC I ANALYSIS OF MELAMINE COMPACTION DATA

|                                  |   |
|----------------------------------|---|
| Ordering of $\tau_i$             | Same as for Kuo, Moore, and Yang Analysis |
| Appearance of $\tau_i$ Curves    | Same as for Kuo, Moore, and Yang Analysis |
| $(\tau_{wp}P_{wp}/\pi D)/\tau_i$ |   |
| 5 g                              | 0.093 + 0.12                              |
| 15 g                             | 0.094 + 0.12                              |
| 25 g                             | Was Not Determined*                       |

\*Calculations were not performed for any 25 g melamine samples because the data did not follow the exponential dependency found in Figure 6.

The same melamine compaction data was next analyzed<sup>6</sup> using the NSWC I approach in which  $\tau_{wp}P_{wp}$  is allowed to vary along the porous bed length. Semilogarithmic plots of intragranular stress and particle-wall friction parameter versus % TMD are given in Figure 15. In analyzing the data in this manner, the  $K_1$  values appearing in Figure 6 were averaged. Calculations were not performed for the 25 g melamine sample because the data did not follow the exponential dependency found in Figure 6 for samples with lower masses. Some observations about these plots appear in Table 7. With the NSWC I analysis, the value of the  $(\tau_{wp}P_{wp}/\pi D)/\tau_i$  ratio was more regular. Various % differences in the intragranular stress values calculated by the first two approaches for the compaction of melamine are listed in Table 8. Reasonably small "representative" % differences are obtained. This indicates that the invariant  $\tau_{wp}P_{wp}$  assumption of Kuo, Moore, and Yang<sup>4</sup> is also satisfactory for analyzing the melamine compaction data. This is so because, even though compacting melamine exhibits a significantly larger wall effect than does Teflon 7C, the magnitude of the loss is still reasonably small, ranging from 0.07 to 0.27  $F_a$ .

Consistent with the linear region observed for Teflon 7C in Figures 12 and 13, the semilogarithmic variation of intragranular stress versus % TMD was also linear, say from 76 to at least 88% TMD. At constant % TMD, the magnitude of the intragranular stress for melamine exceeds that for Teflon 7C, except at the lowest % TMD level obtained. At least for the linear portions of the intragranular stress curves, the difference in magnitude increases with increasing % TMD. The appearance of the intragranular stress curves differs for Teflon 7C and melamine over the same range of % TMD. For Teflon 7C the 5 g curve is not parallel to the 15 and 25 g curves, while the 5 and 15 g curves for melamine are roughly parallel.

Using the first incremental (NSWC II) method of analysis,<sup>22</sup> intragranular stress values were also calculated (Table E-12) for the same 15 and 25 g melamine compaction data that had been analyzed by the Kuo, Moore, and Yang scheme. All of these values were lower (typically a few percent but by as much as ~11% for the 25 g sample at 87.6% TMD) compared to the values determined by the Kuo, Moore, and Yang scheme. Larger differences would result as the L/D ratio of the porous column increased.

The 15 g melamine compaction data treated by the first three analytic methods was also analyzed (Table E-12) by the incremental method of Burchett, Birnbaum, and Oien.<sup>5</sup> Compared to the intragranular stress values calculated by the Kuo, Moore, and Yang method, all of the values were slightly lower. Using Equation (16), the values of the coefficient of friction between the steel mold and the compacted powder increased from 0.06 at 70.5% TMD to 0.14 at 88.8% TMD. An attempt was also made to fit this 15 g compaction data to the equation of state given in Equation (14). The result was analogous to applying this

---

<sup>6</sup>Sandusky, Elban, Kim, Bernecker, Gross, and Clairmont, pp. 843-856.

<sup>4</sup>Kuo, Moore, and Yang, pp. 559-581.

<sup>22</sup>Kim.

<sup>5</sup>Burchett, Birnbaum, and Oien, pp. 11-38.

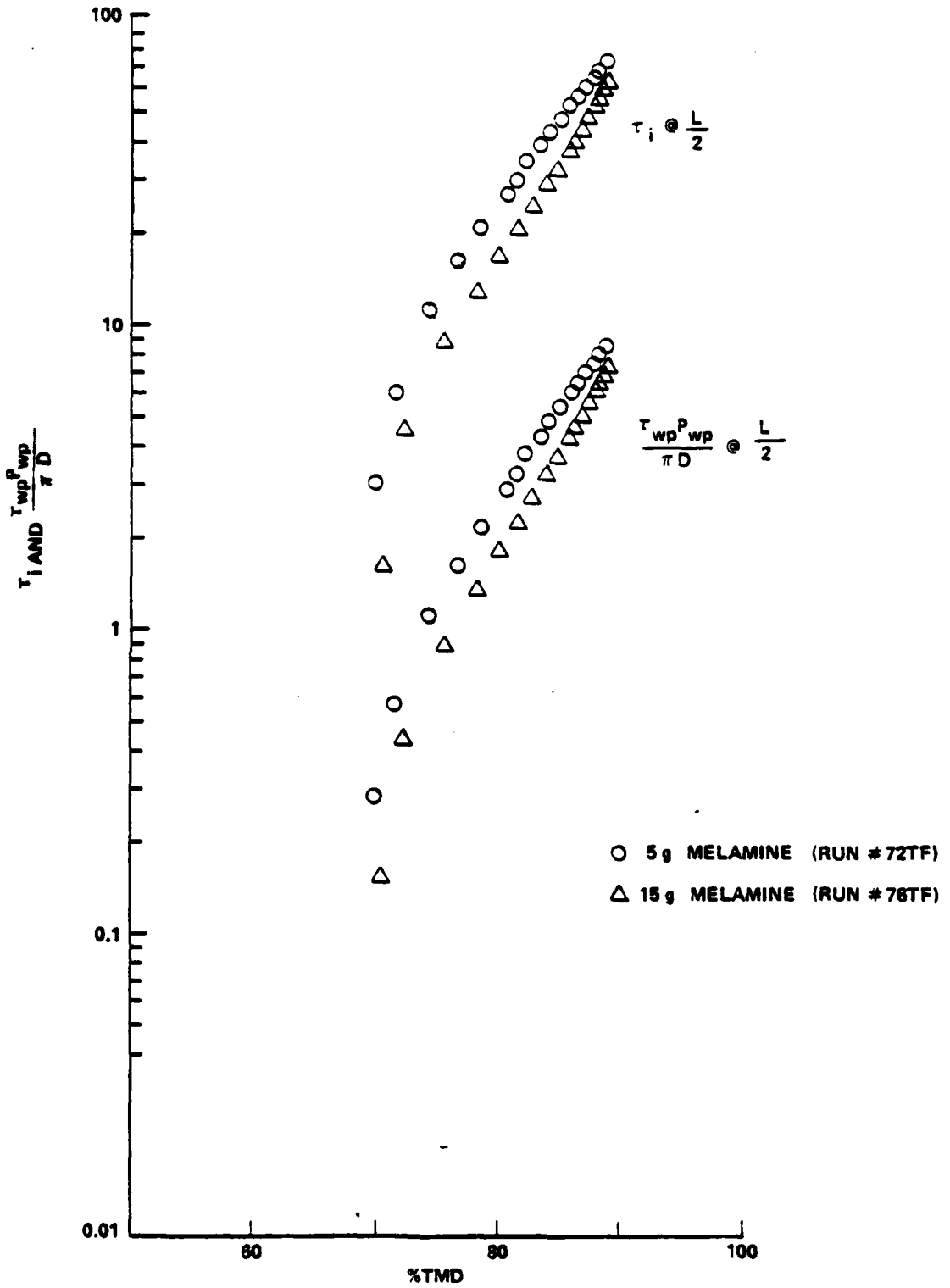


FIGURE 15. SEMILOGARITHMIC VARIATION OF INTRAGRANULAR STRESS AND PARTICLE-WALL FRICTION PARAMETER VERSUS %TMD FOR COMPACTED MELAMINE USING NSWC I ANALYSIS

TABLE 8. DIFFERENCES IN INTRAGRANULAR STRESS VALUES COMPUTED FROM KUO, MOORE, AND YANG ANALYSIS AND FROM NSWC I ANALYSIS OF MELAMINE COMPACTION DATA

| <u>Sample Mass, g</u> | <u>Maximum</u> | <u>% Difference</u><br><u>Minimum</u> | <u>"Representative"</u> |
|-----------------------|----------------|---------------------------------------|-------------------------|
| 5                     | 19.6           | 0.9                                   | 1 + 4                   |
| 15                    | 15.6           | 1.6                                   | 1 + 6                   |

expression to the 25 g Teflon 7C data. Values for the unknown parameters of  $a = -3.72$ ,  $b = 0.513$ , and  $\sigma_0 = 5.78$  MPa were obtained. Since the deformation properties of palladium/aluminum and melamine or Teflon 7C differ significantly, it is not surprising that an equation of state of the form found to be appropriate for describing palladium/aluminum powder compaction would not be satisfactory for the materials compacted in this work.

## VI. SUMMARY AND CONCLUSIONS

A compaction apparatus based on the work of other investigators was successfully used to compact two powdered inert materials, Teflon 7C and melamine. The apparatus is capable of making simultaneous applied force, transmitted force, and sample displacement measurements during the quasi-static compaction of porous beds of both inert and energetic materials (when the apparatus is operated remotely). These measurements permit the variation of transmitted versus applied force and of applied stress versus % TMD to be determined readily.

Extensive quasi-static compaction experiments were performed on porous beds of Teflon 7C, a highly crystalline polymer, and melamine, a molecular crystal. These two materials were selected to be somewhat representative of the range in deformation behavior that can occur for elastomeric plastic bonded explosives and high energy propellants and for crystalline secondary explosives, respectively.

Several important results were obtained from investigating the compaction behavior of Teflon 7C and melamine powders. These include:

(a) the variation of transmitted force versus applied force was linear over the entire applied force range for both of these non-metals and is analogous to compaction measurements on powder metal systems performed by other investigators,

(b) the slope of the plot of transmitted force versus applied force was considerably higher for Teflon 7C than for melamine, which is consistent with the well-known lubrication qualities of Teflon, and

(c) to achieve the same % TMD required an appreciably higher applied stress for melamine than for Teflon 7C.

A portion of the Teflon 7C and melamine compaction data was analyzed to obtain the intragranular stress (average axial compressive force within the granular material comprising a unit cross-sectional area of the porous bed) as a function of compacted powder density. As many as four different methods were applied including two new approaches devised during this work. Minimal numerical differences were found in the intragranular stress values calculated by the various approaches. Thus, the analytic method developed by Kuo, Moore, and Yang appears to be satisfactory for describing the compaction behavior of both Teflon 7C and melamine for the column lengths used in this work.

The semilogarithmic variation of intragranular stress versus % TMD exhibited a linear region for Teflon 7C ( $75 < \% \text{ TMD} < 94$ ) and also for melamine ( $76 < \% \text{ TMD} < 88$ , at least). At constant % TMD, the magnitude of the intragranular stress for melamine exceeded that of Teflon 7C except at the lowest % TMD level obtained.

## VII. BIBLIOGRAPHY

- Bernecker, R. R., Price, D., and Sandusky, H., "Burning to Detonation Transition in Porous Beds of a High Energy Propellant," NSWC TR 79-351, Nov 1979.
- Bernecker, R. R., Sandusky, H. W., and Clairmont, Jr., A. R., "Compaction and the Burning to Detonation Transition at Low Confinement," in Proceedings of the 16th JANNAF Combustion Meeting, Vol. I, 10-14 Sep 1979, Publ. 1979, pp. 91-116.
- Birkett, J. A., "The Acquisition of M30A1 Propellant Rheology Data," IHTR 724, 30 Sep 1981.
- Burchett, O. L., Birnbaum, M. R., and Oien, C. T., "Compaction Studies of Palladium/Aluminum Powders," in Proceedings of the 6th International Pyrotechnics Seminar, 17-21 Jul 1978, pp. 11-38.
- Carroll, M. M., and Holt, A. C., "Static and Dynamic Pore-Collapse Relations for Ductile Porous Materials," Journal of Applied Physics, Vol. 43, No. 4, 1972, pp. 1626-1636.
- Clyens, S., and Johnson, W., "The Dynamic Compaction of Powdered Materials," Materials Science and Engineering, Vol. 30, No. 2, 1977, pp. 121-139.
- Donachie, M. J., and Burr, M. F., "Effects of Pressing of Metal Powders," Journal of Metals, Vol. 15, No. 7, 1963, pp. 849-854.
- Duwez, P., and Zwell, L., "Pressure Distribution in Compacting Metal Powders," Journal of Metals, Vol. 1, No. 2, 1949, pp. 137-144.
- Elban, W. L., "The Development of an Inert Simulant for HNS/Teflon Explosive," NOLTR 72-255, 14 Nov 1972.
- Ensminger, D., Ultrasonics: The Low- and High-Intensity Applications (New York: Marcel Dekker, 1973), pp. 203-218.
- Hartmann, B. and Jarzynski, J., "Immersion Apparatus for Ultrasonic Measurements in Polymers," Journal of the Acoustical Society of America, Vol 56, No. 5, 1974, pp. 1469-1477.
- Hausner, H. H., and Sheinhartz, I., "Friction and Lubrication in Powder Metallurgy," in Proceedings of the 10th Annual Meeting of the Metal Powder Association, Vol. I, 1954, pp. 6-27.

## BIBLIOGRAPHY (Cont.)

- Hinners, N. W., and Mason, P. V., "The Apollo-17 Surface Experiments," Astronautics and Aeronautics, Vol. 10, No. 12, 1972, pp. 40-54.
- Hirschhorn, J. S., and Garey, M. W., "Plastic Deformation of Compacted Iron Powders," International Journal of Powder Metallurgy, Vol. 5, No. 1, 1969, pp. 35-44.
- Hodgman, C. D., Weast, R. C., Shankland, R. S., and Selby, S. M., eds., Handbook of Chemistry and Physics (Cleveland: Chemical Rubber Publishing Co., 1963), p. 2221.
- Hopkins, B. D., Butcher, A. G., Pilcher, D. T., and Beckstead, M. W., "A Comparison of DDT Calculations and Experiments for Granulated Rocket Propellant," in Proceedings of the 16th JANNAF Combustion Meeting, Vol. 3, 10-14 Sep 1979, Publ. 1979, pp. 33-49.
- Kilmer, E. E., "Plastic Bonded, Thermally Stable Explosive for an Apollo Experiment," Journal of Spacecraft and Rockets, Vol. 10, No. 7, 1973, pp. 463-466.
- Kim, K., "Incremental Data Reduction Method for Static Compaction Experiments," presented at 1982 JANNAF Propulsion Systems Hazards Meeting, 19-21 Apr 1982, China Lake, CA.
- Knudsen, F. P., "Dependence of Mechanical Strength of Brittle Polycrystalline Specimens on Porosity and Grain Size," Journal of the American Ceramic Society, Vol. 42, No. 8, 1959, pp. 376-387.
- Kuo, K. K., Moore, B. B., and Yang, V., "Measurement and Correlation of Intragranular Stress and Particle-Wall Friction in Granular Propellant Beds, in Proceedings of the 16th JANNAF Combustion Meeting, Vol. I, 10-14 Sep 1979, Publ. 1979, pp. 559-581. (See also "Intragranular Stress, Particle-Wall Friction and Speed of Sound in Granular Propellant Beds," Journal of Ballistics, Vol. 4, No. 1, 1980, pp. 697-730.)
- Leopold, P. M., and Nelson, R. C., "The Effect of Die-Wall Lubrication and Admixed Lubricant on the Compaction of Sponge-Iron Powder 1. Effect of Lubrication on Powder Compaction," International Journal of Powder Metallurgy, Vol. 1, No. 3, 1965, pp. 37-44.
- Papadakis, E. P. and Petersen, B. W., "Ultrasonic Velocity as a Predictor of Density in Sintered Powder Metal Parts," Materials Evaluation, Vol. 37, No. 5, 1979, pp. 76-80.
- Papadakis, E. P., "Determination of Powder Metal Density by Ultrasonic Velocity," in Proceedings of the IEEE Ultrasonics Symposium, 29 Sep - 1 Oct 1976, Publ. 1976, pp. 133-137.
- Price, D., and Bernecker, R. R., "DDT Behavior of Ground Tetryl and Picric Acid," NSWC TR 77-175, 25 Jan 1978.

## BIBLIOGRAPHY (Cont.)

- Price, D., and Bernecker, R. R., "DDT Behavior of Porous Propellant Models and Porous Samples of Commercial Propellants," NSWC TR 80-65, 13 Mar 1980.
- Price, D., and Bernecker, R. R., "DDT Behavior of Waxed Mixtures of RDX, HMX, and Tetryl," NSWC TR 77-96, 18 Oct 1977.
- Sandusky, H. W., and Bernecker, R. R., "Transparent Tube Studies of Burning to Detonation Transition in Granular Explosives I, Preliminary Framing Camera Studies," NSWC TR 79-79, 27 Oct 1980.
- Sandusky, H. W., Bernecker, R. R., and Clairmont, Jr., A. R., "Dynamic Compaction of Inert Porous Beds," NSWC TR 81-97, to be published.
- Sandusky, H. W., Elban, W. L., Kim, K., Bernecker, R. R., Gross, S. B., and Clairmont, Jr., A. R., "Compaction of Porous Beds of Inert Materials," in Proceedings Seventh Symposium (International) on Detonation, 16-19 Jun 1981, NSWC MP 82-334, pp. 843-856.
- Sheinhartz, I., McCullough, H. M., and Zambrow, J. L., "Method Described for Evaluation of Lubricants in Powder Metallurgy," Journal of Metals, Vol. 6, No. 5, 1954, pp. 515-518.
- Spriggs, R. M., Brissette, L. A., and Vasilos, T., "Effect of Porosity on Elastic and Shear Moduli of Polycrystalline Magnesium Oxide," Journal of the American Ceramic Society, Vol 45, No. 8, 1962, p. 400.
- Spriggs, R. M., "Expression for Effect of Porosity on Elastic Modulus of Polycrystalline Refractory Materials, Particularly Aluminum Oxide," Journal of the American Ceramic Society, Vol. 44, No. 12, 1961, pp. 628-629.
- Strijbos, S., and Vermeer, P. A., "Stress and Density Distributions in the Compaction of Powders," in Processing of Crystalline Ceramics, Materials Science Research, Vol. 11, Eds: H. Palmour III, R. F. Davis, and T. M. Hare (New York: Plenum Press, 1978), pp. 113-123.
- Varghese, J. N., O'Connell, A. M., and Maslen, E. N., "The X-ray and Neutron Crystal Structure of 2,4,6 - Triamino - 1,3,5 - triazine (Melamine)," Acta Crystallographica, Vol. B33, Part 7, 1977, pp. 2102-2108.
- Walker, E. E., "The Properties of Powders Part VI The Compressibility of Powders," Transactions of the Faraday Society, Vol. 19, No. 7, Part 1, 1923, pp. 73-82.
- Waast, R. C., ed., CRC Handbook of Chemistry and Physics (Boca Raton, FL: CRC Press, Inc., 1980), p. C-406.
- Westbrook, J. H., and Conrad, H., eds. The Science of Hardness Testing and Its Research Applications (Metals Park, Ohio: American Society for Metals, 1973).
- 1979 Annual Book of ASTM Standards, Part 35: Plastics-General Test Methods; Nomenclature (Philadelphia: ASTM, 1979), pp. 705-708.

## VIII. NOMENCLATURE

|           |   |                           |
|-----------|---|---------------------------|
| a         | equation of state parameter (Burchett, Birnbaum, and Oien analysis) | --                        |
| b         | equation of state parameter (Burchett, Birnbaum, and Oien analysis) | --                        |
| f         | coefficient of friction between mold and porous bed                 | --                        |
| $g_c$     | unit conversion factors   | $g\text{-cm/s}^2\text{N}$ |
| $h_0$     | precompacted initial sample height                                  | mm                        |
| j         | axial increment number  | --                        |
| $l$       | axial length variable (NSWC I analysis)                             | mm                        |
| m         | mass coordinate (NSWC II analysis)                                  | --                        |
| n         | number of axial increments  | --                        |
| t         | time  | s                         |
| $x_{ave}$ | axial location of the midplane of the porous bed                    | mm                        |
| $x_u$     | axial location of the upper porous bed-ram interface                | mm                        |
| z         | axial position along porous bed                                     | mm                        |
| A         | radial cross-sectional area of the porous bed                       | $\text{mm}^2$             |
| $A_0$     | pre-exponential constant (Equation (D-1))                           | m/s                       |
| AN        | ammonium nitrate  | --                        |
| B         | slope of the semilogarithmic variation of $V_L$ versus % TMD        | --                        |
| D         | mold inner diameter   | mm                        |
| DDT       | deflagration to detonation transition                               | --                        |
| DPH       | diamond pyramid (or Vickers) hardness                               | $\text{kgf/mm}^2$         |

## NOMENCLATURE (Cont.)

|                    |   |                   |
|--------------------|---|-------------------|
| F                  | axial force   | kN                |
| F <sub>a</sub>     | axial applied force   | kN                |
| F <sub>t</sub>     | axial transmitted force   | kN                |
| HMX                | cyclotetramethylenetetranitramine                                       | --                |
| K <sub>1</sub>     | slope of the semilogarithmic variation of F <sub>t</sub> versus L       | --                |
| K <sub>2</sub>     | pre-exponential constant (Equation (D-3))                               | MPa               |
| K <sub>3</sub>     | slope of semilogarithmic variation of M <sub>L</sub> versus % TMD       | --                |
| L                  | porous bed length   | mm                |
| M <sub>L</sub>     | longitudinal modulus  | MPa               |
| M <sub>p</sub>     | total mass of the porous bed  | g                 |
| P <sub>wp</sub>    | contact perimeter between mold and porous bed                           | mm                |
| R                  | radial distance along top of porous bed (Figure F-1)                    | mm                |
| RDX                | cyclotrimethylenetrinitramine   | --                |
| % TMD              | percent theoretical maximum density                                     | --                |
| TNT                | trinitrotoluene   | --                |
| V <sub>L</sub>     | longitudinal sound velocity   | m/s               |
| α                  | porosity $\left( = \frac{\rho_c}{\rho_s} \right)$ at some normal stress | --                |
| α <sub>c</sub>     | correction factor (NSWC II analysis)                                    | --                |
| α <sub>o</sub>     | initial porosity $\left( = \frac{\rho_c}{\rho_o} \right)$               | --                |
| Δl <sub>defl</sub> | change in compaction assembly length (determined by deflectometer)      | mm                |
| δ                  | particle size   | μm                |
| ε                  | correction factor (Appendix C)  | mm                |
| ρ <sub>c</sub>     | crystal density   | g/cm <sup>3</sup> |

## NOMENCLATURE (Cont.)

|                           |   |          |
|---------------------------|---|----------|
| $\rho_j$                  | density of jth increment  | $g/cm^3$ |
| $\rho_{n/2}$              | density of the axial midplane                                       | $g/cm^3$ |
| $\rho_o$                  | initial sample density  | $g/cm^3$ |
| $\rho_r$                  | void free reference density ( $= \rho_c$ )                          | $g/cm^3$ |
| $\rho_s$                  | compacted sample density  | $g/cm^3$ |
| $\sigma$                  | normal stress   | MPa      |
| $\sigma_a$                | axial applied stress  | MPa      |
| $\sigma_j$                | normal stress of the jth increment                                  | MPa      |
| $\sigma_o$                | equation of state parameter (Burchett, Birnbaum, and Oien analysis) | MPa      |
| $\sigma_t$                | axial transmitted stress  | MPa      |
| $\tau_i$                  | intragranular stress  | MPa      |
| $\tau_{wp}$               | particle-wall friction stress                                       | MPa      |
| $\frac{\tau_{wp}}{\pi D}$ | particle-wall friction parameter                                    | MPa      |
| $\phi_{ave}$              | average fractional porosity   | --       |

APPENDIX A

SIEVE ANALYSES OF MELAMINE

Four separate sieve analyses were performed on 200 g samples of the melamine powder used in this work. A nest of five 20.3 cm (8 in) diameter sieves was used for a variety of test conditions as indicated in Table A-1 which includes the actual sieve results and analyses. A semilogarithmic plot of cumulative weight % retained versus particle size appears in Figure A-1.

TABLE A-1. SIEVE ANALYSES ON MELAMINE

| Conditions                              | U.S.A. Sieve Number | Sieve Opening, $\mu\text{m}$ | Weight Retained, g   | Weight % | Cumulative Weight % |
|---|---------------------|------------------------------|----------------------|----------|---------------------|
| 200.00 g initially;                     | 100                 | 150                          | 4.33                 | 2.2      | 2.2                 |
| CENCO-Meiner sieve shaker (setting #2); | 140                 | 106                          | 14.28                | 7.2      | 9.4                 |
|   | 200                 | 75                           | 33.50                | 16.9     | 26.3                |
|   | 270                 | 53                           | 70.76                | 35.8     | 62.1                |
|   | 325                 | 45                           | 33.78                | 17.1     | 79.2                |
| 1 h                                     | pan                 | —                            | 41.03                | 20.8     | 100.0               |
|   |                     |                              | <u>197.68(98.8%)</u> |          |                     |
| 200.00 g initially;                     | 100                 | 150                          | 2.47                 | 1.3      | 1.3                 |
| CENCO-Meiner sieve shaker (setting #5); | 140                 | 106                          | 11.10                | 5.7      | 7.0                 |
|   | 200                 | 75                           | 19.04                | 9.7      | 16.7                |
|   | 270                 | 53                           | 44.63                | 22.7     | 39.4                |
|   | 325                 | 45                           | 26.33                | 13.4     | 52.8                |
| 2 h                                     | pan                 | —                            | 92.69                | 47.2     | 100.0               |
|   |                     |                              | <u>196.26(98.1%)</u> |          |                     |
| 200.00 g initially;                     | 100                 | 150                          | 2.62                 | 1.3      | 1.3                 |
| Tyler Ro-tap;                           | 140                 | 106                          | 10.59                | 5.4      | 6.7                 |
|   | 200                 | 75                           | 21.43                | 10.8     | 17.5                |
| 1 h                                     | 270                 | 53                           | 86.25                | 43.7     | 61.2                |
|   | 325                 | 45                           | 7.78                 | 3.9      | 65.1                |
|   | pan                 | —                            | 68.87                | 34.9     | 100.0               |
|   |                     |                              | <u>197.54(98.8%)</u> |          |                     |
| 200.00 g initially;                     | 100                 | 150                          | 2.71                 | 1.4      | 1.4                 |
| Tyler Ro-tap;                           | 140                 | 106                          | 10.14                | 5.1      | 6.5                 |
|   | 200                 | 75                           | 19.01                | 9.6      | 16.1                |
| 2 h                                     | 270                 | 53                           | 79.46                | 40.3     | 56.4                |
|   | 325                 | 45                           | 8.10                 | 4.1      | 60.5                |
|   | pan                 | —                            | 77.94                | 39.5     | 100.0               |
|   |                     |                              | <u>197.36(98.7%)</u> |          |                     |

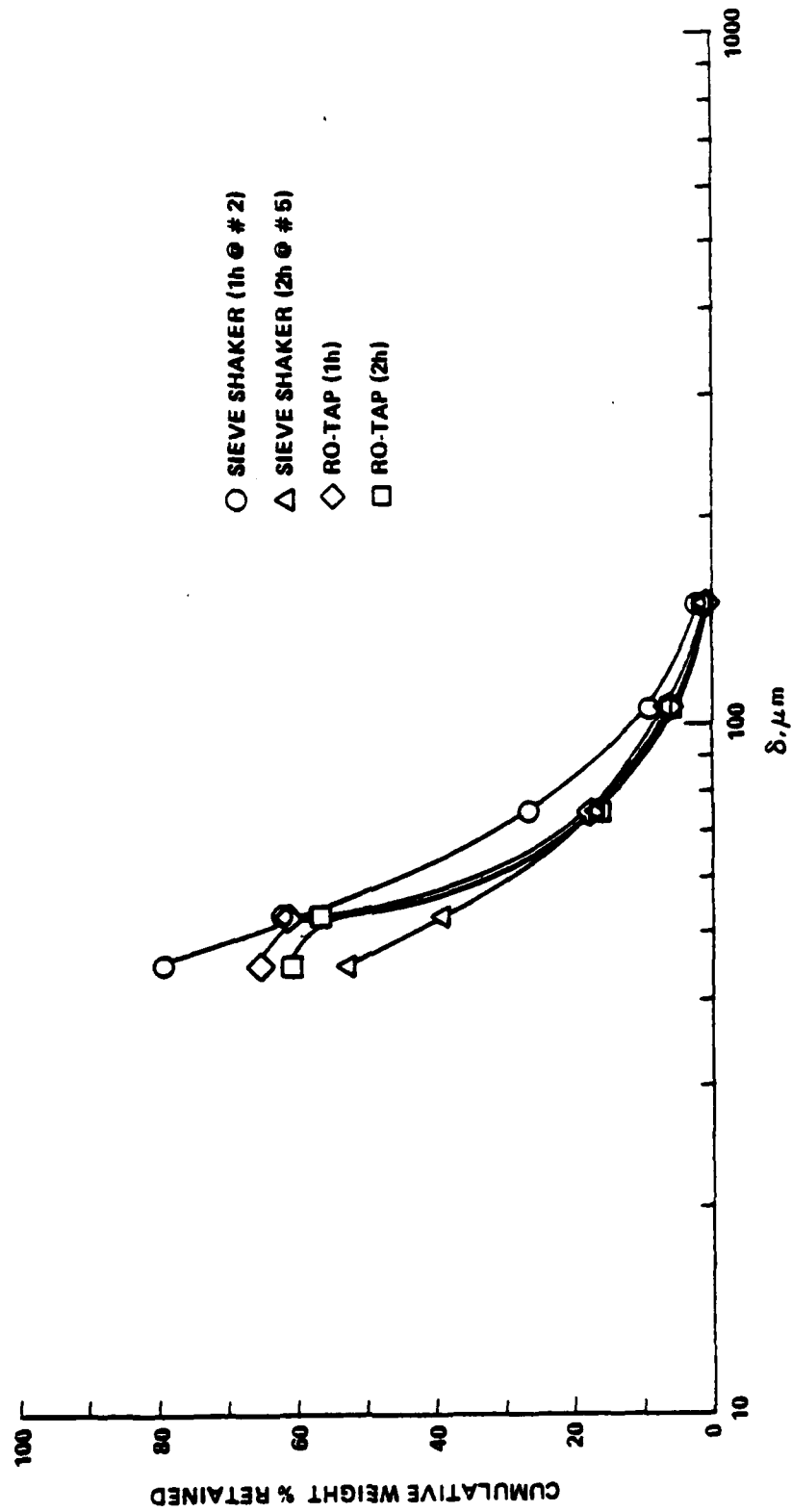


FIGURE A-1. PARTICLE SIZE ANALYSES OF MELAMINE

APPENDIX B

STEP-BY-STEP PROCEDURE OF A COMPLETE COMPACTION EXPERIMENT  
(TWO FORCE MEASUREMENTS)

The following is a step-by-step procedure of a complete compaction experiment on either Teflon 7C or melamine.

1. The sample is weighed to within 0.001 g using a Mettler balance.
2. Both rams and the mold are cleaned with acetone and visually inspected.
3. The strip chart recorders used to follow axial applied force, axial transmitted force, and top ram displacement are adjusted to the proper signal magnification settings.
4. The bottom ram and the mold are assembled and placed on the bottom load cell cover and aligned in the Tinius Olsen machine.
5. The sample is carefully poured into the mold and the top ram is lowered into position.
6. The Tinius Olsen machine is advanced to precompact the sample to approximately 670 N (150 lbf). This precompaction is gauged by the dial register of the Tinius Olsen weighing table (not shown in Figure 3 of the main text). At this level of precompaction, Teflon 7C has a % TMD of about 65% and melamine has a % TMD of about 69%.
7. The cathetometer (which also does not appear in Figure 3 of the main text) is used to determine the initial bed length for the level of precompaction of the sample.
8. The deflectometer is zeroed and engaged.
9. The tracking mechanisms of both strip chart recorders are engaged.
10. The compaction process proceeds stepwise at approximately 1.27 mm/min in intervals determined by applied force levels normally equaling 1/10 to 1/15 of the total compaction force desired.
11. At the maximum load desired, the cathetometer is again used to obtain the final relative displacement of the top ram, yielding an uncorrected final bed length.
12. The Tinius Olsen machine is reversed, and the ram-mold-sample assembly is removed.
13. The sample is removed and retained for possible future characterization.

APPENDIX C

CORRECTION IN COMPACTION APPARATUS ASSEMBLY LENGTH

The correction in apparatus assembly length (without porous bed sample) as a function of applied force was determined experimentally and appears in Figure C-1. Three separate sets of measurements were made to determine the apparatus deformation that would occur during compaction with a maximum applied force of about 53 kN (12000 lbf).

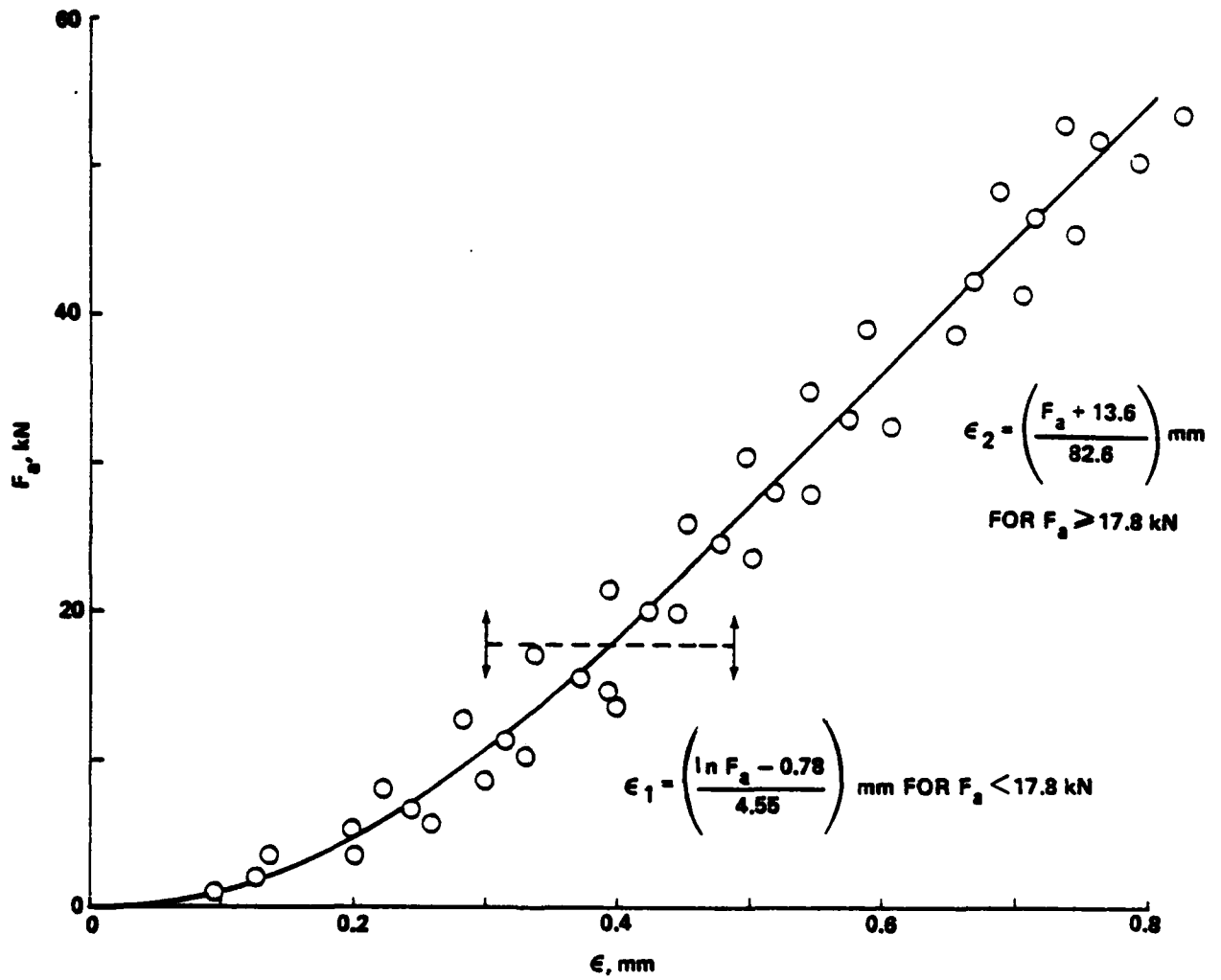


FIGURE C-1. APPLIED FORCE VERSUS STEEL COLUMN DEFLECTION

## APPENDIX D

SOUND VELOCITY MEASUREMENTS ON COMPACTED MELAMINE AND  
TEFLON 7C SAMPLES

Sound velocity measurements have been made on a number of liquids and compacted melamine and Teflon 7C samples at various densities that were contained in a 25.4 mm I.D. Lexan DDT tube (Figure D-1). Radial pulse-echo measurements were made on a series of liquids, each one contained in the bore of the tube which was sealed at the bottom end using a steel plug with an O-ring. These liquids, which are chemically compatible with Lexan (polycarbonate), were chosen to provide a reasonably large range in sound speed. The results appear in Table D-1 along with literature values<sup>D-1</sup> for comparison purposes. The agreement between measured and literature values is excellent, indicating that the pulse-echo scan was being correctly interpreted.

A block diagram of the apparatus used for making these direct contact broadband pulse-echo measurements appears in Figure D-2. The basic component is a broadband\* ultrasonic pulser/receiver (Panametrics Model 5055PR) which is employed with a single broadband contact transducer (taken from the Panametrics Videoscan series). In this work, the transducer had a center frequency, as reported by the manufacturer, of 1 MHz and a 25.4 mm element diameter. A viscous material (Fisher Scientific Nonaq stopcock grease) is used to transmit or couple the ultrasonic energy between the transducer and the sample. Signal amplitude versus time output is displayed on an oscilloscope (Hewlett Packard Model 1743A). A delay feature on the oscilloscope allows transit time measurements (horizontal axis) to be made directly from the cathode ray tube screen using a digital readout display of time.

Radial longitudinal sound velocity measurements (Figure D-1) on powdered melamine columns compacted at 60 and 80% TMD in the 25.4 mm I.D. Lexan tube were attempted with the ultrasonic system operating in pulse-echo as before. Satisfactory measurements on the 60% TMD sample were not possible due to difficulty in the interpreting the pulse-echo scan. However, a value of 1440 m/s was obtained for the 80% TMD sample. It is concluded that radial measurements with the system operating in pulse-echo cannot be made on melamine at 60% TMD for diameters greater than or equal to 25.4 mm and probably at not much below 80% TMD.

---

\*The unit gives an output voltage spike having a minimum rise time less than 10 ns which produces a broadband frequency spectrum in the transducer. The bandwidth of the receiver is from 0.01 to 10 MHz as reported by the manufacturer.

D-1 Ensminger, D., Ultrasonics: The Low- and High-Intensity Applications (New York: Marcel Dekker, 1973), pp. 203-218.

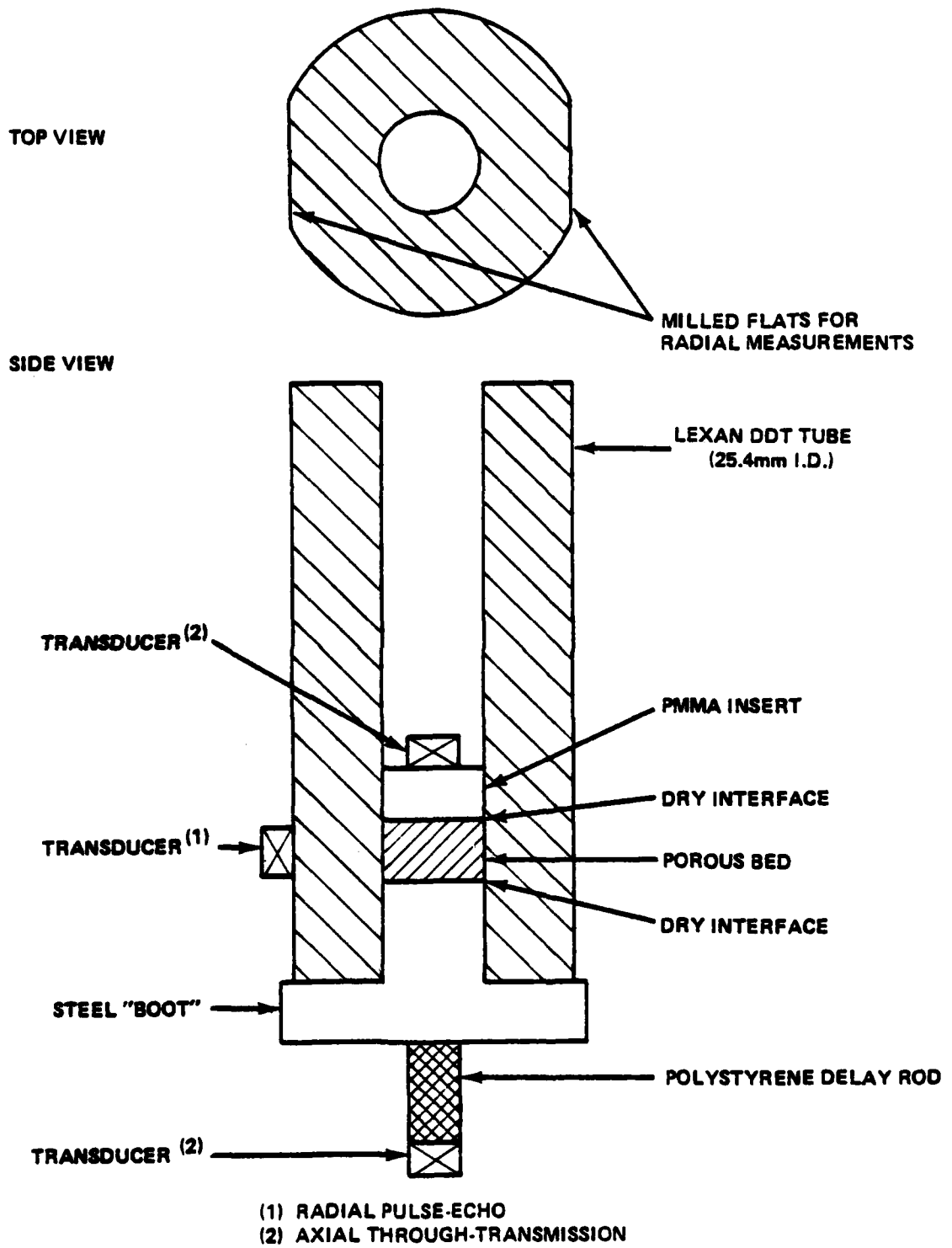


FIGURE D-1. SCHEMATIC OF LEXAN DDT TUBE CONTAINING POROUS BED FOR MAKING SOUND SPEED MEASUREMENTS

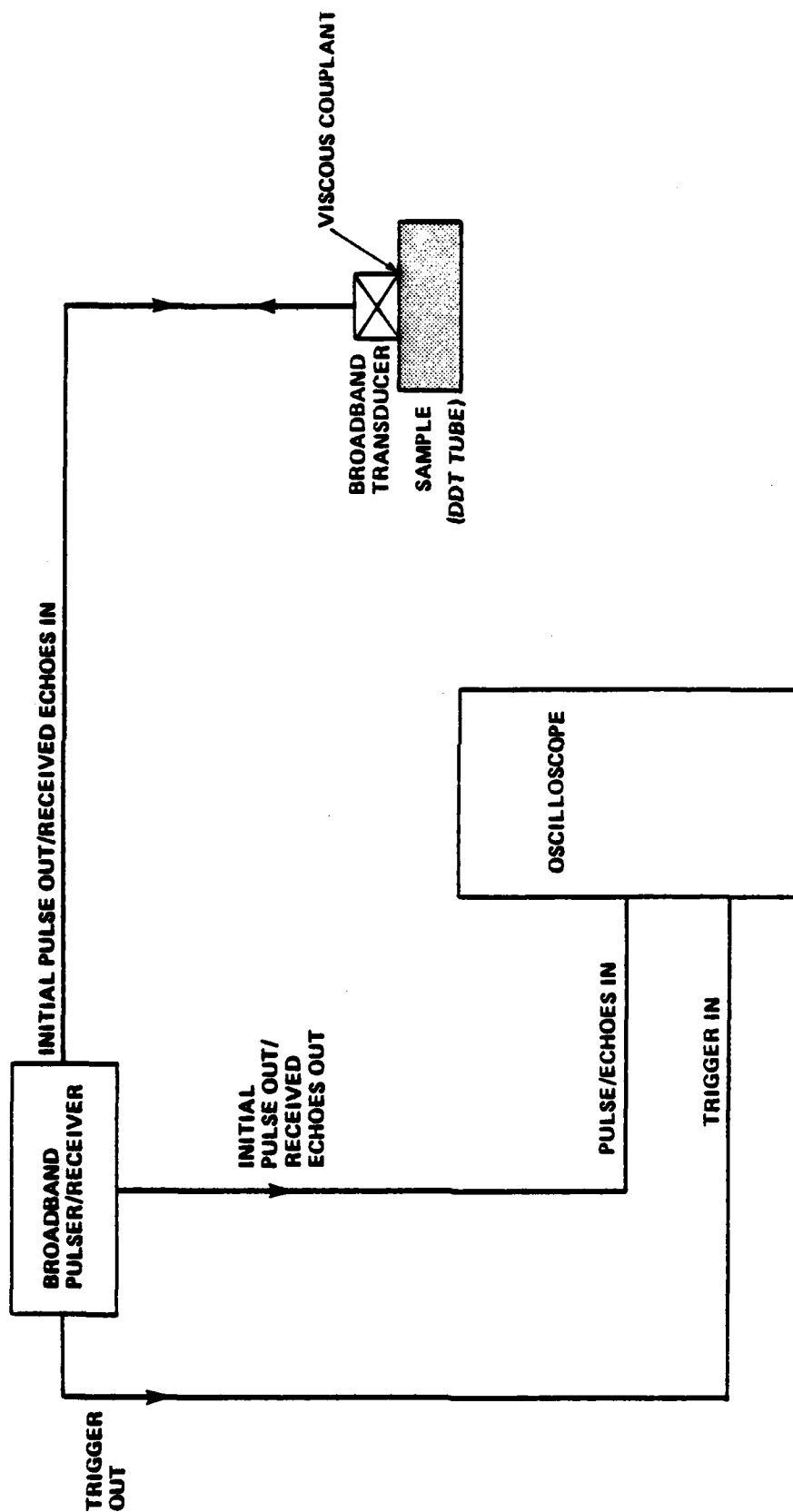


FIGURE D-2. BLOCK DIAGRAM OF BROADBAND ULTRASONIC APPARATUS OPERATING IN DIRECT CONTACT PULSE ECHO

TABLE D-1. SOUND VELOCITY MEASUREMENTS ON VARIOUS LIQUIDS WHILE CONTAINED IN A LEXAN DDT TUBE

| <u>Liquid</u>   | <u>Measured Velocity, m/s</u> | <u>Literature Value, m/s*</u> |
|-----------------|-------------------------------|-------------------------------|
| glycerine       | 1890                          | 1920                          |
| ethylene glycol | 1650                          | 1620                          |
| water           | 1480                          | 1480                          |
| n-heptane       | 1150                          | 1160                          |

\*Taken from Reference D-1.

To better determine the limitation of the broadband ultrasonic system for measuring sound velocities of compacted melamine, a series of axial and radial longitudinal velocity measurements (Figure D-1) were made on a 7.61 g sample\* compacted in the 25.4 mm I.D. Lexan tube. Initial measurements were made on a 18.6 mm high column packed to 51.5% TMD. This single increment of material was then further compacted in stages to 73.1% TMD, corresponding to a final column height of 13.1 mm. Velocity measurements were made after each stage, and these results are given in Table D-2.

TABLE D-2. LONGITUDINAL VELOCITY MEASUREMENTS ON COMPACTED MELAMINE POWDER WHILE CONTAINED IN A LEXAN DDT TUBE

| <u><math>\rho</math>, g/cm<sup>3</sup></u> | <u>% TMD*</u> | <u>V<sub>L</sub>(axial), m/s</u> | <u>V<sub>L</sub>(radial), m/s</u> | <u>Compaction Method</u> |
|--|---------------|----------------------------------|-----------------------------------|--------------------------|
| 0.81                                       | 51.5          | 460                              | No Signal                         | By Hand                  |
| 0.84                                       | 53.4          | 460                              | No Signal                         | By Hand                  |
| 0.99                                       | 62.9          | 480                              | No Signal                         | By Hand                  |
| 1.05                                       | 66.8          | 560                              | No Signal                         | By Hand                  |
| 1.06                                       | 67.4**        | 590                              | No Signal                         | By Hand                  |
| 1.15                                       | 73.1***       | 630                              | No Signal                         | Tinius Olsen Machine     |

\*TMD taken to be 1.573 g/cm<sup>3</sup>.

\*\*Begin to lose transmitted signal amplitude.

\*\*\*Severe loss in transmitted signal amplitude; uncertainty in measuring transit time.

\*This sample mass would yield a 12 mm high column when compacted to 80% TMD.

The axial measurements appearing in Table D-2 were all made in through-transmission with a polystyrene delay rod and using 12.5 mm diameter broadband transducers with a center frequency of 1 MHz. The apparatus (Figure D-3) used for making these broadband through-transmission measurements had two components added to the pulse-echo apparatus described previously. A second receiving transducer, closely matched to the transmitting transducer, is positioned at the backwall of the sample. Now the sound wave simply travels the sample length one time instead of the round trips in pulse-echo. However, with this technique there is insufficient time delay to determine precisely the time (acoustic zero) when the sound wave enters the sample. To circumvent this uncertainty, a piece of low attenuating material is inserted between the transmitting transducer and the sample. Since the acoustic zero is not known precisely, the transit time for the sample is obtained by difference: the transit time for the delay rod is subtracted from the transit time for the sample plus delay rod. All of the interfaces are coupled as before to permit the sound wave to enter the delay rod, then to enter the sample, and finally to pass to the receiving transducer.

The radial measurements were continued in pulse-echo using a single 1 MHz broadband transducer because through-transmission operation yielded a transit time corresponding to the longitudinal velocity for Lexan, indicating that sound propagation was not totally blocked by the center hole. All interfaces involving the porous bed were left dry. To achieve coupling in the axial measurements, the top transducer was vertically loaded with 500 g.

Referring to the results compiled in Table D-2, there is a gradual increase in axial longitudinal velocity with increasing density as expected. However, the loss in transmitted signal amplitude first experienced for material compacted to 67.4% TMD and the severe reduction in the signal for 73.1% TMD melamine were both surprising and puzzling. One possible explanation is that on compaction to 67.4% TMD or higher the melamine crystals are crushed, creating numerous additional interfaces that serve as scattering centers. The loss in signal would then be attributed to the increase in the attenuation in the porous bed. A second explanation may be in the role that the gas phase (air) has in transmitting sound through the bed and in the coupling at the transducer-porous bed interfaces. Clearly, this could only be an important consideration when the gas phase is the sound propagation medium and remains continuous. As the porous bed is compacted, a density is reached where this no longer occurs, which may account for the observed reduced transmitted signal amplitude.

Radial longitudinal velocity measurements on the melamine porous bed having densities listed in Table D-2 were not successful. The observed pulse-echo scan corresponded to the sound traveling in the Lexan cylinder wall, indicating insufficient coupling between the tube and the porous bed. In an effort to eliminate the coupling problems encountered when making velocity measurements on porous melamine beds in the DDT tube, an attempt was made to obtain a bare cylinder that would remain intact. A single increment compaction was made on 7.05 g (corresponding to a column height of 8.8 mm at 100% TMD) of melamine contained in 25.4 mm I.D. steel mold with a single acting ram. This assembly was pressed hydraulically to a pressure of 441 MPa (64,000 psi) for a dwell time of 60 s. On removal the cylinder cracked into numerous pieces.

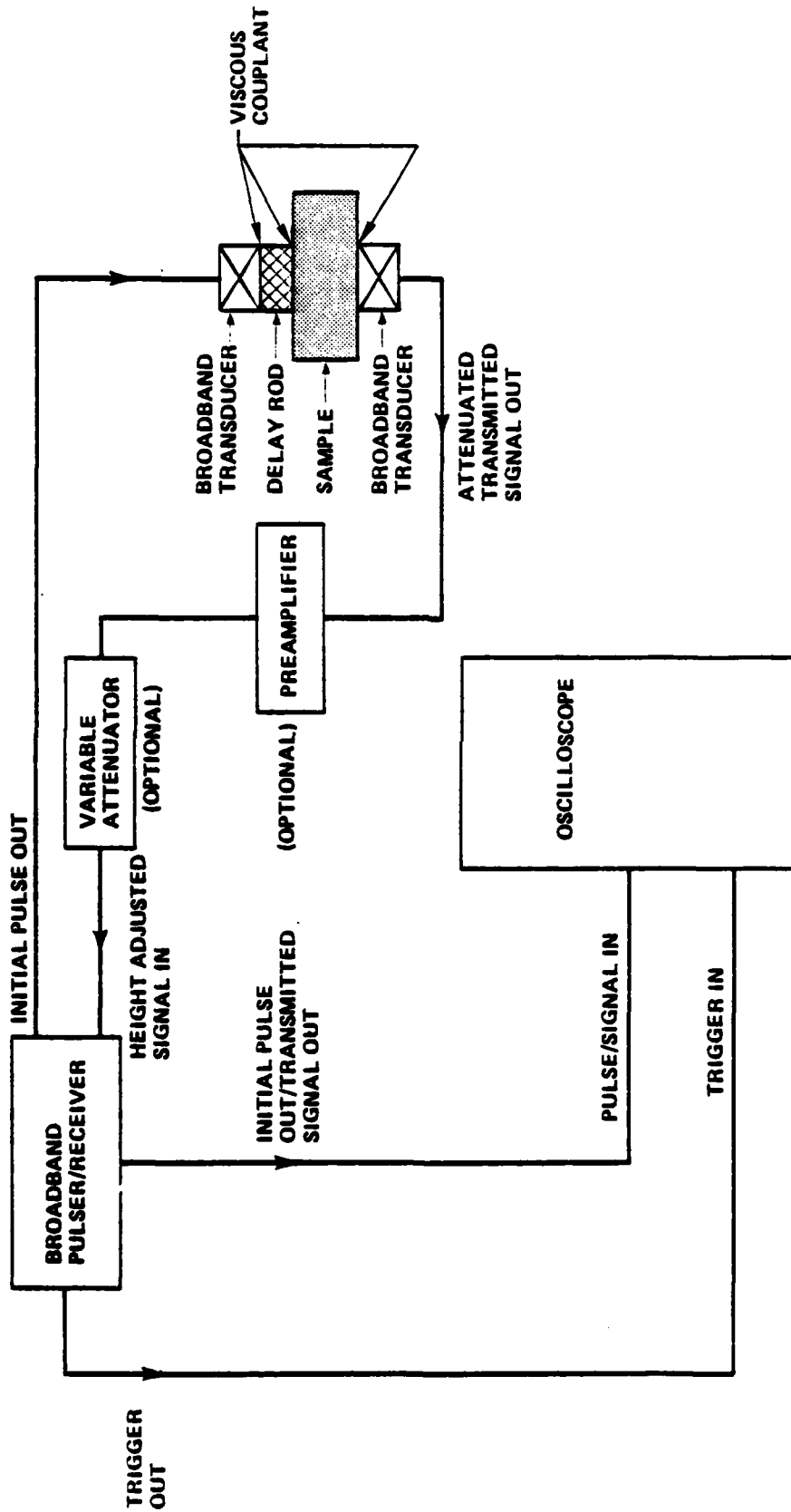


FIGURE D-3. BLOCK DIAGRAM OF BROADBAND ULTRASONIC APPARATUS OPERATING IN THROUGH-TRANSMISSION WITH DELAY ROD

Sound velocity measurements were also made on a number of powdered Teflon 7C samples. Initially, a single 8 g increment of Teflon 7C was compacted by hand in the 25.4 mm I. D. Lexan DDT tube used previously for melamine. Axial and radial longitudinal velocity measurements were attempted, and the results are reported in Table D-3. The ultrasonic procedure worked out for studying powdered melamine was adopted in these measurements on Teflon 7C. No signal could be detected in the axial direction until the material was compacted to 58.1% TMD, corresponding to a column height of 11.8 mm. This was also the highest density porous bed compacted by hand. The remaining densities listed in Table D-3 were achieved using a hammer. The axial longitudinal velocity increased with increasing density until the 80.3% TMD sample was evaluated. For this material the transmitted signal amplitude was severely reduced making correct signal interpretation questionable. Increased pressure (by hand) restored adequate dry pressure coupling to provide a good signal, and a velocity slightly below the value for 77.7% TMD was obtained. As was the case for melamine (Table D-2), no radial velocity measurements were successful; insufficient coupling between the tube and the porous bed is believed to be responsible.

TABLE D-3. LONGITUDINAL VELOCITY MEASUREMENTS ON COMPACTED  
TEFLON 7C POWDER WHILE CONTAINED IN A LEXAN DDT TUBE

| $\rho, \text{g/cm}^3$ | % TMD* | $V_L(\text{axial}), \text{m/s}$ | $V_L(\text{radial}), \text{m/s}$ | Compaction Method |
|-----------------------|--------|---------------------------------|----------------------------------|-------------------|
| 0.70                  | 30.4   | No Signal                       | No Measurement                   | By Hand           |
| 0.82                  | 35.6   | No Signal                       | No Measurement                   | By Hand           |
| 1.00                  | 43.4   | No Signal                       | No Measurement                   | By Hand           |
| 1.22                  | 52.9   | No Signal                       | No Measurement                   | By Hand           |
| 1.34                  | 59.1   | 220                             | No Signal                        | By Hand           |
| 1.52                  | 65.9   | 220                             | No Signal                        | Hammer            |
| 1.61                  | 69.8   | 240                             | No Signal                        | Hammer            |
| 1.79                  | 77.7   | 680                             | No Signal                        | Hammer            |
| 1.85                  | 80.3** | 620                             | No Signal                        | Hammer            |

\*TMD Taken to be  $2.305 \text{ g/cm}^3$ .

\*\*Severe loss in transmitted signal amplitude; signal restored by increased hand pressure.

In an effort to overcome the continuing coupling problems associated with making sound speed measurements on porous beds contained in the DDT tube, an attempt was made to obtain bare cylinders of Teflon 7C. A series of bare cylinders (each weighed close to 8 g) suitable for ultrasonic measurements was achieved having densities ranging from 52.9 to 96.7% TMD. Both axial and radial longitudinal velocities were measured successfully for all of the samples, and these results are given in Table D-4. Axial longitudinal velocity measurements on bare cylinders of more highly compacted Teflon 7C, resulting from the single force-measurement compaction studies, appear in Table D-5. It is important to note that these samples were actually compressed to higher stresses than what appears in Figure 8 of the main text. Measurements on the bare cylinders provided a confirmation of the data obtained on porous beds of Teflon 7C contained in the Lexan DDT tube. Reasonably good agreement was obtained with the only significant deviation occurring for the 65.9 and 69.8% TMD samples. The results of Tables D-3, D-4, and D-5 are plotted in Figure D-4.

Referring to the bare cylinder data, it is clear that the increase in sound speed in porous Teflon 7C with increasing density is non-linear over the density range studied. Below 81.6% TMD, the longitudinal sound velocity is anisotropic with higher velocities being obtained in the radial direction. This is consistent with the measurements for steel powder compacts.<sup>D-2, D-3</sup> In the present work, the transition from anisotropic to isotropic sound propagation corresponded to a change in compaction method. Exactly what influence the impulsive loading, attained from hammering, versus the more uniform (in time) loading, obtained hydraulically, has on the state of the porous bed is unknown. However, a substantial anisotropy was measured for the two lowest density samples compacted by hand. This technique should approximate the hydraulic method used to obtain the higher density samples, indicating that the anisotropy is probably not due to the compaction method.

Axial longitudinal velocity measurements were made on four samples cut from a single piece of 25 mm diameter Teflon bar stock. These results are listed in Table D-6 and are included in Figure D-4 also. Lengths ranged from 6.3 to 50.9 mm while the density was 2.10 g/cm<sup>3</sup> (91.1% TMD) for each cylinder. The velocity varied from 1260 to 1300 m/s; the average value was almost 1290 m/s for all the determinations. This compares with a literature value of 1380 m/s for Teflon having a density of 2.177 g/cm<sup>3</sup> (94.4% TMD).<sup>D-4</sup> At first it was surprising that samples of compacted Teflon 7C had higher densities and longitudinal velocities than Teflon bar stock. However, during a discussion

---

D-2 Papadakis, E. P., "Determination of Powder Metal Density by Ultrasonic Velocity," in Proceedings of the IEEE Ultrasonics Symposium, 29 Sep - 1 Oct 1976, Publ. 1976, pp. 133-137.

D-3 Papadakis, E. P., and Petersen, B. W., "Ultrasonic Velocity as a Predictor of Density in Sintered Powder Metal Parts," Materials Evaluation, Vol. 37, No. 5, 1979, pp. 76-80.

D-4 Hartmann, B., and Jarzynski, J., "Immersion Apparatus for Ultrasonic Measurements in Polymers," Journal of the Acoustical Society of America, Vol. 56, No. 5, 1974, pp. 1469-1477.

TABLE D-4. LONGITUDINAL VELOCITY MEASUREMENTS ON BARE CHARGES  
OF COMPACTED TEFLON 7C POWDER

| <u><math>\rho</math>, g/cm<sup>3</sup></u> | <u>% TMD*</u> | <u><math>V_L</math> (axial) (m/s)</u> | <u><math>V_L</math> (radial) (m/s)</u> | <u>Compaction Method</u> |
|--|---------------|---------------------------------------|--|--------------------------|
| 1.22                                       | 52.9          | 170                                   | 230                                    | By Hand                  |
| 1.38                                       | 59.9          | 250                                   | 330                                    | By Hand                  |
| 1.51                                       | 65.5          | 320                                   | 420                                    | Hammer                   |
| 1.62                                       | 70.3          | 430                                   | 530                                    | Hammer                   |
| 1.67                                       | 72.5          | 440                                   | 560                                    | Hammer                   |
| 1.75                                       | 75.9          | 520                                   | 640                                    | Hammer                   |
| 1.84                                       | 79.8          | 610                                   | 740                                    | Hammer                   |
| 1.88                                       | 81.6          | 810                                   | 830                                    | Hydraulic (Hand)         |
| 1.95                                       | 84.6          | 890                                   | 900                                    | Hydraulic (Hand)         |
| 2.08                                       | 90.2          | 1130                                  | 1110                                   | Hydraulic (Hand)         |
| 2.13                                       | 92.4          | 1310                                  | 1280                                   | Hydraulic (Hand)         |
| 2.18                                       | 94.6          | 1430                                  | 1440                                   | Hydraulic (Hand)         |
| 2.21                                       | 95.9          | 1490                                  | 1480                                   | Hydraulic (Machine)      |
| 2.22                                       | 96.3          | 1520                                  | 1530                                   | Hydraulic (Machine)      |
| 2.23                                       | 96.7          | 1530                                  | 1560                                   | Hydraulic (Machine)      |

---

\*TMD taken to be 2.305 g/cm<sup>3</sup>.

TABLE D-5. LONGITUDINAL VELOCITY MEASUREMENTS ON BARE CHARGES OF TEFLON 7C POWDER COMPACTED USING THE INSTRON UNIVERSAL TESTING MACHINE

| <u>Identification</u> | <u><math>\rho</math>, g/cm<sup>3</sup></u> | <u>% TMD</u> | <u><math>V_L</math> (Axial), m/s</u> |
|-----------------------|--|--------------|--------------------------------------|
| 8 g in Steel Mold     | 2.24                                       | 97.2         | 1570                                 |
| 16 g in Steel Mold    | 2.24                                       | 97.2         | 1570                                 |
| 8 g in Steel Mold     | 2.24                                       | 97.2         | 1660                                 |
| 16 g in Steel Mold    | 2.26                                       | 98.0         | 1650                                 |

---

\*TMD taken to be 2.305 g/cm<sup>3</sup>.

TABLE D-6. LONGITUDINAL VELOCITY MEASUREMENTS ON TEFLON BAR STOCK

| <u>Height, mm</u> | <u><math>\rho</math>, g/cm<sup>3</sup></u> | <u>% TMD</u> | <u><math>V_L</math>(axial), m/s</u> |
|-------------------|--|--------------|-------------------------------------|
| 6.32              | 2.10                                       | 91.1         | 1290                                |
| 12.83             | 2.10                                       | 91.1         | 1300                                |
| 25.48             | 2.10                                       | 91.1         | 1300                                |
| 50.89             | 2.10                                       | 91.1         | 1260                                |

---

\*TMD taken to be 2.305 g/cm<sup>3</sup>.

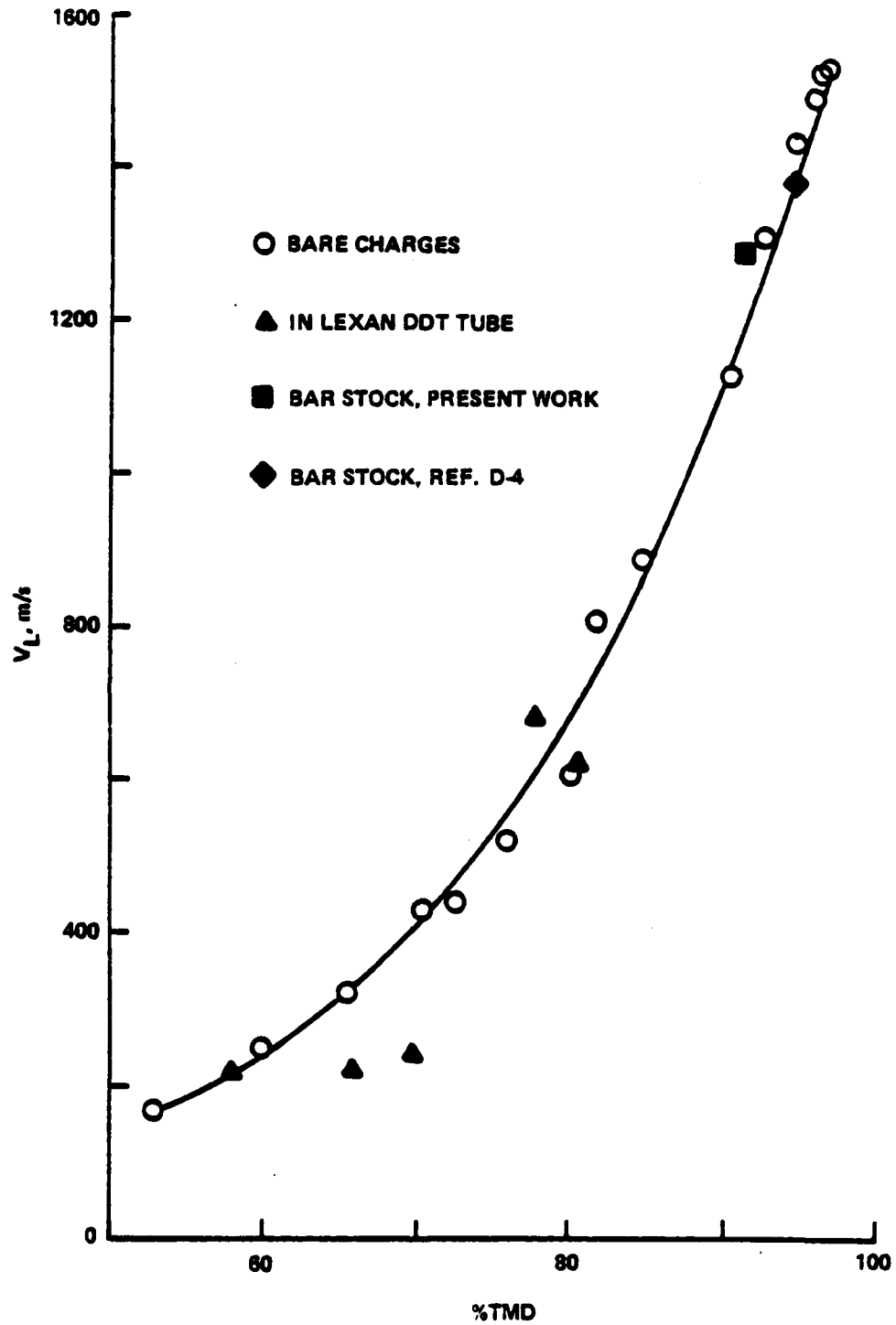


FIGURE D-4. AXIAL LONGITUDINAL VELOCITY VERSUS %TMD FOR COMPACTED TEFLON 7C SAMPLES AND TEFLON BAR STOCK

(Experimental section) with Laurence A. Ferris, a customer services specialist with the DuPont Company, it was revealed that compacted Teflon powder undergoes a crystalline to amorphous phase transition during sintering to form bar stock. This explains why bar stock has a lower density and sound velocity than some of the compacted samples that were prepared in this work.

An attempt was made to find a suitable relationship for the longitudinal velocity versus % TMD data given in Table D-4 for bare cylinders of compacted Teflon 7C powder. There was also an effort to determine whether this data offered any insight into the compaction process, specifically whether a change in compaction mechanism could be detected.

A semilogarithmic plot of longitudinal velocity versus % TMD for both axial and radial measurements appears in Figure D-5. Over the entire density range a straight line relationship is observed for the radial longitudinal velocity measurements suggesting an expression of the form

$$V_L = A_0 e^{B(\% \text{ TMD})}, \quad (\text{D-1})$$

where  $A_0$  and  $B$  are constants. The axial data appears to be best represented by two straight line segments with a jump where the transition from anisotropic to isotropic behavior occurs (between 79.8 and 81.6% TMD). With this exception, there is no indication from plotting the data in this manner that a change in compaction mechanism has occurred over the density range studied.

In investigating the relation between mechanical strength and porosity of brittle polycrystalline materials, Knudsen<sup>D-5</sup> reasoned that a change in strength which accompanies a change in specimen porosity is attributed to a corresponding change in the size of the effective or critical load-bearing area within the specimen. This suggests considering the variation of longitudinal modulus,  $M_L$ , with % TMD as a means of identifying a change in the compaction process.

The longitudinal modulus is calculated simply using the relation

$$M_L = \rho V_L^2, \quad (\text{D-2})$$

where  $\rho$  is the density. Plots of  $M_L$  versus % TMD and  $\log M_L$  versus % TMD are given in Figures D-6 and D-7, respectively, based on the data appearing in Table D-4. The plot of  $M_L$  versus % TMD was non-linear and resembled the plot of  $V_L$  versus % TMD given in Figure D-4. The plot of  $\log M_L$  versus % TMD was linear for the radial longitudinal moduli, suggesting an equation of the form

$$M_L = K_2 e^{K(\% \text{ TMD})}, \quad (\text{D-3})$$

<sup>D-5</sup>Knudsen, F. P., "Dependence of Mechanical Strength of Brittle Polycrystalline Specimens on Porosity and Grain Size," Journal of the American Ceramic Society, Vol. 42, No. 8, 1959, pp. 376-387.

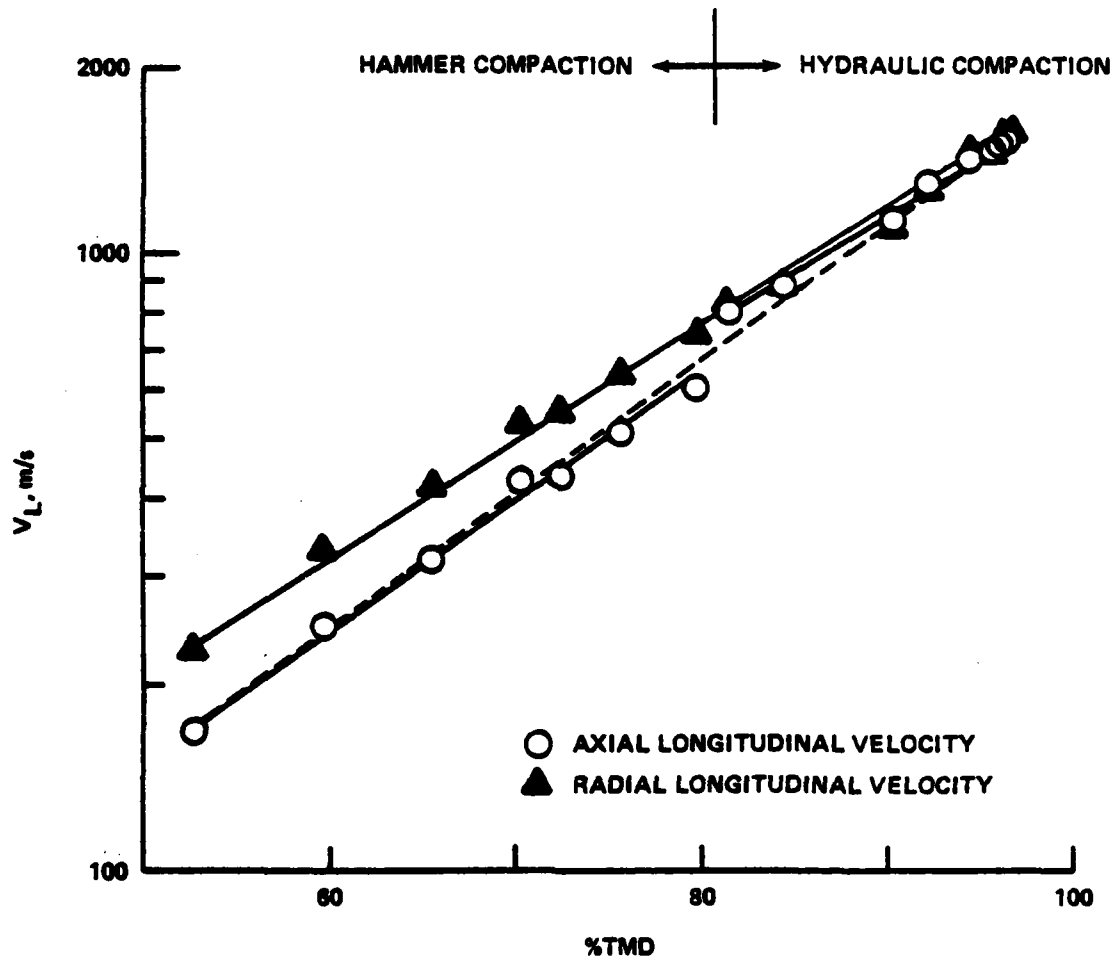


FIGURE D-5. SEMILOGARITHMIC VARIATION OF LONGITUDINAL VELOCITY VERSUS %TMD FOR BARE CHARGES OF COMPACTED TEFLON 7C SAMPLES

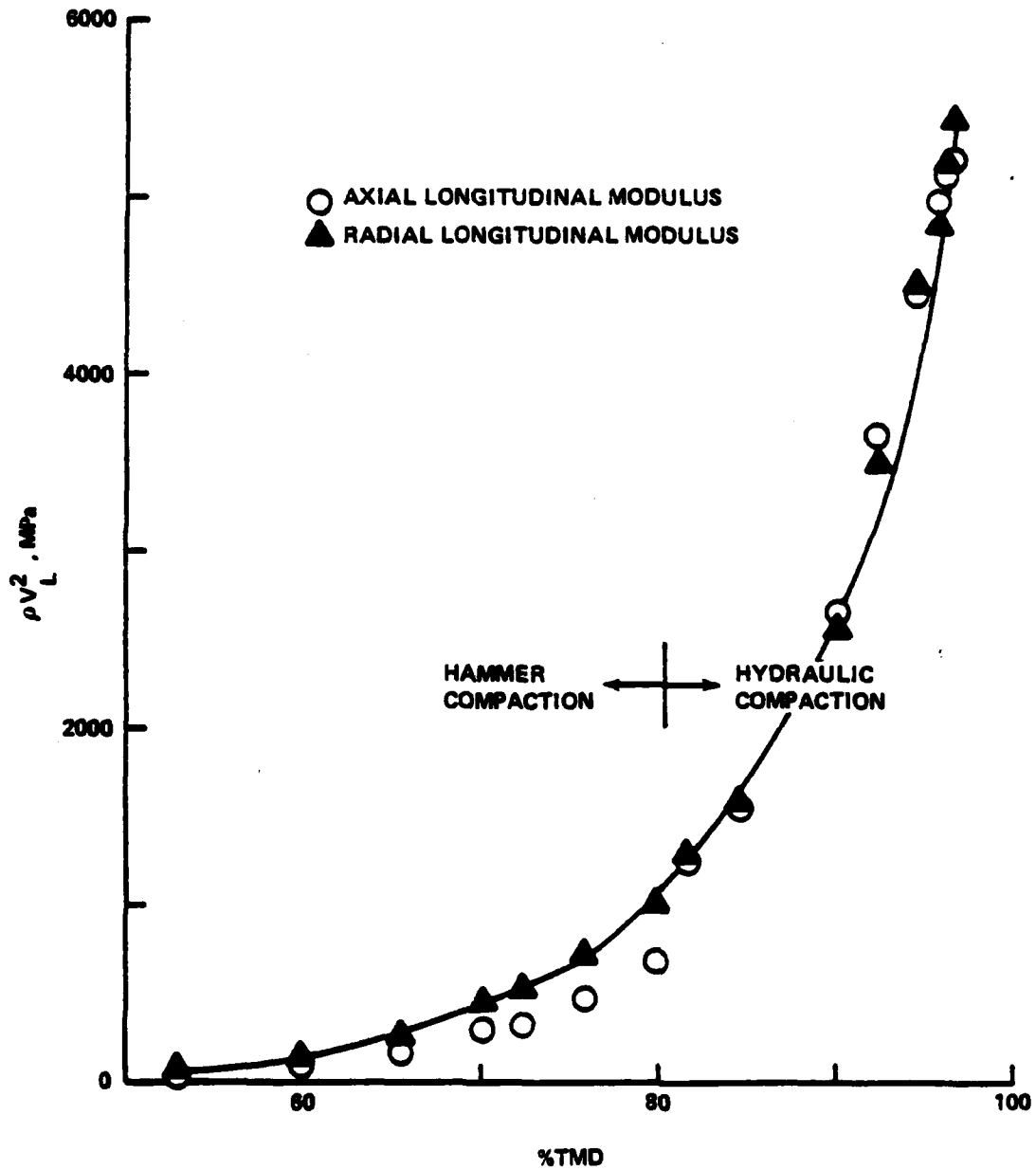


FIGURE D-6. LONGITUDINAL MODULUS VERSUS %TMD OBTAINED FROM LONGITUDINAL VELOCITY MEASUREMENTS ON BARE CHARGES OF COMPACTED TEFLON 7C SAMPLES

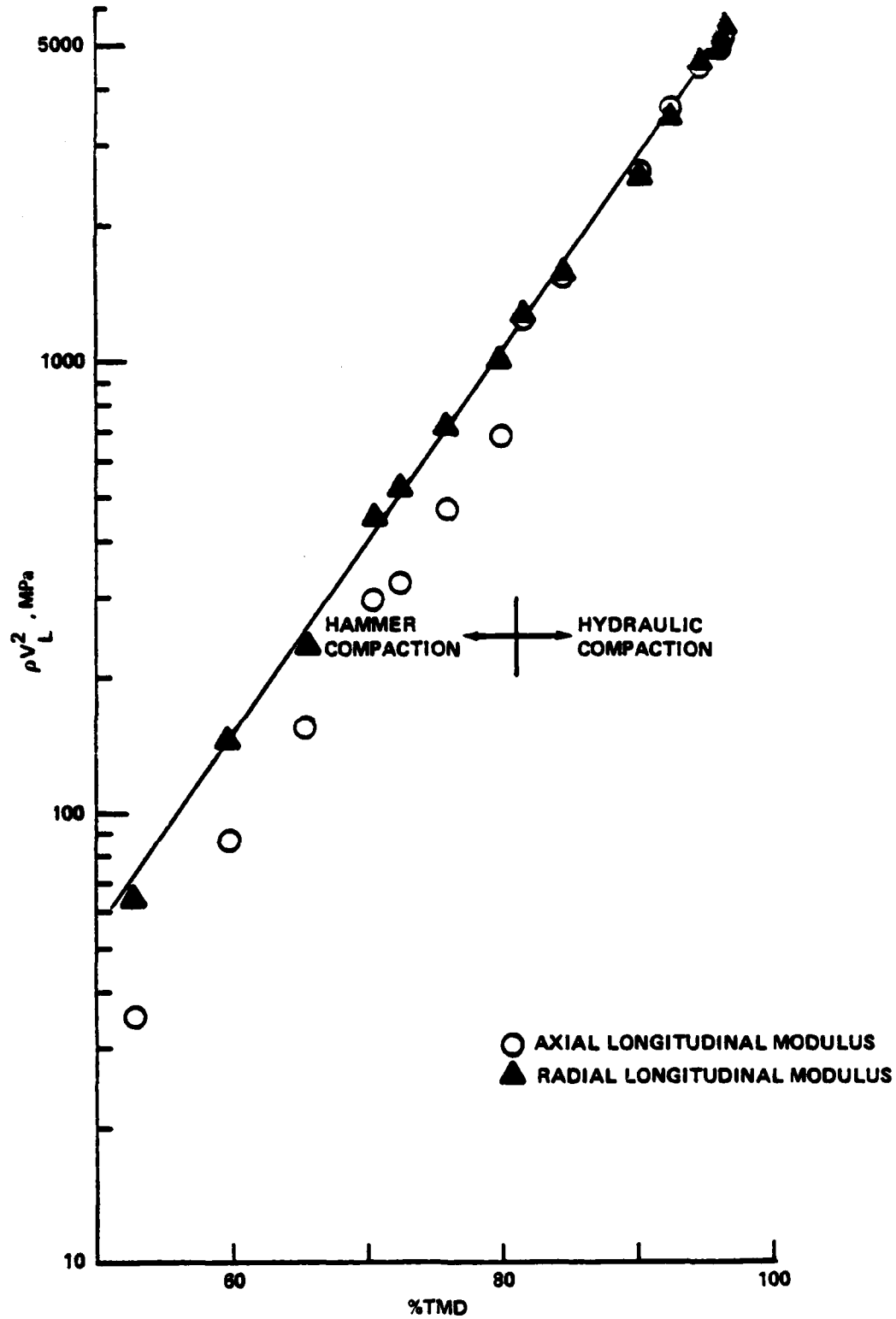


FIGURE D-7. SEMILOGARITHMIC VARIATION OF LONGITUDINAL MODULUS VERSUS %TMD OBTAINED FROM LONGITUDINAL VELOCITY MEASUREMENTS ON BARE CHARGES OF COMPACTED TEFLON 7C SAMPLES

where  $K_2$  and  $K_3$  are constants. There were two straight line segments for the axial longitudinal modulus with a jump again occurring at the anisotropic to isotropic transition. An analogous exponential equation has been shown to satisfactorily relate the effect of porosity on the elastic modulus of polycrystalline aluminum oxide<sup>D-6</sup> and magnesium oxide<sup>D-7</sup> although the porosity range was usually more limited than in the current work on compacted Teflon 7C powder. Spriggs<sup>D-6</sup> suggests that the value of  $K_2$  is related to the proportion of closed and open pores, with the latter exhibiting a stronger influence on the modulus than the former. A change in slope would be expected if the nature of the pore structure changed from primarily open pores to closed pores with increasing % TMD. However, to within experimental error, no change in slope was observed, leading to the conclusion either that it was not possible to detect either a change in the nature of the porosity or a change in the compaction mechanism by plotting the data in this manner or that the formalism described in the studies of ceramic beds does not apply to Teflon 7C.

It is very important to remember, particularly for the compacted samples, that the sound velocity measurements reported in this section were obtained using broadband ultrasonic techniques. No attempt was made to account for the frequency shift associated with these measurements. As such, this work should be regarded as an initial effort and as still requiring an assessment of dispersion.

---

D-6 Spriggs, R. M., "Expression for Effect of Porosity on Elastic Modulus of Polycrystalline Refractory Materials, Particularly Aluminum Oxide," Journal of the American Ceramic Society, Vol. 44, No. 12, 1961, pp. 628-629.

D-7 Spriggs, R. M., Brissette, L. A., and Vasilos, T., "Effect of Porosity on Elastic and Shear Moduli of Polycrystalline Magnesium Oxide," Journal of the American Ceramic Society, Vol. 45, No. 8, 1962, p. 400.

NSWC TR 81-113

APPENDIX E

COMPILATION OF TEFLON 7C AND MELAMINE COMPACTION DATA AND  
INTRAGRANULAR STRESS RESULTS FROM VARIOUS ANALYSES

TABLE E-1. COMPACTION DATA FOR 5 g TEFLON 7C SAMPLES

| <u>Run Number</u> | <u>Applied Force, kN (lbf)</u> | <u>Transmitted Force, kN (lbf)</u> | <u>% TMD</u> |      |
|-------------------|--------------------------------|------------------------------------|--------------|------|
| 54TF              | 0.53 (120)                     | 0.58 (130)                         | 77.8         |      |
|                   | 1.9 (430)                      | 1.8 (400)                          | 86.1         |      |
|                   | 4.4 (980)                      | 4.1 (930)                          | 92.7         |      |
|                   | 5.47 (1230)                    | 5.29 (1190)                        | 93.7         |      |
|                   | 7.30 (1640)                    | 6.94 (1560)                        | 95.3         |      |
|                   | 9.07 (2040)                    | 8.67 (1950)                        | 96.0         |      |
|                   | 10.8 (2430)                    | 10.3 (2320)                        | 96.7         |      |
|                   | 12.7 (2850)                    | 12.2 (2740)                        | 96.9         |      |
|                   | 14.5 (3260)                    | 14.0 (3140)                        | 97.0         |      |
|                   | 16.1 (3630)                    | 15.6 (3500)                        | 97.1         |      |
|                   | 17.9 (4020)                    | 17.3 (3880)                        | 97.2         |      |
|                   | 57TF                           | 0.53 (120)                         | 0.58 (130)   | 69.6 |
|                   |                                | 1.2 (280)                          | 1.1 (240)    | 72.1 |
| 1.9 (420)         |                                | 1.8 (400)                          | 79.7         |      |
| 3.7 (830)         |                                | 3.5 (780)                          | 88.1         |      |
| 5.52 (1240)       |                                | 5.20 (1170)                        | 92.2         |      |
| 7.21 (1620)       |                                | 6.85 (1540)                        | 94.9         |      |
| 9.03 (2030)       |                                | 8.59 (1930)                        | 96.6         |      |
| 10.9 (2440)       |                                | 10.3 (2320)                        | 97.8         |      |
| 12.5 (2810)       |                                | 11.9 (2680)                        | 98.6         |      |
| 14.4 (3230)       |                                | 13.7 (3090)                        | 99.1         |      |
| 16.2 (3650)       |                                | 15.6 (3510)                        | 99.6         |      |
| 18.1 (4060)       |                                | 17.5 (3940)                        | 99.9         |      |
| 59TF              |                                | 0.53 (120)                         | 0.53 (120)   | 70.5 |
|                   | 1.0 (230)                      | 0.93 (210)                         | 72.7         |      |
|                   | 2.8 (620)                      | 2.5 (570)                          | 85.5         |      |
|                   | 4.8 (1070)                     | 4.4 (1000)                         | 91.4         |      |
|                   | 6.36 (1430)                    | 6.01 (1350)                        | 94.2         |      |
|                   | 8.18 (1840)                    | 7.74 (1740)                        | 96.1         |      |
|                   | 9.96 (2240)                    | 9.52 (2140)                        | 97.3         |      |
|                   | 10.9 (2440)                    | 10.4 (2330)                        | 97.9         |      |
|                   | 12.8 (2870)                    | 12.2 (2740)                        | 98.3         |      |
|                   | 14.3 (3210)                    | 13.7 (3080)                        | 98.7         |      |
|                   | 16.1 (3610)                    | 15.5 (3480)                        | 98.9         |      |
|                   | 17.9 (4020)                    | 17.2 (3860)                        | 99.0         |      |

TABLE E-2. COMPACTION DATA FOR 10 g TEFLON 7C SAMPLES

| <u>Run Number</u> | <u>Applied Force, kN (lbf)</u> | <u>Transmitted Force, kN (lbf)</u> | <u>% TMD</u> |
|-------------------|--------------------------------|------------------------------------|--------------|
| 60TF              | 0.58 (130)                     | 0.53 (120)                         | 69.0         |
|                   | 2.0 (440)                      | 1.6 (370)                          | 78.9         |
|                   | 3.7 (840)                      | 3.2 (730)                          | 86.7         |
|                   | 5.52 (1240)                    | 4.9 (1100)                         | 91.2         |
|                   | 7.30 (1640)                    | 6.54 (1470)                        | 93.9         |
|                   | 9.07 (2040)                    | 8.18 (1840)                        | 95.9         |
|                   | 10.9 (2440)                    | 9.88 (2220)                        | 96.7         |
|                   | 12.6 (2840)                    | 11.6 (2600)                        | 97.4         |
|                   | 14.3 (3210)                    | 13.2 (2960)                        | 98.0         |
|                   | 16.2 (3650)                    | 15.0 (3380)                        | 98.4         |
|                   | 18.0 (4050)                    | 16.7 (3760)                        | 98.7         |
|                   | 61TF                           | 0.62 (140)                         | 0.53 (120)   |
| 1.1 (240)         |                                | 0.85 (190)                         | 70.7         |
| 2.0 (440)         |                                | 1.6 (360)                          | 77.9         |
| 2.8 (640)         |                                | 2.4 (530)                          | 82.6         |
| 4.63 (1040)       |                                | 4.0 (900)                          | 88.6         |
| 6.41 (1440)       |                                | 5.60 (1260)                        | 91.9         |
| 8.23 (1850)       |                                | 7.30 (1640)                        | 94.2         |
| 10.1 (2260)       |                                | 8.99 (2020)                        | 95.5         |
| 11.7 (2640)       |                                | 10.6 (2380)                        | 96.5         |
| 13.5 (3040)       |                                | 12.3 (2760)                        | 97.2         |
| 15.3 (3440)       |                                | 14.0 (3140)                        | 97.6         |
| 83TF              |                                | 0.58 (130)                         | 0.62 (140)   |
|                   | 1.9 (420)                      | 1.7 (380)                          | 77.8         |
|                   | 3.6 (820)                      | 3.2 (730)                          | 85.1         |
|                   | 5.47 (1230)                    | 4.98 (1120)                        | 89.6         |
|                   | 7.21 (1620)                    | 6.58 (1480)                        | 92.0         |
|                   | 9.03 (2030)                    | 8.27 (1860)                        | 93.6         |
|                   | 10.9 (2440)                    | 10.0 (2250)                        | 94.6         |
|                   | 12.6 (2830)                    | 11.7 (2620)                        | 95.4         |
|                   | 14.2 (3200)                    | 13.3 (2980)                        | 95.8         |
|                   | 15.5 (3490)                    | 14.5 (3260)                        | 96.0         |
| 17.5 (3940)       | 16.9 (3800)                    | 96.7                               |              |

TABLE E-2. COMPACTION DATA FOR 10 g TEFLON 7C SAMPLES (Cont.)

| <u>Run Number</u> | <u>Applied Force, kN (lbf)</u> | <u>Transmitted Force, kN (lbf)</u> | <u>% TMD</u> |
|-------------------|--------------------------------|------------------------------------|--------------|
| 84TF              | 0.58 (130)                     | 0.58 (130)                         | 71.0         |
|                   | 2.8 (620)                      | 2.5 (570)                          | 82.2         |
|                   | 4.54 (1020)                    | 4.2 (950)                          | 87.8         |
|                   | 6.32 (1420)                    | 5.87 (1320)                        | 90.9         |
|                   | 8.23 (1850)                    | 7.61 (1710)                        | 92.9         |
|                   | 9.96 (2240)                    | 9.30 (2090)                        | 94.1         |
|                   | 11.7 (2640)                    | 11.0 (2470)                        | 94.9         |
|                   | 13.4 (3020)                    | 12.6 (2840)                        | 95.4         |
|                   | 15.2 (3420)                    | 14.3 (3210)                        | 95.9         |
|                   | 17.0 (3820)                    | 16.0 (3600)                        | 96.2         |
|                   | 18.2 (4100)                    | 17.2 (3860)                        | 96.5         |

TABLE E-3. COMPACTION DATA FOR 15 g TEFLON 7C SAMPLES

| <u>Run Number</u> | <u>Applied Force, kN (lbf)</u> | <u>Transmitted Force, kN (lbf)</u> | <u>% TMD</u> |
|-------------------|--------------------------------|------------------------------------|--------------|
| 62TF              | 0.58 (130)                     | 0.49 (110)                         | 66.7         |
|                   | 1.5 (330)                      | 1.4 (310)                          | 74.1         |
|                   | 2.4 (530)                      | 1.9 (420)                          | 79.6         |
|                   | 3.3 (740)                      | 2.7 (600)                          | 83.5         |
|                   | 4.2 (950)                      | 3.6 (800)                          | 86.5         |
|                   | 5.52 (1240)                    | 4.72 (1060)                        | 89.7         |
|                   | 7.30 (1640)                    | 6.27 (1410)                        | 92.3         |
|                   | 9.07 (2040)                    | 7.87 (1770)                        | 94.0         |
|                   | 11.7 (2640)                    | 10.4 (2330)                        | 95.7         |
|                   | 13.6 (3060)                    | 12.1 (2730)                        | 96.5         |
|                   | 15.3 (3450)                    | 13.8 (3100)                        | 97.0         |
|                   | 16.5 (3700)                    | 14.9 (3340)                        | 97.4         |
|                   | 18.3 (4110)                    | 16.6 (3740)                        | 97.7         |
|                   | 70TF                           | 0.49 (110)                         | 0.40 (90)    |
| 1.4 (310)         |                                | 1.1 (240)                          | 73.2         |
| 2.3 (510)         |                                | 1.8 (400)                          | 79.3         |
| 3.6 (810)         |                                | 2.8 (630)                          | 84.7         |
| 5.38 (1210)       |                                | 4.4 (990)                          | 89.6         |
| 7.12 (1600)       |                                | 5.96 (1340)                        | 92.5         |
| 8.94 (2010)       |                                | 7.52 (1690)                        | 94.4         |
| 10.8 (2420)       |                                | 9.25 (2080)                        | 95.6         |
| 12.5 (2810)       |                                | 10.9 (2440)                        | 96.4         |
| 14.3 (3210)       |                                | 12.6 (2830)                        | 97.1         |
| 16.1 (3630)       |                                | 14.3 (3220)                        | 97.6         |
| 17.8 (4010)       |                                | 16.0 (3590)                        | 98.0         |

TABLE E-4. COMPACTION DATA FOR 20 g TEFLON 7C SAMPLES

| <u>Run Number</u> | <u>Applied Force, kN (lbf)</u> | <u>Transmitted Force, kN (lbf)</u> | <u>% TMD</u> |
|-------------------|--------------------------------|------------------------------------|--------------|
| 65TF              | 0.53 (120)                     | 0.53 (120)                         | 68.5         |
|                   | 1.8 (410)                      | 1.6 (360)                          | 77.9         |
|                   | 2.7 (610)                      | 2.4 (530)                          | 82.5         |
|                   | 4.49 (1010)                    | 4.0 (890)                          | 88.0         |
|                   | 6.27 (1410)                    | 5.60 (1260)                        | 91.4         |
|                   | 8.10 (1820)                    | 7.25 (1630)                        | 93.6         |
|                   | 9.88 (2220)                    | 8.90 (2000)                        | 94.8         |
|                   | 11.6 (2610)                    | 10.5 (2360)                        | 95.7         |
|                   | 13.4 (3010)                    | 12.2 (2740)                        | 96.3         |
|                   | 15.2 (3420)                    | 13.9 (3120)                        | 96.7         |
| 16.9 (3810)       | 15.5 (3490)                    | 97.0                               |              |
| 18.0 (4050)       | 16.5 (3710)                    | 97.2                               |              |
| 66TF              | 0.58 (130)                     | 0.53 (120)                         | 68.9         |
|                   | 1.9 (420)                      | 1.6 (360)                          | 78.4         |
|                   | 3.7 (830)                      | 3.2 (720)                          | 86.4         |
|                   | 5.47 (1230)                    | 4.85 (1090)                        | 90.8         |
|                   | 7.25 (1630)                    | 6.45 (1450)                        | 93.3         |
|                   | 8.99 (2020)                    | 8.05 (1810)                        | 94.9         |
|                   | 10.8 (2430)                    | 9.74 (2190)                        | 96.0         |
|                   | 11.7 (2630)                    | 10.5 (2370)                        | 96.5         |
|                   | 13.4 (3020)                    | 12.2 (2740)                        | 97.0         |
|                   | 15.3 (3440)                    | 13.9 (3130)                        | 97.5         |
| 17.0 (3830)       | 15.5 (3490)                    | 97.9                               |              |
| 18.1 (4060)       | 16.5 (3710)                    | 98.1                               |              |
| 85TF              | 0.53 (120)                     | 0.53 (120)                         | 69.3         |
|                   | 1.9 (420)                      | 1.6 (350)                          | 77.0         |
|                   | 3.6 (820)                      | 3.1 (690)                          | 84.6         |
|                   | 5.47 (1230)                    | 4.76 (1070)                        | 89.0         |
|                   | 7.30 (1640)                    | 6.36 (1430)                        | 91.7         |
|                   | 8.99 (2020)                    | 7.92 (1780)                        | 93.3         |
|                   | 10.9 (2440)                    | 9.61 (2160)                        | 94.5         |
|                   | 12.6 (2840)                    | 11.2 (2520)                        | 95.4         |
|                   | 14.3 (3220)                    | 12.8 (2880)                        | 96.0         |
|                   | 16.2 (3640)                    | 14.5 (3250)                        | 96.3         |
| 18.5 (4150)       | 16.5 (3710)                    | 96.7                               |              |

TABLE E-4. COMPACTION DATA FOR 20 g TEFLON 7C SAMPLES (Cont.)

| <u>Run Number</u> | <u>Applied Force, kN (lbf)</u> | <u>Transmitted Force, kN (lbf)</u> | <u>% TMD</u> |
|-------------------|--------------------------------|------------------------------------|--------------|
| 86TF              | 0.58 (130)                     | 0.53 (120)                         | 68.1         |
|                   | 0.93 (210)                     | 0.71 (160)                         | 68.7         |
|                   | 2.8 (630)                      | 2.3 (520)                          | 81.0         |
|                   | 4.58 (1030)                    | 3.9 (870)                          | 86.8         |
|                   | 6.36 (1430)                    | 5.56 (1250)                        | 90.3         |
|                   | 8.14 (1830)                    | 7.12 (1600)                        | 93.0         |
|                   | 9.96 (2240)                    | 8.76 (1970)                        | 93.9         |
|                   | 10.9 (2460)                    | 9.65 (2170)                        | 94.5         |
|                   | 13.6 (3060)                    | 12.1 (2730)                        | 95.6         |
|                   | 15.3 (3440)                    | 13.7 (3070)                        | 96.1         |
|                   | 17.1 (3840)                    | 15.2 (3430)                        | 96.4         |
|                   | 18.1 (4060)                    | 16.1 (3620)                        | 96.7         |

TABLE E-5. COMPACTION DATA FOR 25 g TEFLON 7C SAMPLES

| <u>Run Number</u> | <u>Applied Force, kN (lbf)</u> | <u>Transmitted Force, kN (lbf)</u> | <u>% TMD</u> |
|-------------------|--------------------------------|------------------------------------|--------------|
| 68TF              | 0.58 (130)                     | 0.49 (110)                         | 67.8         |
|                   | 1.8 (410)                      | 1.4 (320)                          | 76.9         |
|                   | 3.6 (820)                      | 2.8 (640)                          | 84.7         |
|                   | 5.43 (1220)                    | 4.58 (1030)                        | 89.8         |
|                   | 7.21 (1620)                    | 6.09 (1370)                        | 92.5         |
|                   | 8.99 (2020)                    | 7.56 (1700)                        | 94.3         |
|                   | 10.9 (2440)                    | 9.25 (2080)                        | 95.5         |
|                   | 12.5 (2820)                    | 10.9 (2440)                        | 96.5         |
|                   | 14.8 (3320)                    | 12.9 (2890)                        | 97.2         |
|                   | 16.2 (3640)                    | 14.2 (3190)                        | 97.5         |
|                   | 18.0 (4040)                    | 15.8 (3550)                        | 97.9         |
| 69TF              | 0.53 (120)                     | 0.40 (90)                          | 67.0         |
|                   | 1.9 (420)                      | 1.3 (300)                          | 75.8         |
|                   | 3.7 (830)                      | 2.7 (600)                          | 83.7         |
|                   | 5.43 (1220)                    | 4.4 (980)                          | 88.9         |
|                   | 7.30 (1640)                    | 5.92 (1330)                        | 91.7         |
|                   | 8.99 (2020)                    | 7.38 (1660)                        | 93.5         |
|                   | 10.9 (2440)                    | 8.99 (2020)                        | 94.8         |
|                   | 12.6 (2840)                    | 10.6 (2380)                        | 95.6         |
|                   | 14.4 (3240)                    | 12.2 (2750)                        | 96.3         |
|                   | 15.5 (3480)                    | 13.2 (2970)                        | 96.7         |
|                   | 17.1 (3840)                    | 14.7 (3300)                        | 97.0         |
| 18.0 (4040)       | 15.5 (3480)                    | 97.3                               |              |

TABLE E-6. COMPACTION DATA FOR 5 g MELAMINE SAMPLES

| <u>Run Number</u> | <u>Applied Force, kN (lbf)</u> | <u>Transmitted Force, kN (lbf)</u> | <u>% TMD</u> |
|-------------------|--------------------------------|------------------------------------|--------------|
| 72TF              | 1.2 (270)                      | 0.62 (140)                         | 69.9         |
|                   | 2.4 (540)                      | 1.7 (390)                          | 71.5         |
|                   | 4.63 (1040)                    | 3.5 (790)                          | 74.2         |
|                   | 6.89 (1550)                    | 5.34 (1200)                        | 76.4         |
|                   | 9.07 (2040)                    | 7.21 (1620)                        | 78.4         |
|                   | 12.1 (2720)                    | 9.79 (2200)                        | 80.5         |
|                   | 13.5 (3040)                    | 11.1 (2490)                        | 81.3         |
|                   | 15.8 (3540)                    | 12.9 (2900)                        | 82.0         |
|                   | 18.1 (4060)                    | 14.8 (3320)                        | 83.2         |
|                   | 20.2 (4530)                    | 16.6 (3740)                        | 83.9         |
|                   | 22.4 (5040)                    | 18.6 (4180)                        | 84.8         |
|                   | 25.1 (5650)                    | 20.9 (4690)                        | 85.6         |
|                   | 27.0 (6070)                    | 22.6 (5070)                        | 86.2         |
|                   | 29.3 (6580)                    | 24.5 (5500)                        | 86.9         |
|                   | 31.4 (7060)                    | 26.3 (5920)                        | 87.5         |
|                   | 33.5 (7540)                    | 28.1 (6320)                        | 87.9         |
|                   | 35.9 (8080)                    | 30.1 (6760)                        | 88.5         |
| 73TF              | 0.71 (160)                     | 0.53 (120)                         | 69.9         |
|                   | 1.8 (400)                      | 1.5 (340)                          | 71.9         |
|                   | 4.6 (1040)                     | 3.6 (800)                          | 74.3         |
|                   | 6.9 (1550)                     | 5.43 (1220)                        | 76.3         |
|                   | 9.0 (2020)                     | 7.25 (1630)                        | 78.4         |
|                   | 11.4 (2570)                    | 9.30 (2090)                        | 80.2         |
|                   | 13.5 (3030)                    | 10.7 (2410)                        | 81.6         |
|                   | 15.7 (3520)                    | 12.9 (2910)                        | 82.7         |
|                   | 18.0 (4050)                    | 14.9 (3360)                        | 83.7         |
|                   | 20.3 (4560)                    | 16.9 (3800)                        | 84.6         |
|                   | 22.6 (5080)                    | 18.9 (4240)                        | 85.4         |
|                   | 24.6 (5540)                    | 20.6 (4640)                        | 86.1         |
|                   | 27.2 (6120)                    | 22.9 (5140)                        | 86.8         |
|                   | 29.2 (6560)                    | 24.6 (5530)                        | 87.4         |
|                   | 31.6 (7110)                    | 26.7 (6010)                        | 88.0         |
|                   | 34.1 (7660)                    | 28.8 (6480)                        | 88.5         |
|                   | 35.7 (8020)                    | 30.2 (6800)                        | 88.6         |

TABLE E-7. COMPACTION DATA FOR 10 g MELAMINE SAMPLES

| <u>Run Number</u> | <u>Applied Force, kN (lbf)</u> | <u>Transmitted Force, kN (lbf)</u> | <u>% TMD</u> |
|-------------------|--------------------------------|------------------------------------|--------------|
| 74TF              | 0.71 (160)                     | 0.71 (160)                         | 68.5         |
|                   | 2.3 (510)                      | 1.9 (430)                          | 70.3         |
|                   | 4.54 (1020)                    | 3.5 (780)                          | 73.0         |
|                   | 6.85 (1540)                    | 5.07 (1140)                        | 75.1         |
|                   | 8.99 (2020)                    | 6.67 (1500)                        | 76.9         |
|                   | 11.2 (2510)                    | 8.32 (1870)                        | 78.5         |
|                   | 13.4 (3020)                    | 9.96 (2240)                        | 79.9         |
|                   | 15.8 (3550)                    | 11.7 (2630)                        | 81.1         |
|                   | 18.0 (4050)                    | 13.3 (2980)                        | 81.9         |
|                   | 21.1 (4740)                    | 15.3 (3440)                        | 83.1         |
|                   | 22.5 (5060)                    | 16.4 (3680)                        | 83.5         |
|                   | 24.7 (5560)                    | 18.0 (4050)                        | 84.3         |
|                   | 26.9 (6050)                    | 19.6 (4410)                        | 84.9         |
|                   | 29.1 (6540)                    | 21.2 (4760)                        | 85.5         |
|                   | 31.3 (7040)                    | 22.9 (5140)                        | 86.1         |
| 33.5 (7540)       | 24.6 (5520)                    | 86.5                               |              |
| 35.8 (8040)       | 26.2 (5890)                    | 87.0                               |              |
| 75TF              | 1.2 (270)                      | 0.80 (180)                         | 68.9         |
|                   | 2.3 (510)                      | 1.5 (340)                          | 70.7         |
|                   | 4.63 (1040)                    | 3.2 (720)                          | 73.5         |
|                   | 6.85 (1540)                    | 4.89 (1100)                        | 75.6         |
|                   | 9.07 (2040)                    | 6.49 (1460)                        | 77.5         |
|                   | 11.3 (2530)                    | 8.18 (1840)                        | 79.0         |
|                   | 13.5 (3030)                    | 9.79 (2200)                        | 80.3         |
|                   | 15.7 (3520)                    | 11.4 (2560)                        | 81.3         |
|                   | 17.9 (4020)                    | 13.1 (2940)                        | 82.3         |
|                   | 20.1 (4510)                    | 14.6 (3280)                        | 83.1         |
|                   | 22.5 (5060)                    | 16.4 (3680)                        | 83.9         |
|                   | 24.6 (5540)                    | 17.9 (4020)                        | 84.6         |
|                   | 26.7 (6000)                    | 19.5 (4380)                        | 85.2         |
|                   | 29.1 (6550)                    | 21.2 (4770)                        | 85.8         |
|                   | 31.3 (7040)                    | 22.9 (5140)                        | 86.3         |
| 33.6 (7560)       | 24.5 (5510)                    | 86.8                               |              |
| 35.7 (8020)       | 26.1 (5860)                    | 87.1                               |              |

TABLE E-8. COMPACTION DATA FOR 15 g MELAMINE SAMPLES

| <u>Run Number</u> | <u>Applied Force, kN (lbf)</u> | <u>Transmitted Force, kN (lbf)</u> | <u>% TMD</u> |
|-------------------|--------------------------------|------------------------------------|--------------|
| 76TF              | 0.76 (170)                     | 0.62 (140)                         | 70.5         |
|                   | 2.2 (500)                      | 1.4 (320)                          | 72.2         |
|                   | 4.45 (1000)                    | 2.8 (640)                          | 75.5         |
|                   | 6.67 (1500)                    | 4.4 (980)                          | 78.1         |
|                   | 8.90 (2000)                    | 5.83 (1310)                        | 79.9         |
|                   | 11.0 (2480)                    | 7.16 (1610)                        | 81.5         |
|                   | 13.3 (2980)                    | 8.63 (1940)                        | 82.6         |
|                   | 15.6 (3500)                    | 10.1 (2270)                        | 83.8         |
|                   | 17.8 (4000)                    | 11.4 (2560)                        | 84.6         |
|                   | 20.6 (4620)                    | 13.2 (2960)                        | 85.6         |
|                   | 22.2 (5000)                    | 14.1 (3180)                        | 86.0         |
|                   | 24.6 (5520)                    | 15.5 (3480)                        | 86.7         |
|                   | 26.7 (6000)                    | 16.9 (3810)                        | 87.2         |
|                   | 29.1 (6540)                    | 18.4 (4130)                        | 87.7         |
|                   | 31.1 (7000)                    | 19.6 (4400)                        | 88.1         |
|                   | 33.4 (7510)                    | 21.0 (4720)                        | 88.4         |
| 35.5 (7990)       | 22.3 (5020)                    | 88.8                               |              |
| 77TF              | 1.5 (340)                      | 0.89 (200)                         | 72.0         |
|                   | 4.54 (1020)                    | 1.6 (580)                          | 74.9         |
|                   | 6.89 (1550)                    | 4.1 (920)                          | 77.7         |
|                   | 9.07 (2040)                    | 5.60 (1260)                        | 79.9         |
|                   | 11.3 (2540)                    | 7.03 (1580)                        | 81.4         |
|                   | 13.5 (3030)                    | 8.41 (1890)                        | 82.7         |
|                   | 15.8 (3550)                    | 9.96 (2240)                        | 83.8         |
|                   | 18.0 (4040)                    | 11.4 (2570)                        | 84.8         |
|                   | 20.3 (4560)                    | 12.8 (2880)                        | 85.6         |
|                   | 22.4 (5040)                    | 14.1 (3180)                        | 86.2         |
|                   | 26.2 (5900)                    | 16.5 (3710)                        | 87.3         |
|                   | 27.7 (6220)                    | 17.6 (3960)                        | 87.5         |
|                   | 29.4 (6620)                    | 18.6 (4190)                        | 88.0         |
|                   | 31.4 (7060)                    | 19.9 (4480)                        | 88.3         |
|                   | 33.5 (7540)                    | 21.4 (4800)                        | 88.7         |
|                   | 35.6 (8010)                    | 11.6 (5080)                        | 89.1         |

TABLE E-9. COMPACTION DATA FOR 20 g MELAMINE SAMPLES

| <u>Run Number</u> | <u>Applied Force, kN (lbf)</u> | <u>Transmitted Force, kN (lbf)</u> | <u>% TMD</u> |
|-------------------|--------------------------------|------------------------------------|--------------|
| 78TF              | 1.1 (240)                      | 0.53 (120)                         | 68.3         |
|                   | 2.3 (520)                      | 1.1 (240)                          | 69.9         |
|                   | 4.54 (1020)                    | 2.3 (520)                          | 73.6         |
|                   | 6.89 (1550)                    | 3.6 (800)                          | 76.0         |
|                   | 8.99 (2020)                    | 4.76 (1070)                        | 77.9         |
|                   | 11.2 (2520)                    | 6.01 (1350)                        | 79.5         |
|                   | 13.5 (3040)                    | 7.30 (1640)                        | 80.8         |
|                   | 15.7 (3540)                    | 8.59 (1930)                        | 81.9         |
|                   | 18.2 (4100)                    | 9.88 (2220)                        | 82.8         |
|                   | 20.2 (4540)                    | 10.9 (2460)                        | 83.4         |
|                   | 22.5 (5060)                    | 12.1 (2730)                        | 84.0         |
|                   | 24.8 (5580)                    | 13.4 (3020)                        | 84.7         |
|                   | 26.9 (6050)                    | 14.5 (3260)                        | 85.2         |
|                   | 29.5 (6640)                    | 15.7 (3540)                        | 85.6         |
|                   | 31.3 (7030)                    | 16.9 (3810)                        | 86.1         |
|                   | 33.5 (7540)                    | 18.1 (4080)                        | 86.5         |
| 35.7 (8020)       | 19.3 (4340)                    | 86.9                               |              |
| 79TF              | 0.89 (200)                     | 0.36 (80)                          | 68.7         |
|                   | 2.3 (520)                      | 1.1 (240)                          | 70.6         |
|                   | 4.63 (1040)                    | 2.2 (500)                          | 73.7         |
|                   | 6.85 (1540)                    | 3.4 (760)                          | 76.0         |
|                   | 8.90 (2000)                    | 4.72 (1060)                        | 78.0         |
|                   | 11.3 (2530)                    | 6.09 (1370)                        | 79.6         |
|                   | 13.4 (3020)                    | 7.47 (1680)                        | 80.8         |
|                   | 15.8 (3550)                    | 8.81 (1980)                        | 81.9         |
|                   | 17.9 (4030)                    | 10.1 (2260)                        | 82.7         |
|                   | 20.1 (4520)                    | 11.3 (2540)                        | 83.5         |
|                   | 22.5 (5060)                    | 12.5 (2810)                        | 84.1         |
|                   | 24.6 (5540)                    | 13.7 (3090)                        | 84.7         |
|                   | 26.9 (6040)                    | 14.9 (3360)                        | 85.3         |
|                   | 29.1 (6540)                    | 16.3 (3660)                        | 85.7         |
|                   | 31.2 (7020)                    | 17.4 (3920)                        | 86.1         |
|                   | 33.5 (7540)                    | 18.6 (4190)                        | 86.5         |
| 35.7 (8030)       | 20.0 (4500)                    | 86.9                               |              |

TABLE E-10. COMPACTION DATA FOR 25 g MELAMINE SAMPLES

| <u>Run Number</u> | <u>Applied Force, kN (lbf)</u> | <u>Transmitted Force, kN (lbf)</u> | <u>% TMD</u> |
|-------------------|--------------------------------|------------------------------------|--------------|
| 80TF              | 0.98 (220)                     | 0.36 (80)                          | 68.6         |
|                   | 1.4 (320)                      | 0.53 (120)                         | 69.6         |
|                   | 2.3 (520)                      | 2.0 (440)                          | 70.5         |
|                   | 4.58 (1030)                    | 3.1 (700)                          | 73.8         |
|                   | 6.98 (1570)                    | 4.1 (920)                          | 76.4         |
|                   | 8.99 (2020)                    | 5.16 (1160)                        | 78.2         |
|                   | 11.2 (2520)                    | 6.32 (1420)                        | 79.6         |
|                   | 13.5 (3040)                    | 7.47 (1680)                        | 81.0         |
|                   | 15.7 (3540)                    | 8.54 (1920)                        | 82.1         |
|                   | 17.9 (4020)                    | 9.30 (2090)                        | 83.0         |
|                   | 20.3 (4560)                    | 9.79 (2200)                        | 83.9         |
|                   | 22.5 (5050)                    | 10.9 (2440)                        | 84.6         |
|                   | 24.6 (5540)                    | 12.0 (2700)                        | 85.2         |
|                   | 26.9 (6050)                    | 13.1 (2940)                        | 85.7         |
|                   | 29.0 (6520)                    | 14.1 (3160)                        | 86.2         |
|                   | 31.3 (7030)                    | 15.0 (3370)                        | 86.6         |
|                   | 33.5 (7540)                    | 16.1 (3630)                        | 87.1         |
| 35.9 (8060)       | 17.3 (3900)                    | 87.5                               |              |
| 82TF              | 0.98 (220)                     | 0.62 (140)                         | 69.5         |
|                   | 2.3 (510)                      | 1.2 (270)                          | 71.6         |
|                   | 4.54 (1020)                    | 2.5 (570)                          | 74.7         |
|                   | 6.76 (1520)                    | 3.7 (840)                          | 77.0         |
|                   | 8.90 (2000)                    | 4.89 (1100)                        | 78.8         |
|                   | 11.4 (2560)                    | 6.05 (1360)                        | 80.5         |
|                   | 13.3 (3000)                    | 7.12 (1600)                        | 81.5         |
|                   | 15.6 (3510)                    | 8.32 (1870)                        | 82.6         |
|                   | 17.8 (4010)                    | 9.47 (2130)                        | 83.5         |
|                   | 20.0 (4500)                    | 10.5 (2370)                        | 84.3         |
|                   | 22.3 (5020)                    | 11.6 (2600)                        | 84.9         |
|                   | 24.8 (5580)                    | 12.8 (2880)                        | 85.6         |
|                   | 26.6 (5980)                    | 13.7 (3070)                        | 86.0         |
|                   | 29.9 (6720)                    | 15.0 (3380)                        | 86.6         |
|                   | 31.3 (7030)                    | 15.8 (3560)                        | 86.9         |
| 33.4 (7510)       | 16.8 (3770)                    | 87.3                               |              |
| 35.8 (8040)       | 17.8 (4000)                    | 87.6                               |              |

TABLE E-11. INTRAGRANULAR STRESS RESULTS FROM VARIOUS ANALYSES OF  
TEFLON 7C COMPACTION DATA

| Sample Mass, g | Run Number | Intragranular Stress, MPa (psi) |        | Burchett et al. | % TMD  |                |      |
|----------------|------------|---------------------------------|--------|-----------------|--------|----------------|------|
|                |            | Kuo et al.                      | NSWC I |                 |        |                |      |
| 5              | 54TF       | 1.4                             | (200)  | 1.4             | (200)  | Not Determined | 77.8 |
|                |            | 4.3                             | (620)  | 4.4             | (640)  | Determined     | 86.1 |
|                |            | 9.1                             | (1300) | 9.2             | (1300) |                | 92.7 |
|                |            | 11.4                            | (1650) | 11.4            | (1650) |                | 93.7 |
|                |            | 14.8                            | (2150) | 14.9            | (2160) |                | 95.3 |
|                |            | 18.3                            | (2650) | 18.4            | (2670) |                | 96.0 |
|                |            | 21.6                            | (3130) | 21.8            | (3160) |                | 96.7 |
|                |            | 25.4                            | (3680) | 25.5            | (3700) |                | 96.9 |
|                |            | 29.1                            | (4220) | 29.1            | (4220) |                | 97.0 |
|                |            | 32.3                            | (4680) | 32.4            | (4700) |                | 97.1 |
| 35.8           | (5190)     | 35.8                            | (5190) |                 | 97.2   |                |      |
| 15             | 62TF       | 1.6                             | (230)  | 1.6             | (230)  | Not Determined | 66.7 |
|                |            | 3.8                             | (550)  | 3.7             | (540)  | Determined     | 74.1 |
|                |            | 5.3                             | (770)  | 5.5             | (800)  |                | 79.6 |
|                |            | 7.1                             | (1000) | 7.4             | (1100) |                | 83.5 |
|                |            | 8.9                             | (1300) | 9.1             | (1300) |                | 86.5 |
|                |            | 11.3                            | (1640) | 11.6            | (1680) |                | 89.7 |
|                |            | 14.6                            | (2120) | 14.9            | (2160) |                | 92.3 |
|                |            | 17.8                            | (2580) | 18.2            | (2640) |                | 94.0 |
|                |            | 22.9                            | (3320) | 23.1            | (3350) |                | 95.7 |
|                |            | 26.4                            | (3830) | 26.6            | (3860) |                | 96.5 |
| 29.7           | (4310)     | 29.8                            | (4320) |                 | 97.0   |                |      |
| 31.8           | (4610)     | 31.9                            | (4630) |                 | 97.4   |                |      |
| 35.4           | (5130)     | 35.3                            | (5120) |                 | 97.7   |                |      |

TABLE E-11. INTRAGRANULAR STRESS RESULTS FROM VARIOUS ANALYSES OF  
TEFLON 7C COMPACTION DATA (Cont.)

| Sample Mass, g | Run Number | Intragranular Stress, MPa (psi) |        | NSWC II | Burchett et al. | % TMD          |     |       |        |      |
|----------------|------------|---------------------------------|--------|---------|-----------------|----------------|-----|-------|--------|------|
|                |            | Kuo et al.                      | NSWC I |         |                 |                |     |       |        |      |
| 25             | 68TF       | 1.5                             | (220)  | 1.5     | (220)           | Not Determined | 1.5 | (220) | 67.8   |      |
|                |            | 4.2                             | (610)  | 4.3     | (620)           |                |     | 4.2   | (610)  | 76.9 |
|                |            | 7.6                             | (1100) | 7.8     | (1100)          |                |     | 7.5   | (1100) | 84.7 |
|                |            | 11.0                            | (1600) | 11.0    | (1600)          |                |     | 11.0  | (1600) | 89.8 |
|                |            | 14.3                            | (2070) | 14.2    | (2060)          |                |     | 14.2  | (2060) | 92.5 |
|                |            | 17.4                            | (2520) | 17.4    | (2520)          |                |     | 17.3  | (2510) | 94.3 |
|                |            | 20.8                            | (3020) | 20.7    | (3000)          |                |     | 20.8  | (3020) | 95.5 |
|                |            | 24.0                            | (3480) | 23.8    | (3450)          |                |     | 24.0  | (3480) | 96.5 |
|                |            | 28.1                            | (4080) | 27.7    | (4020)          |                |     | 28.1  | (4080) | 97.2 |
|                |            | 30.8                            | (4470) | 30.3    | (4390)          |                |     | 30.8  | (4470) | 97.5 |
|                |            | 34.1                            | (4950) | 33.5    | (4860)          |                |     | 34.1  | (4950) | 97.9 |

TABLE E-12. INTRAGRANULAR STRESS RESULTS FROM VARIOUS ANALYSES OF MELAMINE COMPACTION DATA

| Sample Mass, g | Run Number | Intragranular Stress, MPa (psi) |           |         |                 | % TMD |   |
|----------------|------------|---------------------------------|-----------|---------|-----------------|-------|---|
|                |            | Kuo et al.                      | NSWC I    | NSWC II | Burchett et al. |       |   |
| 5              | 72TF       | 2.6                             | (380)     | 3.1     | (450)           | 69.9  | Not Determined  |
|                |            | 5.7                             | (830)     | 6.1     | (880)           | 71.5  |   |
|                |            | 10.8                            | (1570)    | 11.3    | (1640)          | 74.2  |   |
|                |            | 15.8                            | (2290)    | 16.4    | (2380)          | 76.6  |   |
|                |            | 20.6                            | (2990)    | 21.1    | (3060)          | 78.4  |   |
|                |            | 26.9                            | (3900)    | 27.4    | (3970)          | 80.5  |   |
|                |            | 29.9                            | (4340)    | 30.4    | (4410)          | 81.3  |   |
|                |            | 34.6                            | (5020)    | 35.1    | (5090)          | 82.0  |   |
|                |            | 39.0                            | (5660)    | 39.7    | (5760)          | 83.2  |   |
|                |            | 43.4                            | (6290)    | 43.9    | (6370)          | 83.9  |   |
|                |            | 47.9                            | (6950)    | 48.4    | (7020)          | 84.8  |   |
|                |            | 53.2                            | (7720)    | 53.8    | (7800)          | 85.6  |   |
|                |            | 56.9                            | (8250)    | 57.5    | (8340)          | 86.2  |   |
|                |            | 61.2                            | (8880)    | 61.9    | (8980)          | 86.9  |   |
| 65.3           | (9470)     | 65.9                            | (9560)    | 87.5    |                 |       |   |
| 69.4           | (10100)    | 70.0                            | (10200)   | 87.9    |                 |       |   |
| 73.8           | (10700)    | 74.6                            | (10800)   | 88.5    |                 |       |   |
| 15             | 76TF       | 1.9                             | (280)     | 1.6     | (230)           | 70.5  | 1.9 (280)<br>4.8 (700)<br>9.32 (1350)<br>13.7 (1990)<br>17.9 (2600)<br>21.6 (3130)<br>25.6 (3710)<br>29.7 (4310)<br>33.3 (4830) |
|                |            | 5.0                             | (730)     | 4.6     | (670)           | 72.2  |   |
|                |            | 9.54                            | (1380)    | 8.94    | (1300)          | 75.5  |   |
|                |            | 14.0                            | (2030)    | 13.1    | (1900)          | 78.1  |   |
|                |            | 18.2                            | (2640)    | 17.2    | (2490)          | 79.9  |   |
|                |            | 22.1                            | (3210)    | 21.0    | (3050)          | 81.5  |   |
|                |            | 26.2                            | (3800)    | 25.0    | (3630)          | 82.6  |   |
|                |            | 30.3                            | (4390)    | 29.1    | (4220)          | 83.8  |   |
|                |            | 34.1                            | (4950)    | 32.9    | (4770)          | 84.6  |   |
|                |            |                                 |           |         | 9.4 (1400)      |       |   |
|                |            |                                 |           |         | 14 (2000)       |       |   |
|                |            |                                 |           |         | 18 (2600)       |       |   |
|                |            |                                 |           |         | 22 (3200)       |       |   |
|                |            |                                 |           |         | 26 (3800)       |       |   |
|                |            |                                 | 30 (4400) |         |                 |       |   |
|                |            |                                 | 34 (4900) |         |                 |       |   |

TABLE E-12. INTRAGRANULAR STRESS RESULTS FROM VARIOUS ANALYSES OF  
MELAMINE COMPACTION DATA (Cont.)

| Sample Mass, g | Run Number       | Intragranular Stress, MPa (psi) |                       | % TMD              |                      |                |
|----------------|------------------|---------------------------------|-----------------------|--------------------|----------------------|----------------|
|                |                  | Kuo et al.                      | NSWC I                |                    |                      |                |
| 15<br>(Cont.)  | 76TF             | 39.0                            | (5660) 37.7 (5470) 38 | (5500) 38.0 (5510) |                      |                |
|                |                  | 41.9                            | (6080) 40.7 (5900) 41 | (5900) 40.8 (5920) |                      |                |
|                |                  | 45.7                            | (6630) 44.6 (6470) 45 | (6500) 44.5 (6450) |                      |                |
|                |                  | 49.5                            | (7180) 48.3 (7010) 49 | (7100) 48.3 (7010) |                      |                |
|                |                  | 53.6                            | (7770) 52.5 (7600) 53 | (7700) 52.2 (7570) |                      |                |
|                |                  | 57.0                            | (8270) 55.9 (8110) 56 | (8100) 55.5 (8050) |                      |                |
|                |                  | 60.9                            | (8830) 59.8 (8670) 60 | (8700) 59.3 (8600) |                      |                |
|                |                  | 64.5                            | (9350) 63.4 (9200) 63 | (9100) 62.8 (9110) |                      |                |
|                |                  | 25                              | 82TF                  | 2.3                | (330) Not Determined | Not Determined |
|                |                  |                                 |                       | 4.8                | (700) 4.5 (650)      | Determined     |
|                |                  |                                 |                       | 9.3                | (1300) 8.8 (1300)    |                |
|                |                  |                                 |                       | 13.5               | (1960) 13 (1900)     |                |
|                |                  |                                 |                       | 17.3               | (2510) 17 (2500)     |                |
|                |                  |                                 |                       | 21.4               | (3100) 20 (2900)     |                |
| 24.8           | (3600) 24 (3500) |                                 |                       |                    |                      |                |
| 28.7           | (4160) 27 (3900) |                                 |                       |                    |                      |                |
| 32.4           | (4700) 31 (4500) |                                 |                       |                    |                      |                |
| 35.9           | (5210) 34 (4900) |                                 |                       |                    |                      |                |
| 39.5           | (5730) 36 (5200) |                                 |                       |                    |                      |                |
| 43.5           | (6310) 40 (5800) |                                 |                       |                    |                      |                |
| 46.4           | (6730) 43 (6200) |                                 |                       |                    |                      |                |
| 51.4           | (7450) 46 (6700) |                                 |                       |                    |                      |                |
| 53.6           | (7770) 48 (7000) |                                 |                       |                    |                      |                |
| 56.9           | (8250) 51 (7400) |                                 |                       |                    |                      |                |
| 60.5           | (8770) 54 (7800) |                                 |                       |                    |                      |                |

## APPENDIX F

## HARDNESS STUDIES OF COMPACTED TEFLON 7C SAMPLES

The microhardness profile was measured radially for a 5 and 25 g sample of Teflon 7C, both compacted above 95% TMD. These measurements were made using a diamond pyramid or Vickers indenter and appear in Figure F-1. It was determined that the hardness is essentially constant (diamond pyramid hardness (DPH) =  $2.4 \pm 0.1 \text{ kgf/mm}^2$ ) from the center of the top surface to within 0.7 mm of the circumference. A nearly 30% increase in hardness was observed for the outer annular region from the circumference to an inward radial distance of about 0.7 mm. Although the relationship between diamond pyramid hardness and density was not established in this work, Hirschhorn and Garey<sup>F-1</sup> found hardness to increase with increasing density for compacted iron powders. The outer annular region of increased hardness is consistent with various studies of the density and stress distribution in the compaction of metal powders.<sup>F-2, F-3</sup>

Instantaneous Shore hardness measurements in accordance with ASTM Method D 2240-75 (Reference F-4) were made on a series of compacted Teflon 7C samples with widely varying % TMD. These are most of the same samples used in the sound velocity measurements work described in Appendix D. Both Shore A-2 and D measurements were made because of the limitation in the recommended<sup>F-4</sup> hardness measurement range for each durometer. These values appear in Figures F-2 and F-3, respectively, in which the appropriate recommendations are indicated. All measurements were made on the top and bottom surfaces of the cylindrical samples and were found to be essentially the same. No correction was made on these measurements based on the calibrated test block measurements (Figures F-2 and

---

F-1 Hirschhorn, J. S., and Garey, M. W., "Plastic Deformation of Compacted Iron Powders," International Journal of Powder Metallurgy, Vol. 5, No. 1, 1969, pp. 35-44.

F-2 Duwez, P., and Zwell, L., "Pressure Distribution in Compacting Metal Powders," Journal of Metals, Vol. 1, No. 2, 1949, pp. 137-144.

F-3 Strijbos, S., and Vermeer, P. A., "Stress and Density Distributions in the Compaction of Powders," in Processing of Crystalline Ceramics, Materials Science Research, Vol. 11, Eds: H. Palmour III, R. F. Davis, and T. M. Hare (New York: Plenum Press, 1978), pp. 113-123.

F-4 1979 Annual Book of ASTM Standards, Part 35: Plastics-General Test Methods; Nomenclature (Philadelphia: ASTM, 1979), pp. 705-708.

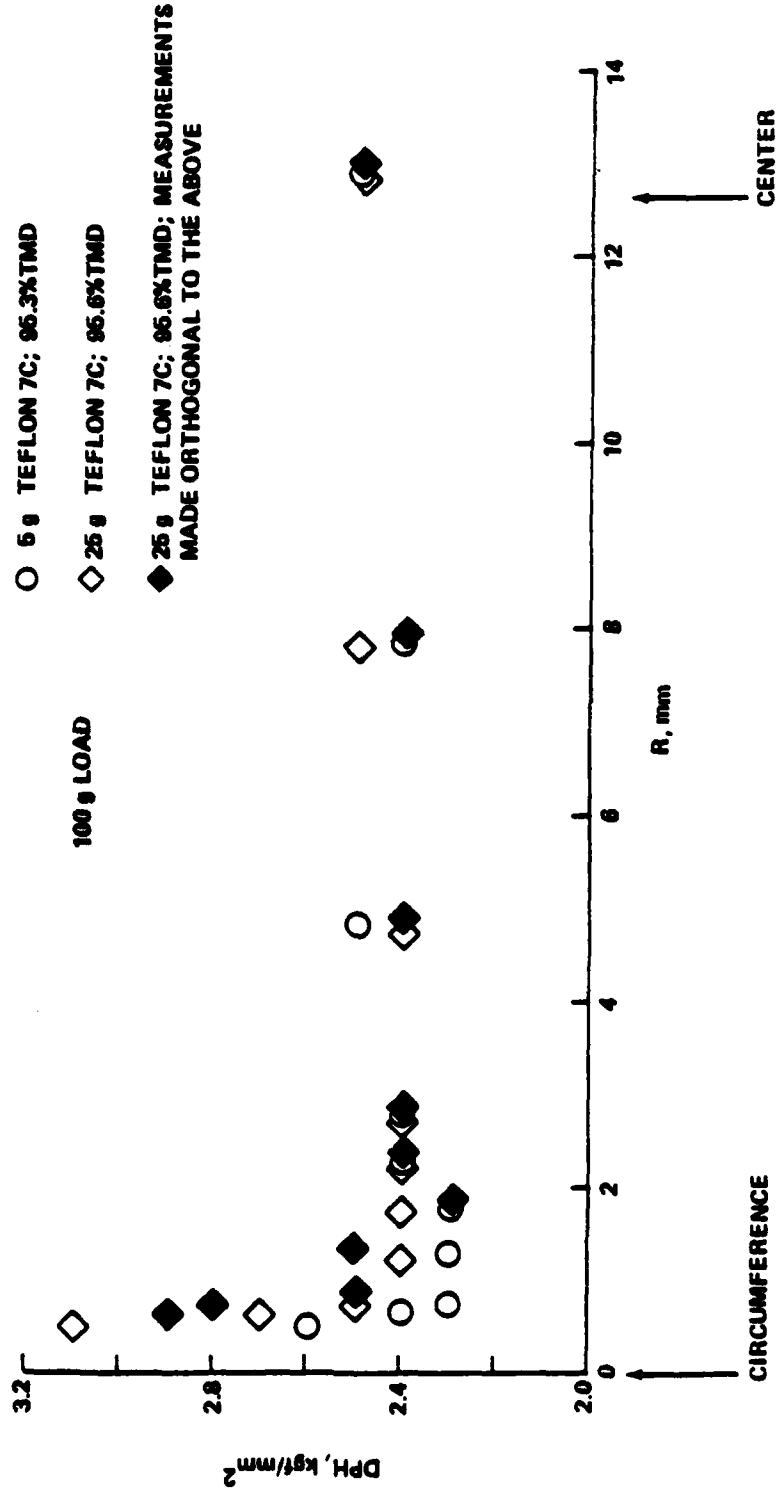


FIGURE F-1. DIAMOND PYRAMID (VICKERS) HARDNESS VERSUS RADIAL DISTANCE ALONG TOP SURFACE OF COMPACTED TEFLON 7C SAMPLES

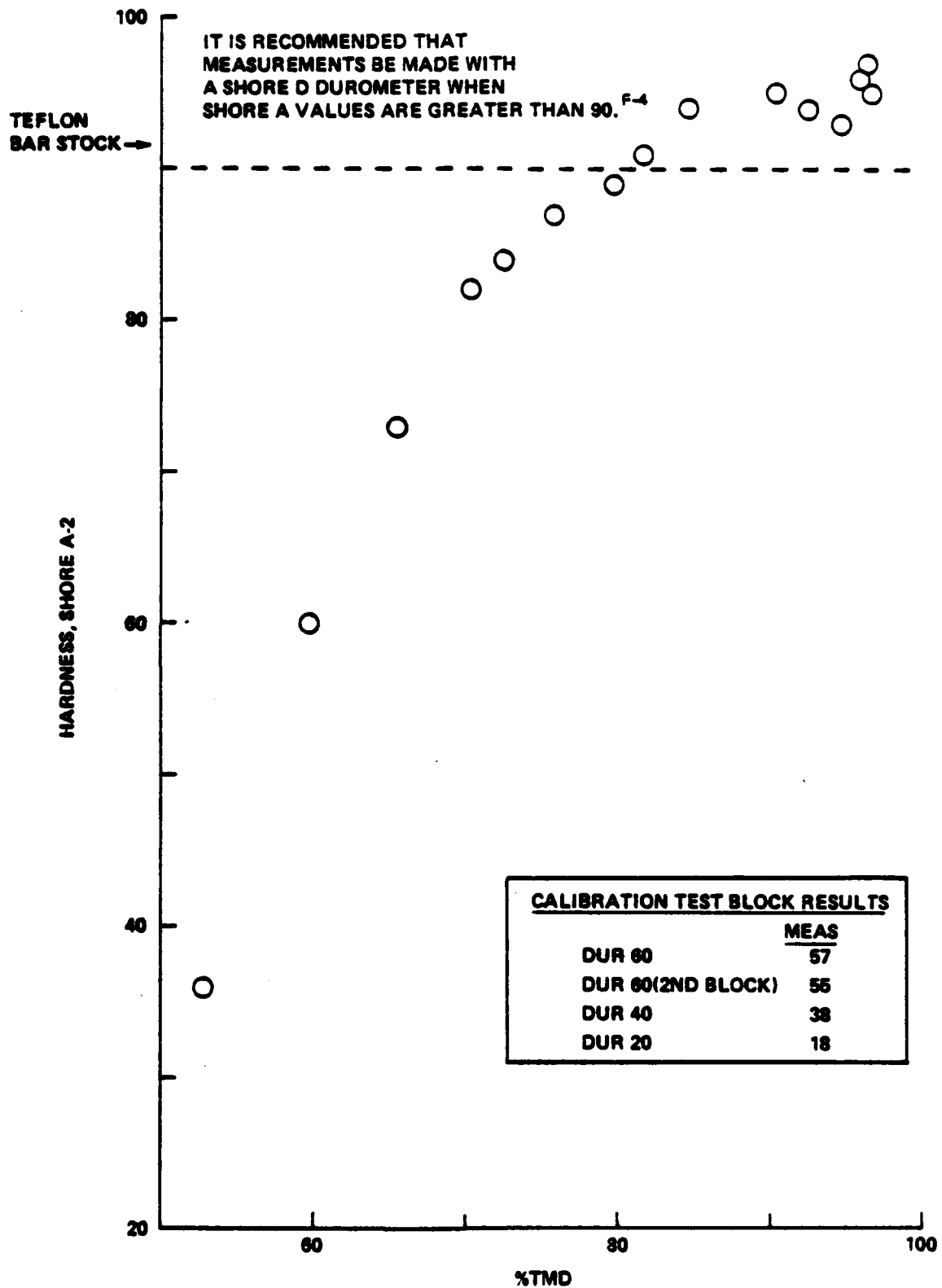


FIGURE F-2. SHORE A-2 HARDNESS VERSUS %TMD FOR COMPACTED TEFLON 7C SAMPLES

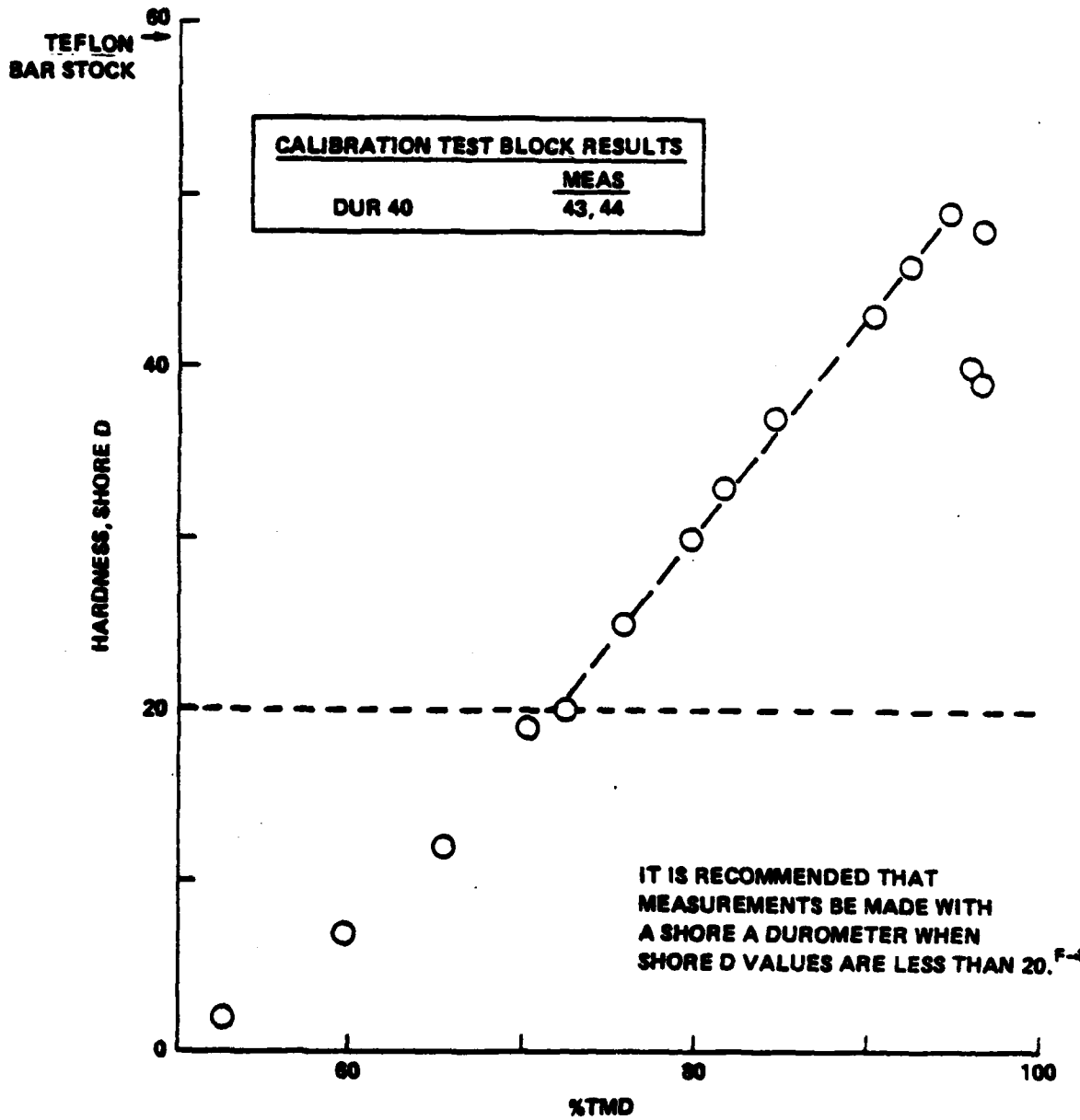


FIGURE F-3. SHORE D HARDNESS VERSUS %TMD FOR COMPACTED TEFロン 7C SAMPLES

F-3), which would indicate that all reported values are actually a little lower. Rather, emphasis was given to determining how the data was trending. Referring to Figure F-2, the rate of change of hardness, below a Shore A-2 value of 90 was found to decrease with increasing % TMD indicating that an increasing amount of plastic deformation is occurring to accommodate the indenter in the higher density samples. By comparison, the variation of Shore D hardness (above a Shore D value of 20) with % TMD given in Figure F-3 is linear below 95% TMD, but hardness values fall significantly off this linear dependency above 95% TMD. This suggests an enhanced plasticity in samples compacted above 95% TMD. It is important to note that all of the Shore D values for compacted Teflon 7C samples are significantly below the Shore D value of 59 for Teflon bar stock.

## DISTRIBUTION

|  | <u>Copies</u> |   | <u>Copies</u> |
|--|---------------|---|---------------|
| Chief of Naval Material<br>Washington, DC 20360                          | 1             | Office of Naval Technology<br>Attn: MAT-07P (J. Enig)<br>Department of the Navy<br>800 North Quincy Street<br>Arlington, VA 22217 | 1             |
| Commander<br>Naval Air Systems Command<br>Attn: AIR-350                  | 1             |   |               |
| AIR-330  | 1             | Commander<br>Naval Weapons Center<br>Attn: Technical Library  | 1             |
| Department of the Navy<br>Washington, DC 20361                           |               | Code 3264   | 1             |
| Commander<br>Naval Sea Systems Command                                   |               | Code 3205 (C. Thelin)   | 1             |
| Attn: SEA-99612  | 2             | Code 32052 (L. Smith)   | 1             |
| SEA-62R  | 1             | Code 388 (R. L. Derr)   | 1             |
| SEA-62R2   | 1             | Code 3882 (T. Boggs)  | 1             |
| SEA-62R3   | 1             | Code 3882 (C. Price)  | 1             |
| SEA-62R32  | 1             | Code 383 (H. D. Mallory)  | 1             |
| SEA-64E  | 1             | Code 3835 (K. Graham)   | 1             |
| Department of the Navy<br>Washington, DC 20362                           |               | China Lake, CA 93555  |               |
| Director<br>Strategic Systems Project<br>Office (PM-1)<br>Attn: SP-2731  |               | Director<br>Naval Research Laboratory<br>Attn: Technical<br>Information Section   | 2             |
| (E. L. Throckmorton, Jr.)  | 1             | Washington, DC 20375  |               |
| J. F. Kincaid  | 1             | Office of Chief of Naval<br>Operations<br>Operations Evaluation Group<br>(OP03EG)<br>Washington, DC 20350                         | 1             |
| Department of the Navy<br>Washington, DC 20376                           |               |   |               |
| Office of Naval Research<br>Attn: RADM L. S. Kollmorgen                  | 1             | Director<br>Office of the Secretary of Defense<br>Advanced Research Projects Agency<br>Washington, DC 20301                       | 1             |
| ONR-430 (R. S. Miller)   | 1             |   |               |
| ONR-471 (Technical<br>Library)   | 1             | Commanding Officer<br>Naval Weapons Station<br>Attn: R&D Division<br>Code 50<br>Yorktown, VA 23691                                | 1             |
| Department of the Navy<br>800 North Quincy Street<br>Arlington, VA 22217 |               |   |               |

## DISTRIBUTION (Cont.)

|   | <u>Copies</u> |  | <u>Copies</u>         |
|---|---------------|--|-----------------------|
| Commanding Officer<br>Naval Propellant Plant<br>Attn: Technical Library<br>Indian Head, MD 20640                                  | 1             | Naval Plant Representative<br>Office<br>Strategic Systems Project Office<br>Lockheed Missiles and Space<br>Company<br>Attn: SPL-332 (R. H. Guay)<br>C. Vanek<br>P. O. Box 504<br>Sunnyvale, CA 94088 | 1<br>1                |
| Commanding Officer<br>Naval Explosive Ordnance<br>Disposal Facility<br>Attn: Information Services<br>Indian Head, MD 20640        | 1             | Hercules Incorporated<br>Allegany Ballistics Laboratory<br>Attn: Library<br>P. O. Box 210<br>Cumberland, MD 21502  | 1                     |
| Commanding Officer<br>Naval Ordnance Station<br>Attn: J. A. Birkett<br>Indian Head, MD 20640                                      | 1             | AMCRD<br>5001 Eisenhower Avenue<br>Alexandria, VA 22302  | 1                     |
| McDonnell Aircraft Company<br>Attn: M. L. Schimmel<br>P. O. Box 516<br>St. Louis, MO 63166  | 1             | Redstone Scientific<br>Information Center<br>U. S. Army Missile Command<br>Attn: Chief, Documents<br>Redstone Arsenal, AL 35809  | 1                     |
| Commanding Officer<br>Naval Ammunition Depot<br>Crane, IN 47522   | 1             | Commanding Officer<br>Army Armament Research and<br>Development Command<br>Energetic Materials Division<br>Attn: Louis Avrami, DRDAR-LCE<br>Technical Library<br>Dover, NJ 07801                     | 1<br>1                |
| Commanding Officer<br>Naval Underwater Systems<br>Center<br>Attn: LA 151-Technical<br>Library<br>Newport, RI 02840                | 1             | Director<br>Ballistics Research Laboratories<br>Attn: Library<br>N. Gerri<br>P. Howe<br>B. Frey<br>D. Kooker   | 1<br>1<br>1<br>1<br>1 |
| Commanding Officer<br>Naval Weapons Evaluation<br>Facility<br>Attn: Code AT-7<br>Kirtland Air Force Base<br>Albuquerque, NM 87117 | 1             | Aberdeen Proving<br>Ground, MD 21005   | 1                     |
| Commanding Officer<br>Naval Ammunition Depot<br>Attn: QEL<br>Concord, CA 94522  | 1             | Commanding Officer<br>Harry Diamond Laboratories<br>Attn: Library<br>Keith Warner<br>2800 Powder Mill Road<br>Adelphi, MD 20783  | 1<br>1                |
| Superintendent Naval Academy<br>Attn: Library<br>Annapolis, MD 21402  | 1             |  |                       |

## DISTRIBUTION (Cont.)

|   | <u>Copies</u> |   | <u>Copies</u> |
|---|---------------|---|---------------|
| Armament Development &<br>Test Center           |               | Sandia National Laboratories                  |               |
| Attn: B. G. Craig                               | 1             | Attn: R. J. Lawrence,                         |               |
| DLOSL/Technical Library                         | 1             | Div. 5166                                     | 1             |
| Eglin Air Force Base, FL 32542                  |               | J. Nunziato                                   | 1             |
|   |               | R. Setchell                                   | 1             |
|   |               | D. Hayes                                      | 1             |
| Commanding Officer                              |               | P. O. Box 5800                                |               |
| Naval Ordnance Station                          |               | Albuquerque, NM 87115                         |               |
| Louisville, KY 40124                            | 1             |   |               |
| Director  |               | Director                                      |               |
| Applied Physics Laboratory                      |               | Los Alamos National Laboratory                |               |
| Attn: Library                                   | 1             | Attn: Library                                 | 1             |
| Johns Hopkins Road                              |               | R. L. Rabie                                   | 1             |
| Laurel, MD 20707                                |               | A. Bowman                                     | 1             |
|   |               | H. Flaugh                                     | 1             |
|   |               | C. A. Forest                                  | 1             |
| U. S. Department of Energy                      |               | J. D. Wackerle                                | 1             |
| Attn: DMA                                       | 1             | A. W. Campbell                                | 1             |
| Washington, DC 20545                            |               | J. K. Dienes                                  | 1             |
|   |               | P. O. Box 1663                                |               |
| Research Director                               |               | Los Alamos, NM 87544                          |               |
| Pittsburgh Mining and Safety<br>Research Center |               | Chairman                                      |               |
| Bureau of Mines                                 |               | DOD Explosives Safety Board                   |               |
| 4800 Forbes Avenue                              |               | Attn: Dr. T. A. Zoker                         | 1             |
| Pittsburgh, PA 15213                            | 1             | 2461 Eisenhower Avenue                        |               |
|   |               | Alexandria, VA 22331                          |               |
| Director  |               |   |               |
| Defense Technical Information<br>Center         |               | Aerojet Ordnance and<br>Manufacturing Company |               |
| Cameron Station                                 |               | 9236 East Hall Road                           |               |
| Alexandria, VA 22314                            | 1             | Downey, CA 90241                              | 1             |
|   |               |   |               |
| Goddard Space Flight<br>Center, NASA            |               | Hercules Incorporated Research<br>Center      |               |
| Glenn Dale Road                                 |               | Attn: Technical Information                   |               |
| Greenbelt, MD 20771                             | 1             | Division                                      | 1             |
|   |               | B. E. Clouser                                 | 1             |
| Lawrence Livermore National<br>Laboratory       |               | Wilmington, DE 19899                          |               |
| University of California                        |               |   |               |
| Attn: M. Finger                                 | 1             | Thiokol/Huntsville Division                   |               |
| E. James  | 1             | Attn: Technical Library                       | 1             |
| E. L. Lee                                       | 1             | Huntsville, AL 35807                          |               |
| P. Urtiew                                       | 1             |   |               |
| L. Green  | 1             | Shock Hydrodynamics Division                  |               |
| C. Tarver                                       | 1             | Whittaker Corporation                         |               |
| W. Von Holle                                    | 1             | Attn: Dr. L. Zernow                           | 2             |
| K. Scribner                                     | 1             | 4716 Vineland Avenue                          |               |
| P. O. Box 808                                   |               | North Hollywood, CA 91706                     |               |
| Livermore, CA 94550                             |               |   |               |

## DISTRIBUTION (Cont.)

|  | <u>Copies</u> |   | <u>Copies</u>         |
|--|---------------|---|-----------------------|
| SRI, International<br>Attn: D. Curran<br>333 Ravenswood Avenue<br>Menlo Park, CA 94025   | 1             | Paul Gough Associates<br>1048 South Street<br>Portsmouth, NH 03801  | 1                     |
| Thiokol/Wasatch Division<br>Attn: Technical Library<br>P. O. Box 524<br>Brigham City, UT 84302   | 1             | Hercules Incorporated,<br>Bacchus Works<br>Attn: Library 100-H<br>K. B. Iscm<br>D. Caldwell<br>J. H. Thacher<br>A. Butcher                        | 1<br>1<br>1<br>1<br>1 |
| Thiokol/Elkton Division<br>Attn: Technical Library<br>P. O. Box 241<br>Elkton, MD 21921  | 1             | P. O. Box 98<br>Magna, UT 84044   | 1                     |
| Teledyne McCormick Selph<br>P. O. Box 6<br>Hollister, CA 95023   | 1             | Professor H. Krier<br>144 MEB, University of IL, at U-C<br>1206 West Green Street<br>Urbana, IL 61801   | 1                     |
| R. Stresau Laboratory, Inc.<br>Star Route<br>Spooner, WI 54801   | 1             | Chemical Propulsion Information<br>Agency<br>The Johns Hopkins University<br>Applied Physics Laboratory<br>Johns Hopkins Road<br>Laurel, MD 20707 | 1                     |
| Rohm and Haas<br>Huntsville, Defense Contract<br>Office<br>Arthur Murray Building<br>Attn: H. M. Shuey<br>723-A Arcadia Circle<br>Huntsville, AL 35801 | 1             | ITT Research Institute<br>Attn: H. S. Napadensky<br>10 West 35th Street<br>Chicago, IL 60616  | 1                     |
| U. S. Army Foreign Service<br>and Technology Center<br>220 7th Street, N.E.<br>Charlottesville, VA 22901   | 1             | Erion Associates, Inc.<br>Attn: W. Petray<br>600 New Hampshire Avenue,<br>Suite 870<br>Washington, DC 20037                                       | 1                     |
| Princeton Combustion Research<br>Laboratories, Inc.<br>1041 U. S. Highway One North<br>Attn: M. Summerfield<br>N. Messina<br>Princeton, NJ 08540       | 1<br>1        | Brigham Young University<br>Department of Chemical<br>Engineering<br>Attn: Prof. M. W. Becksted<br>Provo, UT 84601                                | 1                     |
| Pennsylvania State University<br>Department of Mechanical<br>Engineering<br>Attn: K. Kuo<br>University Park, PA 16802                                  | 1             | Library of Congress<br>Attn: Gift and Exchange<br>Division<br>Washington, DC 20540  | 4                     |

## DISTRIBUTION (Cont.)

|                              | <u>Copies</u> | <u>Copies</u>                |
|------------------------------|---------------|------------------------------|
| Department of the Navy       |               | Internal Distribution:       |
| Office of Naval Research     |               |                              |
| Branch Office                |               | R10 1                        |
| Box 39                       |               | R11 1                        |
| Attn: R. W. Armstrong        | 1             | R12 1                        |
| FPO, New York 09510          |               | R13 1                        |
|                              |               | R14 1                        |
|                              |               | R15 1                        |
|                              |               | R16 1                        |
| Department of Commerce       |               | H. G. Adolph (R11) 1         |
| National Bureau of Standards |               | C. Gotzmer (R11) 1           |
| Attn: G. V. Blessing         | 1             | M. J. Kamlet (R11) 1         |
| Bldg. 233/A147               |               | H. G. Nielsen (R11) 1        |
| Washington, DC 20234         |               | V. D. Ringbloom (R11) 1      |
|                              |               | E. W. Anderson (R12) 1       |
| E. T. Toton                  |               | G. R. Liab (R12) 1           |
| BDM Corporation              |               | J. M. Short (R12) 1          |
| 7915 Jones Branch Drive      | 1             | L. A. Roslund (R121) 1       |
| McLean, VA 22102             |               | M. J. Stosz (R122) 1         |
|                              |               | R. R. Bernecker (R13) 2      |
| Lockheed Palo Alto Reserach  |               | A. R. Clairmont, Jr. (R13) 1 |
| Laboratory                   |               | C. S. Coffey (R13) 1         |
| Attn: Technical Library      | 1             | V. F. DeVost (R13) 1         |
| H. P. Marshall               | 1             | W. L. Elban (R13) 25         |
| 3251 Hanover Street          |               | J. W. Forbes (R13) 1         |
| Palo Alto, CA 94304          |               | C. L. Groves (R13) 1         |
|                              |               | S. J. Jacobs (R13) 1         |
| Air Force Rocket Propulsion  |               | H. D. Jones (R13) 1          |
| Laboratory                   |               | K. Kim (R13) 10              |
| Attn: Technical Library      | 1             | T. P. Liddiard (R13) 1       |
| R. L. Geisler                | 1             | D. Price (R13) 1             |
| Edwards Air Force Base,      |               | H. W. Sandusky (R13) 1       |
| CA 93523                     |               | L. E. Starr (R13) 1          |
|                              |               | G. B. Green (R31) 1          |
| Loyola College               |               | B. Hartmann (R31) 1          |
| Attn: Prof. P. J. Coyne, Jr. | 1             | R. W. Warfield (R31) 1       |
| 4501 N. Charles Street       |               | T. A. Orlow (K34) 1          |
| Baltimore, MD 21210          |               |                              |
|                              |               |                              |
| L. A. Ferris                 |               |                              |
| E. I. DuPont de Nemours and  |               |                              |
| Co, Inc.                     |               |                              |
| Polymer Products Department  |               |                              |
| Concord Plaza, Read Building |               |                              |
| Wilmington, DE 19898         | 1             |                              |
|                              |               |                              |
| A. W. Weston                 |               |                              |
| William M. Brobeck & Assoc.  |               |                              |
| 1235 10th Street             |               |                              |
| Berkeley, CA 94710           | 1             |                              |

**SUPPLEMENTARY**

**INFORMATION**

AD-A135292



DEPARTMENT OF THE NAVY  
NAVAL SURFACE WEAPONS CENTER  
DAHLGREN, VIRGINIA 22448

WHITE OAK LABORATORY  
SILVER SPRING, MD. 20910  
(202) 994-1800

DAHLGREN LABORATORY  
DAHLGREN, VA. 22448  
(703) 663-

IN REPLY REFER TO:  
E421:WJO:wjo

To all holders of NSWC TR 81-113  
Title: Quasi-Static Compaction Studies for DDT  
Investigations: Inert Materials

Change 1

2 page(s)

**This publication is changed as follows:**

Replace pages D-9 and D-10 with the attached pages. This replacement is being made due to a printing error on page D-9.

Insert this change sheet between the cover and the DD Form 1473 in your copy.  
Write on the cover "Change 1 inserted"

*I. L. Welch*  
I. L. WELCH  
By direction